UNIVERSIDADE FEEVALE

ROBERTA ZILLES HAHN

SANGUE SECO EM PAPEL COMO AMOSTRA ALTERNATIVA PARA AVALIAÇÃO DA EXPOSIÇÃO AO IRINOTECANO EM PACIENTES COM TUMORES DIGESTIVOS

Orientador: Prof. Dr. Rafael Linden

Novo Hamburgo, fevereiro de 2018.

ROBERTA ZILLES HAHN

SANGUE SECO EM PAPEL COMO AMOSTRA ALTERNATIVA PARA AVALIAÇÃO DA EXPOSIÇÃO AO IRINOTECANO EM PACIENTES COM TUMORES DIGESTIVOS

Dissertação apresentada como requisito para obtenção do grau de Mestre em Toxicologia e Análises Toxicológicas pela Universidade Feevale.

Orientador: Prof. Dr. Rafael Linden

Novo Hamburgo, fevereiro de 2018.

DADOS INTERNACIONAIS DE CATALOGAÇÃO NA PUBLICAÇÃO (CIP)

Hahn, Roberta Zilles.

Sangue seco em papel como amostra alternativa para avaliação da exposição ao irinotecano em pacientes com tumores digestivos / Roberta Zilles Hahn. – 2018.

93 f. il. color. ; 30 cm.

Dissertação (Mestrado em Toxicologia e Análises Toxicológicas) – Feevale, Novo Hamburgo-RS, 2018.

Inclui bibliografia.

"Orientador: Prof. Dr. Rafael Linden".

1. Toxicologia. 2. Monitoramento terapêutico. 3. Irinotecano. 4. Farmacologia. I. Título.

CDU 615.9-047.36

Bibliotecária responsável Patrícia Mentz– CRB 10/2143

Universidade Feevale
Mestrado Acadêmico em Toxicologia e Análises Toxicológicas

SANGUE SECO EM PAPEL COMO AMOSTRA ALTERNATIVA PARA AVALIAÇÃO DA EXPOSIÇÃO AO IRINOTECANO EM PACIENTES COM TUMORES DIGESTIVOS

Dissertação de mestrado aprovada pela banca examinadora em 23 de fevereiro de 2018, conferindo à autora o título de Mestre em Toxicologia e Análises Toxicológicas.

Componentes da Banca Examinadora:

Prof. Dr. Rafael Linden – FEEVALE (orientador)

Profª. Drª. Ana Paula Cappra Silva – FEEVALE

Profª. Drª. Flávia Valladão Thiesen – PUCRS

AGRADECIMENTOS

Agradeço ao meus pais por sempre priorizarem o meu estudo, sempre estarem presentes e por mais este apoio financeiro.

Ao meu Amor por todo apoio, companheirismo e paciência nos momentos difíceis. Por me fazer acreditar que no final tudo sempre dá certo.

Aos colegas do laboratório de toxicologia, colegas de mestrado e demais colaboradores do projeto irinotecano por toda ajuda técnica, apoio e incentivo.

Aos meus amigos que sempre estiveram ao meu lado mesmo eu estando mais ausente para poder me dedicar ao mestrado.

Em especial ao meu orientador, o qual admiro e respeito muito. Agradeço por todo conhecimento científico, tempo dedicado e incentivo. Rumo à próxima orientação.

RESUMO

O câncer é uma doença crônica de incidência crescente em todo o mundo, particularmente em países de baixa e média renda, com mais de 20 milhões de novos casos de câncer esperados para 2025. O quimioterápico irinotecano (IRI) é amplamente utilizado, sendo um importante componente dos regimes combinados de quimioterapia FOLFIRI e FOLFIRINOX, que são utilizados como tratamento de primeira linha contra o câncer colorretal e câncer de pâncreas avançado. Apesar da sua utilidade clínica, o uso do IRI está associado a toxicidades hematopoiéticas e gastrointestinais potencialmente graves, que podem ocasionar a interrupção do tratamento e comprometer sua eficácia além de uma significativa variabilidade na resposta terapêutica e na ocorrência de toxicidade. Estas diferenças interindividuais estão associadas à sua farmacocinética variável. Uma parte significativa da atividade do IRI é devida ao seu metabólito ativo SN-38, que é 100 a 1000 vezes mais citotóxico do que IRI, sendo metabolizado ao seu glicuronídeo inativo SN-38G. A disponibilidade de metodologias sensíveis para quantificar IRI e metabolitos, aliadas a técnicas de amostragem de fácil execução e minimamente invasivas, pode permitir o estabelecimento de relações entre exposição ao IRI e metabolitos e respostas clínicas, resultando no uso de doses individualizadas de IRI. O presente trabalho disponibiliza metodologias bioanalíticas que podem ser utilizadas no monitoramento terapêutico do IRI. Foi desenvolvido e validado um método para determinação de IRI, SN-38 e SN-38G em amostras de plasma e um método para IRI e SN-38 em amostras de manchas de sangue seco em papel (*dried blood spots*, DBS). Ambos métodos empregaram cromatografia líquida de alta eficiência associada ao detector de fluorescência (CLAE-FL) e apresentaram desempenhos aceitáveis para a implementação em laboratórios clínicos. Os métodos foram aplicados às amostras de plasma e DBS obtidas de 19 voluntários que receberam IRI em regimes de quimioterapia combinados ou como único agente, coletados 1 e 24 horas após o início da infusão. Com a quantificação dessas duas coletas foi possível calcular a área sob a curva (ASC) do IRI, de acordo com uma estratégia de amostragem limitada e modelo farmacocinético populacional. Os ensaios desenvolvidos e validados neste estudo podem ser utilizados para a avaliação da exposição individual ao IRI e seus metabólitos em condições clínicas, a fim de avaliar a exposição individual a este fármaco.

Palavras-chave: Irinotecano; SN-38; DBS; CLAE-FL; monitoramento terapêutico de fármacos.

ABSTRACT

Cancer is a chronic disease of increasing worldwide incidence, particularly in low- and middle-income countries, with more than 20 million new cases of cancer expected by 2025. The chemotherapeutic drug irinotecan (IRI) is widely used as an important component of the combined chemotherapy regimens FOLFIRI and FOLFIRINOX, which are used as first-line treatment against colorectal cancer and advanced pancreatic cancer. Despite its clinical utility, the use of IRI is associated with potentially serious hematopoietic and gastrointestinal toxicities, which can lead to discontinuation of treatment and compromise its efficacy. Moreover, there is a significant variability in therapeutic responses and the occurrence of toxicity among patients. These interindividual differences are associated to the variable pharmacokinetics. A significant part of IRI activity is due to its active metabolite SN-38, which is 100 to 1000 times more cytotoxic than IRI. The metabolite SN-38 is metabolized to its inactive glucuronide SN-38G. The availability of sensitive methodologies to quantify IRI and metabolites, coupled with easy to perform and minimally invasive sampling techniques, may allow the establishment of relationships between exposure to IRI and metabolites and clinical responses, resulting in the use of individualized doses of IRI. The present work presents bioanalytical methodologies that may allow the therapeutic monitoring of IRI. A method for determining IRI, SN-38 and SN-38G in plasma samples and a method for measuring IRI and SN-38 concentrations in dried blood spots (DBS) samples were developed and validated. Both methods employed high performance liquid chromatography associated with the fluorescence detector (HPLC-FL) and presented acceptable performances for the implementation in clinical laboratories. The methods were applied to plasma and DBS samples obtained from 19 volunteers who received IRI in combined chemotherapy regimens or as single agent, collected 1 and 24 hours after start of infusion. With the quantification of these two collections it was possible to calculate the area under the curve (AUC) of IRI, according to a limited sampling strategy and population pharmacokinetic model. The assays developed and validated in this study can be used to assess the individual exposure to IRI and its metabolites under clinical conditions in order to assess individual exposure to this drug.

Keywords: Irinotecan; SN-38; DBS; HPLC-FL; therapeutic drug monitoring.

SUMÁRIO

1. INTRODUÇÃO GERAL

O câncer é uma doença de incidência crescente em todo o mundo. Segundo estimativas da Organização Mundial da Saúde (OMS) de 2012, o câncer já provoca mais mortes do que todas as doenças cardiovasculares (FERLAY et al., 2015).

A quimioterapia é um dos fundamentos do tratamento do câncer. Dentre os diversos fármacos disponíveis, o irinotecano (IRI) é um importante componente dos regimes combinados de quimioterapia FOLFIRI (ácido folínico, 5-fluorouracil e irinotecano) e FOLFIRINOX (ácido folínico, 5-fluorouracil, irinotecano e oxaliplatina), que são utilizados como tratamento de primeira linha contra o câncer colorretal (TOURNIGAND et al., 2004) e câncer de pâncreas avançado (CONROY et al., 2013).

A prática atual é selecionar as doses de IRI com base na área de superfície corporal do paciente (DE JONG et al., 2004). Entretanto, esta estratégia não reduz a conhecida variabilidade interindividual na exposição ao IRI, o que torna essa estratégia de dosagem de pouca utilidade para este quimioterápico, tal como para muitos outros medicamentos contra o câncer (INNOCENTI et al., 2014). Esta prática pode resultar em subdosagem em alguns pacientes, assim como exposições excessivas e toxicidade severa em outros (VAN DE BOL et al., 2010).

IRI é um pró-fármaco convertido no seu metabólito ativo SN-38 através da ação das carboxilesterases hepáticas, principalmente. O SN-38 é 100 a 1.000 vezes mais potente que o IRI (Figura 1). A atividade antineoplásica do IRI é atribuída ao efeito inibitório do SN-38 sobre a DNA topoisomerase I, que desempenha um papel importante na replicação e transcrição do DNA (MATHIJSSEN et al., 2001; BASU et al., 2016). O SN-38 é metabolizado pela uridina difosfato glicuroniltransferase (UGT), especialmente UGT1A1, para formar o glicuronideo inativo SN-38G (POUJOL et al., 2006). O IRI também é metabolizado pela CYP3A4 em vários metabólitos inativos, incluindo a APC (VAN SCHAIK, 2004), sendo também biotransformado em menor extensão pela CYP3A5 (SANTOS et al., 2000). Variações na atividade destas enzimas estão relacionadas a diferenças na exposição sistêmica ao metabólito ativo SN-38 (KEHRER et al., 2002; MATHIJSSEN et al., 2002). O SN-38 é o principal responsável pela resposta antitumoral, e também pelas toxicidades dose-limitantes, neutropenia e diarreia (CANAL et al., 1996; INNOCENTI et al., 2014).

Figura 1. Rota metabólica do IRI.

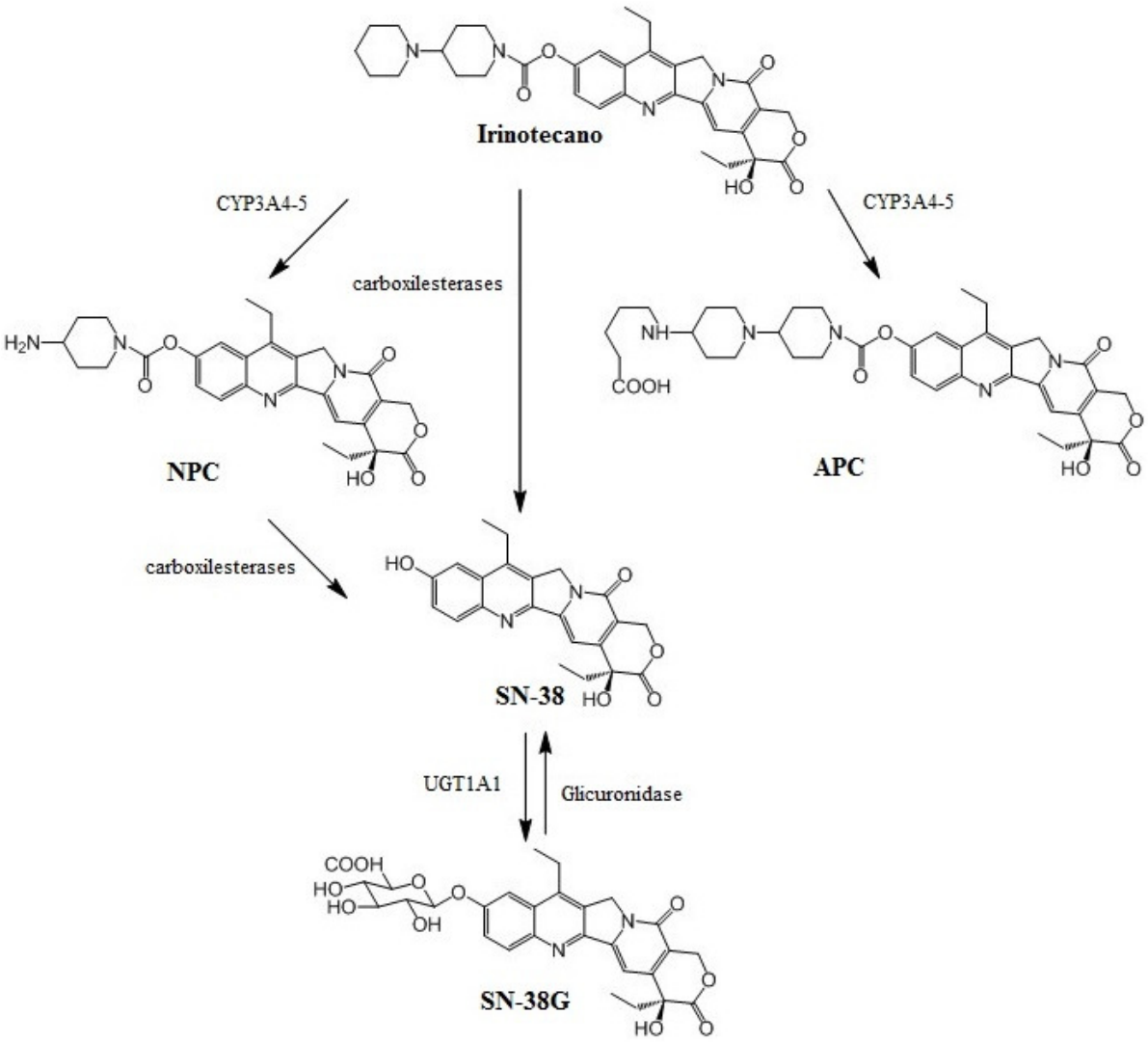

Como a maioria dos fármacos oncológicos, IRI tem uma janela terapêutica estreita (VAN DER BOL et al., 2010). Portanto, uma limitação importante associada ao seu uso é a ampla variabilidade interindividual na tolerabilidade com ocorrência de toxicidade grave, especialmente neutropenia, e na eficácia, em parte devido ao metabolismo complexo deste fármaco (MEYERHARDT & MAYER, 2005). Esta variabilidade está relacionada parcialmente a diferenças farmacocinéticas e farmacogenéticas interindividuais, especialmente na glicuronidação do metabólito ativo através da ação da UGT. Como consequência, são observadas grandes diferenças na exposição ao fármaco e metabólito ativo quando avaliadas através da área sob a curva (ASC) (DI PAOLO et al., 2011; INNOCENTI et al., 2014).

Recentemente foram propostos marcadores endógenos para caracterizar a atividade das enzimas CYP3A4/5. A proporção entre as concentrações séricas de colesterol e seu metabólito 4β-hidroxicolesterol (4β-HC), formado pela CYP3A4/5, foi sugerida como um marcador para a atividade da enzima (BJÖRKHEM-BERGMAN et al., 2013).

O risco de neutropenia grave associada ao tratamento com IRI está relacionado, também, com a presença do alelo *UGT1A1*28*, uma variante que reduz a eliminação de SN-38, o metabolito ativo do IRI (TOFFOLI et al., 2010; INNOCENTI et al., 2014). A presença do alelo *UGT1A1*28* é um biomarcador da neutropenia mencionado na bula do IRI. As concentrações séricas de bilirrubina têm sido utilizadas como indicativo da atividade de glicuronidação no fígado (DI PAOLO et al., 2011) uma vez que seus níveis estão mais elevados nos pacientes homozigotos para o alelo *UGT1A1*28* em comparação com homozigotos e heterozigotos para o alelo selvagem (ROUITS et al., 2008). O uso da razão de concentração [SN-38G]/[SN-38], denominada razão de glicuronidação (RG) do SN-38, foi descrita como um índice farmacocinético útil para identificar pacientes com risco de efeitos adversos graves (HIROSE et al., 2012; HIROSE et al., 2014).

A determinação das concentrações plasmáticas do fármaco e sua utilização para a individualização da farmacoterapia é o fundamento do monitoramento terapêutico de fármacos (MTF) (SALEEM et al., 2012). A estimativa de parâmetros farmacocinéticos do IRI e de seus metabólitos com modelos de farmacocinética populacionais previamente descritos exigem esquemas de amostragem de sangue complexos, limitando sua aplicação clínica (KLEIN et al., 2002; POUJOL et al., 2007). Neste contexto, o uso de manchas de sangue secas (*dried blood spots*, DBS), geralmente obtidas a partir de perfuração digital, pode permitir estratégias de amostragem mais complexas através de realização de múltiplas coletas de forma pouco invasiva e sem a necessidade de um flebotomista (ANTUNES, CHARÃO & LINDEN, 2016). Assim, a quantificação de IRI e seu metabólito ativo SN-38 em DBS pode ser uma alternativa para individualizar a dose do fármaco através de um método de coleta minimamente invasivo e de fácil execução, inclusive pelo próprio paciente.

Nesta perspectiva, o presente estudo buscou contribuir para a individualização do tratamento oncológico do IRI ao disponibilizar métodos totalmente validados e com desempenhos aceitáveis para análise de IRI e metabólitos tanto em plasma como em DBS. Com essas metodologias foi possível determinar os níveis plasmáticos de IRI e metabólitos e estabelecer a exposição sistêmica ao IRI através da ASC.

Essa dissertação é apresentada na forma de três capítulos, cada um consistindo de um artigo científico. O **capítulo 1** descreve a revisão da literatura científica com respeito à

farmacologia do IRI e dos possíveis marcadores farmacogenéticos e farmacocinéticos que permitam prever a ocorrência de toxicidade no tratamento do câncer com IRI (artigo de revisão submetido à revista *Current Medicinal Chemistry*). O **capítulo 2** descreve um ensaio para a determinação simultânea de IRI, SN-38 e SN-38G em amostras de plasma empregando cromatografia líquida de alta eficiência com detecção por fluorescência (CLAE-FL) (artigo publicado na revista *Latin American Journal of Pharmacy*). O **capítulo 3** descreve, pela primeira vez, um método para a determinação de IRI e SN-38 em DBS e sua aplicação em um grupo de pacientes em tratamento quimioterápico com IRI (artigo publicado na revista *Journal of Pharmaceutical and Biomedical Analysis*).

2. CAPÍTULO 1 – PHARMACOKINETIC AND PHARMACOGENETIC MARKERS OF IRINOTECAN TOXICITY

Roberta Zilles Hahn[a,b], Simone Gasparin Verza[b], Magda Susana Perassolo[b], Edna Sayuri Suyenaga[b], Marina Venzon Antunes[a,b], Gilberto Schwartsmann[c], Rafael Linden[a,b]

[a]*Laboratory of Analytical Toxicology, Institute of Health Sciences, Universidade Feevale, Novo Hamburgo-RS, Brazil*

[b]*Graduate Program on Toxicology and Analytical Toxicology, Universidade Feevale, Novo Hamburgo-RS, Brazil*

[c]*Oncology Service, Hospital de Clínicas de Porto Alegre, Porto Alegre-RS, Brazil*

**Address correspondence to this author at the Laboratory of Analytical Toxicology*
Institute of Health Sciences
Universidade Feevale
Novo Hamburgo-RS, Brazil
Tel/Fax: +555135868800, +5551999873090
E-mail: rafael.linden@feevale.br

ABSTRACT

Background: Irinotecan (IRI) is a widely used chemotherapeutic drug, used for first-line treatment of colorectal and pancreatic cancer, with doses usually established based on patient's body surface area. Toxic and therapeutic effects of IRI are also due to its active metabolite SN-38, reported to be up to 100 times more cytotoxic than IRI. SN-38 is detoxified by the formation of SN-38 glucuronide, through UGT1A1. Genetic polymorphisms in the *UGT1A1* gene are associated to higher exposures to SN-38 and severe toxicity. Pharmacokinetic models to describe IRI and SN-38 kinetic profiles are available, with few studies exploring pharmacokinetic and pharmacogenetic-based dose individualization. The aim of this manuscript is to review the available evidence supporting pharmacogenetic and pharmacokinetic dose individualization of IRI. **Methods:** The PubMed database was searched, considering papers published in the period from 1995-2017, using the keywords irinotecan, pharmacogenetics, metabolic genotyping, dose individualization, therapeutic drug monitoring, pharmacokinetics and pharmacodynamics, either alone or in combination, with original papers being selected based on the presence of relevant data. **Conclusions:** The findings of this review confirm the importance of considering individual patient characteristics to select IRI doses. Currently, the most straightforward approach for IRI dose individualization is *UGT1A1* genotyping. However, this strategy is sub-optimal due to several other genetic and environmental contributions to the variable pharmacokinetics of IRI and its active metabolite. The use of dried blood spot sampling could allow the clinical application of complex sampling for the clinical use of limited sampling and population pharmacokinetic models for IRI doses individualization.

Keywords: irinotecan, SN-38, pharmacokinetics, pharmacogenetics, dose individualization.

INTRODUCTION

Irinotecan (IRI, 7-ethyl-10-[4-(1-piperidino)-1-piperidino]carbonyloxycamptothecin) is a pentacyclic semisynthetic derivative of the alkaloid camptothecin, which is isolated from the barks of the Chinese tree Camptotheca acuminate [1–3]. IRI is a topoisomerase I inhibitor used either alone or in combination with other chemotherapeutic agents as the first line in the treatment against colorectal [3,4] and pancreatic cancer [3,5]. IRI also has antitumor activity in other solid tumors, such gastro-esophageal [6] and ovarian [7].

The recommended doses of IRI are selected on body surface area (BSA). When monotherapy is adopted, IRI doses range from 50 to 350 mg/m^2, depending on regimen or dosing schedule. In combined chemotherapy with other agents, IRI doses usually are comprised between 180 and 240 mg/m^2. Other associated therapies were approved for concomitant treatment with IRI, such as monoclonal antibodies and angiogenesis inhibitors [8,9].

IRI is a prodrug converted in the liver by carboxylesterases (CES) to 7-ethyl-10-hydroxycamptothecin (SN-38) which is more active and cytotoxic than its parent drug [10]. Treatment with IRI is usually associated with dose-limiting toxicities, mainly diarrhea and neutropenia/leukopenia [11–13]. The occurrence of severe toxicity due to IRI is dependent of the specific regimen and dosage schedule, also being affected by clinical variables such as age, body weight, gender, and co-medication, as well as pharmacogenetic variations [8,12].

Besides being an approved drug by the Food and Drug Administration (FDA) for more than twenty years, IRI has recently gained renewed interest due to results showing an extended survival of pancreatic cancer patients treated with a new nanolipossomal formulation when compared to standard chemotherapy [14]. The observed relation between exposure to IRI and its principal active metabolite SN-38 to its clinical effects, both for the classical [15] and the new nanolipossomal formulation [16], suggest this drug can be a candidate for therapeutic drug monitoring (TDM), based on either pharmacogenetic or pharmacokinetic approach.

Considering the clinical relevance of IRI and the potentialities of dose individualization, this manuscript aims to review relevant information on the pharmacology of IRI, with a particular focus on data pertinent to dose individualization. For this purpose, the PubMed database, considering papers published in the period from 1995-2017, was searched using the keywords irinotecan, pharmacogenetics, metabolic genotyping, dose

individualization, therapeutic drug monitoring, pharmacokinetics and pharmacodynamics, either alone or in combination.

PHARMACODYNAMICS

IRI anticancer activity is based on the inhibition of topoisomerase I [17], which is an enzyme involved in all transactions of DNA (replication, transcription, recombination, and DNA chain repair) [18]. During the cell division process, the DNA double helix is opened into two singles strands to serve as templates [18]. Topoisomerase I is responsible by catalyzing the relax supercoiled DNA and alleviate the DNA helical constraints to restore the integrity to the DNA double helix [18,19]. During the action of topoisomerase I, DNA damages, mutations and cell death may occur. In fact, levels of the topoisomerase I are found to be elevated in several types of lymphoma, leukemia, and colon carcinoma cells [19].

IRI and its active metabolite SN-38 induce cytotoxicity and cause apoptosis [20]. Both inhibit topoisomerase I by binding to the DNA-topoisomerase I complex and blocking the re-ligation of the DNA double helix [17]. This process involves the non-covalent bound between IRI and SN-38 with the DNA-topoisomerase I complex [18]. Indeed, this complex formed by IRI and SN-38 with DNA-topoisomerase I inhibit tumor growth [21]. The IRI rings intercalate DNA, simulating a DNA base pair at the site of cleavage. The E ring is the most activated moiety of the IRI; its lactone carbonyl interacts with 2 hydrogen bonds with arginine site (Arg364) of the topoisomerase I and the hydroxyl group of C-20 position increase hydrogen bond at aspartic acid (Asp533) of the polypeptide chain. The ethyl substitution at C-7 facilitates reaction with DNA due to increased lipophilicity, leading to more significant cytotoxicity and higher chemical stability in human plasma [22].

Associated with its anticancer activity, toxicities of IRI can be severe and may cause morbidity, treatment delay and rare cases of death. The principals side effects observed in use of IRI are massive diarrhea (by intestinal toxicity) and neutropenia (by myelosuppression) [23,24]. Other observed adverse effects are fatigue and vomiting [23]. On the other hand, IRI generates high oxidative stress levels [25], that may contribute to the drug toxicity and lead to normal cellular functions failure [24,26].

PHARMACOKINETICS

The pharmacokinetics of IRI and its main metabolites was extensively investigated, with mean population pharmacokinetic parameters being presented in table 1. Mean peak IRI maximum concentrations (C_{max}) is generally observed at the end of the 90 min infusion. SN-38 C_{max} is reached within one hour after the end of the IRI infusion and is about 25% of the corresponding IRI C_{max} [27]. IRI plasma concentrations can be described using a three-compartment model and that of SN-38 with a two-compartment model, with first-order formation of SN-38 from IRI [28,29]. Disposition of SN-38G can be described with an one-compartment open model with first-order formation from SN-38 [29]. The mean terminal half-life ($t_{½}$) varies from 6.2 to 14.6 h for IRI, from 10.6 to 28.5 h for SN-38 and from 10.9 to 35.5 h for SN-38G. IRI volume of distribution at steady-state (VD_{ss}) ranges from 84 to 297 L/m^2, and the total body clearance is 12.4 to 17.5 L/h/m^2 (Table 1) [27–38].

The lactone ring of IRI and SN-38 is chemically unstable and can be hydrolyzed to the inactive carboxylate form. Only the closed lactone forms of the drug inhibit topoisomerase I. The rate of hydrolysis is dependent on pH, ionic strength and protein concentration [39]. In solutions at pH 3–5, the lactone form is stable, whereas at basic pH it rapidly converts into the carboxylate form [40]. Quantification of total forms of IRI and SN-38 has substantially the same clinical relevance as monitoring the lactone forms of the two analytes, because the pharmacokinetics of total IRI and total SN-38 are significantly correlated with those of lactone forms [39].

Table 1. Mean pharmacokinetics parameters of IRI, SN-38 and SN-38G.

No. of patients	Regimen	Dose (mg/m^2)	IRI time of infusion (min)	IRI				SN-38		SN-38G		Ref.
				$t_{½}$ (h)	AUC (mg x h/L)	VD_{ss} (L/m^2)	CL ($L/h/m^2$)	$t_{½}$ (h)	AUC (mg x h/L)	$t_{½}$ (h)	AUC (mg x h/L)	
107	IRI	33-750	30	10.8	-	150	14.3	10.6	-	-	-	[30]
47	IRI	350	30	-	24.8	-	15.2	-	0.50	-	-	[31]
26	FOLFIRI	100	90	6.0	-	153	16.6	12.7	-	-	-	[32]
10	IRI/cisplatin	200	90	13.5	-	138	14.0	23.8	-	-	-	[33]
34	FOLFIRI	240-340	90	12.4	21.5	123	13.0	21.1	0.72	18.3	2.28	[34]
45	IRI/cisplatin	175-300	90	12.1	-	151	17.5	22.5	-	-	-	[35]
8	FOLFIRI	125[a]	90	14.6	8.8	297	12.4	28.5	0.40	35.5	1.74	[36]
56	IRI	125-325	90	7.2[b]	15.1	146	14.0	13.4[b]	0.43	12.7[b]	1.77	[27]
78	IRI	100-340	90	14	-	152	14.6	24.3	-	-	-	[29]
3	IRI	180	90	10.1	11.9	-	15.6	25.3	0.30	22.2	1.49	[37]
74	FOLFIRI	180-225	90	11.5	14.9[c]	230	14.5	32.2	0.42 [c]	-	-	[28]
6	IRIS	125	120	6.6	9.8	86	12.5	13.7	0.15	13.2	1.03	[38]
12	FOLFIRI	150	90	6.2	11.0	84	13.3	11.0	0.27	10.9	0.98	[38]

[a] Dose (14C), mg/m^2. [b] Harmonic mean half-life.[c] Normalized to a 330 mg administered dose.
AUC: Area under the curve; CL: clearance; FOLFIRI: irinotecan plus 5-fluoururacil (continuous infusion) and leucovorin; IRI: Irinotecan; IRIS: irinotecan plus S-1; $t_{½}$: mean terminal half-life; VD_{ss}: volume of distribution at steady-state.

IRI is converted into its active metabolite SN-38 by the action of CES of the liver (Figure 1). SN-38 is 100 to 1,000 times more cytotoxic than IRI. SN-38 is metabolized by uridine diphosphate glucuronyltransferase (UGT) to form SN-38G, an inactive glucuronide, especially by UGT1A1 [41,42]. IRI is also metabolized by CYP3A4 in several inactive metabolites, including 7-ethyl-10-[4-N-(5-aminopentanoic acid)-1-piperidino]-carbonyloxycamptothecin (APC) and 7-ethyl-10-(4-amino-1-piperidino)-carbonyloxy-camptothecin (NPC) [43]. IRI is also biotransformed to a lesser extent by CYP3A5 in APC and NPC metabolites [44]. The variable activity of these metabolizing enzymes is associated to differences in systemic exposure to the active metabolite SN-38 [45,46].

Figure 1. Metabolic pathways of IRI.

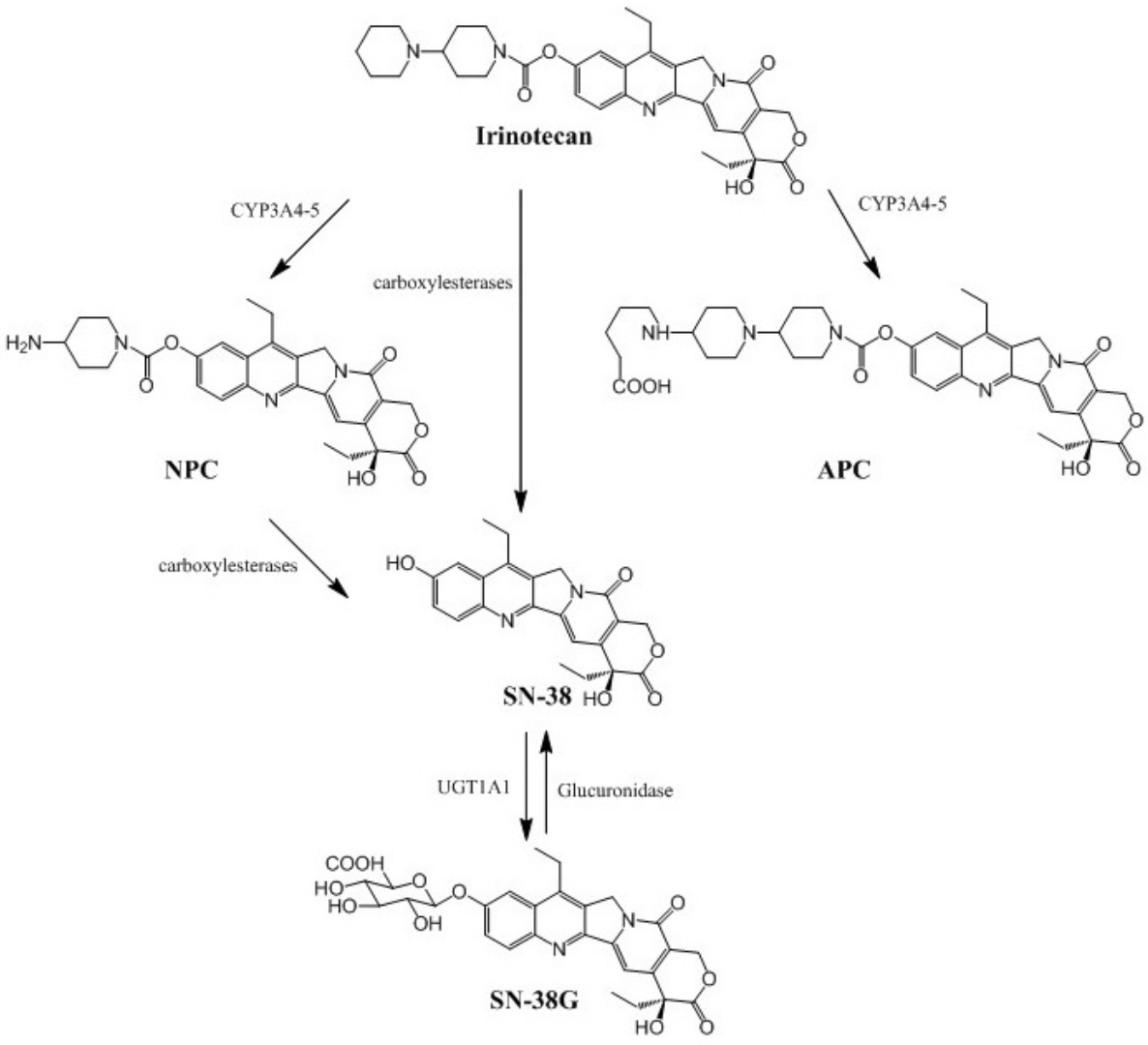

In humans, human hepatic CES (hCE1) and human intestinal CES (hiCE) present significant ability to hydrolyze IRI into SN-38. Despite the higher affinity of hiCE to IRI [47,48], hCE1 is responsible for up to 50% of the total formation of SN-38 due to its higher concentration in the liver [49]. On the other hand, in the human duodenum, jejunum, ileum and kidney, where the expression of hCE1 is very low, more than 99% of the conversion of IRI to SN-38 is mediated by hiCE [49]. In addition, analysis of lung microsomal extracts indicated that IRI activation was more efficient in samples obtained from smokers, suggesting that exposure to tobacco increases the activity of CES. Overall, the study by Hatfield *et al.* [49], showed that hCE1 plays a significant role in IRI hydrolysis, even though it is up to 100-fold less efficient in converting IRI to its active metabolite than hiCE. Moreover, membrane transporters are responsible for the uptake of SN-38 from plasma into hepatocytes like organic anion-transporting polypeptides (OATP), which mediate the hepatic uptake of several drugs, thus defining their clearance. Impaired hepatic clearance due to low activity polymorphisms in human *OATP1B1* gene may increase systemic exposure to SN-38 [50]. ABC transporters including ABCB1, ABCC1, ABCC2, and ABCG2 regulate the hepatic and biliary efflux of SN-38 and SN-38G [51]. Polymorphisms of *SLCO1B1*, *ABCB1*, and *ABCC2* genes have recently been associated with significant impact on the pharmacokinetics and pharmacodynamics of IRI and SN-38 [52,53].

SN-38 is the main responsible for the antitumor response of IRI, and also for the dose-limiting toxicities, namely neutropenia and diarrhea [31,54]. Diarrhea is related to concentrations of SN-38 at the intestinal lumen resulting from the biliary excretion of SN-38, and potentially enhanced by the intraluminal conversion of SN-38G to SN-38 by bacterial glucuronidases [55]. The wide interindividual variability in tolerability with occurrence of severe toxicity is partially related to interindividual pharmacokinetic and pharmacogenetic differences, especially in glucuronidation of the active metabolite through the action of UGT. Consequently, large differences in exposure to the drug and its active metabolite, evaluated trough area under the curve (AUC), are observed [54,56].

CYP3A enzyme activity (mainly 3A4) also significantly influences plasma concentrations and the occurrence of toxicity in IRI treatment [43]. IRI is detoxified by CYP3A4 to APC, which has no known pharmacological activity [55]. CYP3A4 also produces NPC, being further transformed into SN-38 by liver CES. Other 4 minor metabolites, called M1 up to M4, were identified in urine samples of patients receiving IRI and *in vitro* studies demonstrated that, with some differences of the metabolic profile, CYP3A4 and CYP3A5 isoforms contributes to their formation from IRI [44]. Moreover, authors have found that

AUC of SN-38 or the ratio between AUC of SN-38G to AUC of SN-38 is associated with neutropenia after IRI administration [31,57]. These findings support that IRI and SN-38 pharmacokinetics is as important as *UGT1A1* gene polymorphism assay in predicting IRI related toxic effects.

The plasma protein binding of IRI and SN-38 was reported as 65 and 95%, respectively. The AUC of both increase proportionally to the administered dose, although interpatient variability is important. SN-38 plasmatic levels are about 100 fold lower than corresponding IRI concentrations [58].

After i.v. infusion of 125 mg/m^2 of IRI, fecal excretion represents 63.7%, whereas urinary excretion accounted for 32.1% of the administered dose. IRI is the major elimination product in urine, feces, and bile. APC and SN-38G were the most significant metabolites in urine and bile, whereas SN-38 and APC were the most significant metabolites in feces. The relatively higher amount of SN-38 in feces compared with bile is probably due to hydrolysis of SN-38G to SN-38 by bacterial β-glucuronidases [36].

Nanoliposomal irinotecan (nal-IRI) is a liposomal formulation with a longer half-life ($t_{1/2}$), higher total plasma IRI concentration, and lower SN-38 maximum concentration (C_{max}) compared with nonliposomal IRI. Nal-IRI formulation (MM-398, PEP02, BAX2398) is used as intravenous injection, being designed to combine the properties of long plasma circulation and increased delivery of IRI to tumor lesions via the enhanced permeability and retention effect, creating a local depot for drug release [16]. The clinical pharmacokinetics of nal-IRI was previously compared with those of nonliposomal IRI in a phase II study in patients with gastric cancer [59]. Results showed that compared with IRI 300 mg/m^2 every 3 weeks, nal-IRI 100 mg/m^2 every 3 weeks had a total IRI C_{max} 13.4-times higher, $t_{1/2}$ 2.0 times longer, and $AUC_{0-\infty}$ 46.2-times higher. The $t_{1/2}$ and $AUC_{0-\infty}$ of SN-38 were also increased relative to nonliposomal IRI (3.0- and 1.4-times, respectively), while maintaining a 5.3-times lower SN-38 C_{max} [59]. In a phase 3 trial, Wang Gillam *et al*. [14] showed an extended survival of pancreatic cancer patients treated with a nal-IRI formulation in combination with fluorouracil and folinic acid when compared to standard chemotherapy. Adiwijaya *et al*. [16] results support the benefit of nal-IRI dose of 70 mg/m^2. These results indicate the potential benefit in extending duration of plasma and tumor exposure via liposomal encapsulation.

PHARMACOGENETICS

Several studies focused on IRI pharmacogenetic have identified specific inherited differences in glucuronidation capacity that influence drug exposure and outcomes, as this reaction is critical to SN-38 detoxification [52,60–76]. The interindividual variability on IRI pharmacokinetics has been attributed mostly to genetic variations in the *UGT1A1* gene, which encodes for UGT1A1, a strategic enzyme in IRI metabolism [72]. To date, approximately 100 polymorphisms of the *UGT1A1* gene have been identified [77]. Allelic variations in the gene promoter and its 5 exons are known to decrease the enzyme activity, leading to constitutional unconjugated Gilbert's syndrome [60,78].

The wild type (wt) allele *UGT1A1*1* contain six thymine–adenine (TA) repeats in the promoter region (TATA box), while a higher number of repeats is associated to reduced transcription rate and lower enzyme level. The *UGT1A1*28* variant allele has seven TA repeats (A(TA)7TAA), resulting in about 30% of the activity from the functional enzyme. As a consequence, patients with the *UGT1A1*28/*28* genotype might glucuronidate SN-38 less efficiently than the carriers of at least one wt allele (*UGT1A1*1/*28* or **1/*1*) [9].

The allele frequency of *UGT1A1*28* is higher in Caucasians (30 to 39%) and African-American (35 to 45%) than in Asians (6.8 to 13% in Japanese and Koreans). In contrast, the *UGT1A1*6* allele is relatively common in Asians (1.3 to 24% in Japanese and Korean), while in Caucasians its occurrence is unusually low (<1.0%) [79].

As displayed in table 2, carriers of the *UGT1A1*28* allele have consistently shown lower glucuronidation ratio, with decreased SN-38G to SN-38 ratio [52,62,68,69,74] and higher biliary index, expressed as [(IRI AUC) x (SN-38 AUC/SN-38G AUC)] [68]. Because of the higher systemic exposure to the SN-38 metabolite, patients with impaired UGT metabolism are at higher risk of developing drug-induced toxicity. Although a few studies have been partly conflicting [63,65,71] most of them have found a significant association between the *UGT1A1*28* polymorphism and severe neutropenia [62,64–70] and/or diarrhea [60,67]. Similar results were found for the *UGT1A1*6* polymorphism in Asians, indicating a central role of the variant allele in this ethnic population. A Japanese study showed a significant association of the allele **6* with reduced glucuronidation ratio and severe neutropenia [69]. In Koreans, the homozygous variant genotype was an independent predictor of SN-38 plasma exposure and grade IV leukopenia [75]. In another hand, the *UGT1A1*6* was associated with grade III/IV diarrhea, but not with severe neutropenia in Chinese [65].

Table 2. Summary of IRI pharmacogenetic studies.

Gene	Population	Chemotherapy	Type of Cancer	Allele	Main Findings		Ref.
					Association with irinotecan exposure	**Association with outcomes (Toxicity and/or response)**	
UGT1A1	Japanese N=118	IRI (n=35) IRI/ platinum (n=58) IRI/other (n=25)	Small cell lung (n=21) Non-small cell lung (n=65) Colorectal (n=21)	*UGT1A1 *6, *7, *27, *28, *29*	-	*UGT1A1*28* was a significant predictor of severe toxicity (OR: 7.23, P<.001) No significant association of *UGT1A1*6* with the occurrence of severe toxicity (OR: 0.55; P>.2)	[60]
UGT1A1	North American N=20	IRI	Lung (n=7) Colonrectal (n=4) Esophageal (n=2) Liver (n=2) Other (n=5)	*UGT1A1 *28*	SN-38G/SN-38 AUC ratios were inversely correlated with the number of *28* alleles (P=.001)	More severe grades of diarrhea and neutropenia were observed only in patients with *28 allele, however not statistically significant	[61]
UGT1A1	North	IRI	Lung (n=19)	*UGT1A1 *6, *27, *28,*	SN-38 AUC was directly	*UGT1A1*28/*28* higher frequency	

	American N=65		Gastroesophageal (n=14) Colorectal (n=10) Other (n=23)	**60, *93*	correlated with number of **28* alleles (P=.03) SN-38G/SN-38 AUC ratios were inversely correlated with the number of **28* alleles (P=.03) **28* allele showed no impact on SN-38G AUC	(P=.001) and risk of grade 4 neutropenia (RR: 9.3, 95% CI: 2.4-36.4) **93* allele and the SN-38 AUC were significant predictors of ANC nadir; (r^2= 0.51, p<.0.01)	[62]
UGT1A1	European N=95	IRI (n=12) FOLFIRI (n=56) IRI/ tomudex (n=9) IRI/5-FU (n=18)	Colorectal	*UGT1A1 *28*	-	No relationship was found between the *UGT1A1*28* genotypes and infection, nausea or mucositis In a multivariate analysis, the genotype was not related to clinical response or to OS.	[63]
UGT1A1	North American N=520	IFL (n=114) IROX (n=107) FOLFOX (n=299)	Colorectal	*UGT1A1 *28*	-	*28/*28 genotype was associated with grade 4 neutropenia (IROX, P=.004; and all patients, P=.007) and grade 3 febrile neutropenia (IROX, P=.006) No association was seen between *UGT1A1* and diarrhea, tumor	[64]

						response, TTP, or OS	
UGT1A1	Chinese N=167	FOLFIRI (n=101) IRI /monoclonal antibody (n=30) IRI/ raltitrexed (n=18) XELIRI (n=18)	Colorectal	*UGT1A1 *6, *28*	-	*UGT1A1*28* and **6* were associated with severe diarrhea (OR: 3.56, P=.01, and OR: 4.19, P=.003, respectively) No significant association of *UGT1A1* 28 or *6* with the occurrence of severe neutropenia No significant differences of either response rate or PFS were found among different genotypes	[65]
UGT1A1	Israeli N=329	FOLIFIRI (n=125) IFL (n=135) XELIRI or TEGAFIRI (n=69)	Colorectal	*UGT1A1 *28*	-	Grade 3-4 hematological toxicity was higher in **28/*28* carriers (48%) compared with **1/*28* (10.2%) and *1/*1 (7.7%) (P < .001) Median OS was worse in the **28/*28* (1.6 *vs* 2.0, and 2.4 years, respectively; P < .01)	[66]
UGT1A1	Chinese	IRI/ platinum	Small-cell lung	*UGT1A1 *6, *28*	-	Higher incidence of severe thrombocytopenia in **28* carriers	[67]

	N=67					(P=.017) Patients *UGT1A1*6/*28* were prone to suffering severe delayed diarrhea and neutropenia (P<.05) None of the genotypes associated significantly with OS	
UGT1A1	Italian N=250	FOLFIRI	Colorectal	*UGT1A1*28*	*UGT1A1*28/*28* showed higher biliary index [irinotecan AUC) x (SN38 AUC/SN38G AUC)] (P=.007) and lower glucuronidation ratio (SN38G AUC/SN38 AUC) (P=.01)	*UGT1A1*28/*28* was associated with higher risk of severe hematologic toxicity (OR: 8.63, P=.02) and higher response rate (OR:0.32, P<.05)	[68]
UGT1A1 ***UGT1A7*** ***UGT1A9*** ***UGT1A10***	Japanese N=177	IRI (n=56) IRI / platinum (n=72) IRI /5-FU (n=36) IRI /other (n=13)	Lung (n=81) Colon (n=63) Stomach (n=19) Other (n=14)	*UGT1A1*6, *27, *28, *60* *UGT1A7*2, *3, *4* *UGT1A9*22, *T11, *141C, *4, *5* *UGT1A10*2T, *2, *67G, *3*	*UGT1A1*6* and **28* carriers had reduced SN-38G/SN-38 AUC ratios (P<.001), with a gene dose effect (median 5.55, 3.62, and 2.07 for 0, 1, and 2 haplotypes, respectively, P < .0001)	*UGT1A1*6* and **28* were associated with severe neutropenia (P<.0001)	[69]

UGT1A1 ***UGT1A7*** ***UGT1A9***	Spanish N=149	FUIRI FOLFIRI	Colorectal	*UGT1A1*28,* *UGT1A9*22* *UGT1A7*3*	-	*UGT1A1*28/*28* was predictive for haematologic toxicity (OR=6.27, P=0.04), specifically for neutropenia alone (OR=6.40, P=.038) or together with diarrhea (OR=18.87, P=.008) *UGT1A9*1/*1* was associated with non-haematologic toxicity (OR=2.70, P=.035) None of the genotypes were significantly associated with treatment response	[70]
UGT1A1 ***UGT1A7*** ***UGT1A6***	North American N=67	XELIRI	Colorectal	*UGT1A1 *28, *36* *37* *UGT1A7 *2, *3, *4* *UGT1A6 *2,*3, *4* *UGT1A9 *1B*	-	*UGT1A7*2/*2* and *UGT1A7*3/*3* genotypes were associated with improved efficacy (P=.013) and reduced toxicity (P=.003) *UGT1A9*1B* genotype was associated with increased response (P=.047) and reduced toxicity (P=.002)	[71]

						UGT1A1 genotypes was not associated with efficacy and toxicity	
UGT1A1 ***UGT1A7*** ***UGT1A6*** ***UGT1A9***	Canadian N=167	FOLFIRI (n=98) FOLFIRI/ monoclonal antibody (n=69)	Colorectal	*UGT1A1 *28,* *UGT1A7 *3* *UGT1A6 *2* *UGT1A9 -1212, -688, -440*	-	*UGT1A1*28* was associated with a higher risk of severe neutropenia (OR: 2.43, P=.004) Other variations associated with increased risk of severe neutropenia *UGT1A9 -688* (OR: 5.65, P=.028), *UGT1A7*3* (OR: 2.00, P=.025) and *UGT1A6 *2* (OR: 3.55, P=.017)	[72]
UGT1A1 ***UGT1A6*** ***CYP2A6***	Korean N=43	IRI/oxaliplatin	Colorectal	*UGT1A1 *6, *28, *60* *UGT1A6 *2* *UGT1A7 *3* CYP2A6 *4, *7, *9	-	There was no significant relationship between haematologic toxicities and genotypes *UGT1A1*60* and *CYP2A6* variant alleles had significantly poorer response rates (OR:0.16, P=.043, and OR: 0.2, P=.049, respectively) None of the genotypes associated significantly with PFS.	[82]
UGT1A1	North	IRI	NI	*UGT1A1 *6, *27, *28,*	*UGT1A1*28, *60*, *93* and	*UGT1A1*28*, *60* and *93* were	[52]

UGT1A7 ***UGT1A9*** ***CYP3A4*** ***CYP3A5*** ***HNF1A*** ***CES2*** ***SLCO1B1*** ***ABCB1*** ***ABCG2*** ***ABCC1*** ***ABCC2***	American N=85	**60, *93* *UGT1A7*4, 387T>G, 391C>A, 392G>A* *UGT1A9 *1B, _275T>A, _2152C>T* *CYP3A4*1B* *CYP3A5*3* *HNF1A 79A>C* *CES2 -363C>G, IVS1+1361ª>G, 108C>G* *SLCO1B1 *1b,*5* *ABCB1 3435C>T, 2677G>A/T, IVS14 +38A>G, IVS13+24C>T, 1236C>T, IVS9-44A>G* *ABCG2 34G>A, 421C>A,*	*UGT1A7*4* were associated with decreased SN-38G/SN-38 AUC ratios (P<.0001, P=.004, P=.001, and P=.011, respectively) *UGT1A1*28, *93, ABCB1 IVS9 -44A>G,* and *ABCC1 1684T>C* were associated with increased SN-38 AUC (P=.002, P=0.002, P=.03, P=.032, respectively) *ABCC2 3972C>T* was associated with increased SN-38G AUC (P<.001)	associated with decreased in ANC nadir (P<.001, P=.016 and P<.001, respectively) *ABCC1 IVS11 -48C>T* and *SLCO1B1*1b* were associated with decreased in ANC nadir (P=.002 and P=.034, respectively)

				ABCC1 1684T>C, IVS11 -48C>T *ABCC2 3972C>T*			
UGT1A1 ***CES1*** ***CYP3A4*** ***CYP3A5*** ***ABCB1*** ***ABCG2*** ***ABCC2*** ***ABCC5*** ***SLCO1B1*** ***SLCO1B3***	Canada N=127	IRI (n=8) FOLFIRI/ bevacizumab (n=85) FOLFIRI (n=19) FOLFIRINOX (n=14)	Colorectal (n=107) Pancreatic (n=13) Other (n=7)	*UGT1A1*28* *CES1 14506G>A, 27467A>C* *CYP3A4*22* *CYP3A5*3* *ABCB1 3435C>T* *ABCG2 421C>A, 34G>A* *ABCC2 24C>T, 1249G>A* *ABCC5 T>C* *SLCO1B1*1b, *5* *SLCO1B3 699G>A*	*SLCO1B1 521C* was associated with increased SN-38 exposure (P<.001), which was additive with *UGT1A1*28* (P<.001). *ABCC5 C* carriers and CYP3A5 expressers had reduced SN-38G plasma concentrations (P<.001) *ABCB1 3435TT* had lower irinotecan levels (P<.05)	*ABCC2–24CT* was associated with reduced risk of neutropenia (OR:0.22, P<.05) and *CES1 27467A* with reduced risk of diarrhea (OR:0.29, P<.05) CYP3A5 expressers had higher-grade oral mucositis (OR:8.10, P<.05) *PFS* was longer in *SLCO1B1 *1b/*1b* patients (HR: 1.6, P<.05) and reduced in *ABCC2–24TT* (HR: 0.62, P<.05) and *UGT1A1*28* (HR: 0.60, P<.05) carriers Higher *OATP1B3* tumour expression was associated with reduced PFS.	[74]
UGT1A1 ***ABCB1***	Swedish and Norwegian	FOLFIRI (n=75) Lv5FU2-IRI (n=65)	Colorectal	*UGT1A1*28* *ABCB1 3435C>T,*	-	Increased risk of early toxicity: *ABCB1 3435 T/T* (OR: 3.79, P<.05)	[76]

	N=182			*1236C>T, 2677G>T/A*	and *UGT1A1*28/*28* (OR: 4.43, P<.05) *UGT1A1*28/*28* high risk of neutropenia (OR: 6.87, P<.05) *ABCB1 1236T-2677T-3435T* haplotype responded to treatment less frequently (43 vs 67%, P=0.027), and survived shorter time, OR: 1.56, P<.05).	
UGT1A1 ***UGT1A9*** ***ABCB1*** ***ABCC2*** ***ABCG2*** ***SLCO1B1*** ***CYP3A5***	Korean N=107	IRI	Non-Small Cell Lung Cancer	*UGT1A1 *6, *28* *UGT1A9*22* *ABCB1 3435C>T, 1236C>T, 2677G>T/A* *ABCC2 _24C > T, 1249G > A, 3972C> T* *ABCG2 34G > A, 421C > A* *SLCO1B1*1b 11187G>A,,521T>C*	Independent predictors of SN-38 plasma exposure: *UGT1A1*6/*6* (P< .0001), *UGT1A9*1/*1* or **1/*22* (P =.011), and *SLCO1B1 521TC* or *CC* (P =.017) variants	Independent predictors of grade 4 neutropenia *SLCO1B1* 521TC or TT (OR: 3.8, P=.007) and *UGT1A1*6*/*6 (OR: 7.4, P=. 028) Independent predictors of grade 3 diarrhea *UGT1A9*1/*1* (OR: 6.3, P=. 024), *ABCC2 3972CC* (OR: 5.6, P=.0041) and *ABCG2 34GA* or *AA* (OR 5.1, P=.038)	[75]

				*CYP3A5 *3*			
CES1A	Japanese N=58	IRI		*CES 1A1, 1A2, 1A3, var1A1*	The median [(SN-38 + SN-38G)/IRI] AUC ratio of patients having three or four functional CES1 genes was 1.24-fold of that in patients with two functional CES1 genes (0.31 *vs*. 0.25, P =.0134)	Incidence of severe neutropenia was not significantly influenced by the number of functional CES1 genes (50% for four genes and 16% for two or three genes, P =.09).	[84]
ABCB1 ***ABCC2*** ***ABCG2*** ***SLCO1B1***	Japanese N=117	IRI (n=55) IRI/cisplantin (n=62)	Lung (n=79) Colon (n=28) Other (n=10)	*ABCB1 -1789G>A, 2677G>T/A, IVS27-182G>T* *ABCC2 3972C> T, -1774delG* *ABCG2 34G > A, 421C > A* IVS12 + 49G>T *SLCO1B1*1b, 521T>C*	Higher SN-38 AUC values were observed in ABCB1 2677G>T (P=.008)	Associations of grade 3/4 neutropenia were observed with *ABCC2 -1774delG (P=.014)* and *ABCG2 421C>A, IVS12 + 49G>T* (P=.042) in the IRI monotherapy	[53]
ABCB1 ***ABCC2*** ***ABCG2***	Korean N=107	IRI/cisplatin	Non-Small Cell Lung Cancer	*ABCB1 3435C>T* *ABCB1 1236C>T* *ABCB1 2677G>T/A*	*ABCB1 3435TT* and *2677TT* were associated with SN-38G AUC and CL *ABCB1 2677TT/3435TT*	*ABCB1 2677GG* was associated with grade 4 neutropenia (P=.03) and *3435TT* with grade 3 diarrhea (P =.047).	[83]

				ABCC2 _24C > T *ABCC2 1249G > A* *ABCC2 3972C > T* *ABCG2 34G > A* *ABCG2 421C > A*	haplotypes showed significantly lower SN-38G AUC (P=.006), whereas *2677GG/3435CC* carriers showed significantly higher SN-38 AUC (P =.039).	In tumor response, *ABCC2 _24TT* and *3972TT* genotypes were associated with higher response rates (P =.031 and, P= .046, respectively) and longer progression-free survival (P =.035 and .038, respectively)	
ABCB1 ***ABCC1*** ***ABCC2*** ***ABCG2*** ***SLCO1B1***	Italian N=250	FOLFIRI	Colorectal	Several single nucleotide polymorphisms and haplotypes for each evaluated gene	None of the variants were seen to be associated with IRI PK (evaluation of 71 patients)	*ABCG2 –15622C>T* was associated with lower tumor response rate (OR: 0.48, P=.0087) *ABCB1 2677T* polymorphism improved patient OS (P=.007) but not response rate. *ABCG2 rs7699188* was associated with severe non-hematological toxicity (OR: 15.15, P=.001) and higher tumor response rate (OR: 2.23, P=.0071) None of the tested *ABC/SLC* genetic markers were associated with TTP (P<.01)	[85]

						ABCB1 2677 G> T was the only polymorphism significantly associated with the OS (P=.0074)	
SLCO1B1 ***SLC19A1***	Chinese N=137	FOLFIRI (n=104) XELIRI (n=33)	Colorectal	*SLCO1B1*1b* *SLCO1B1*5* *SLC19A1* 80G>A	-	*SLCO1B1*1b* and *SLC19A1 GG* genotypes were associated with a higher rapid response rate (OR =3.58, P=.011 and 3.521, P=.013, respectively) *SLCO1B1*1b* was an independent prognostic factor of longer PFS (HR=0.40, P=.037)	[102]
SLCO1B1	Asian N=71	IRI	Nasopharyngeal (n=28) Gastrointestinal (n=33) Other (n=10)	*SLCO1B1*1a, *1b, *5, *15*	IRI CL was 3-fold lower in **15* carriers than in patients with the reference genotype **1a/*1a* (9.57± vs. 28.86 l/h/m^2; P=.001) IRI AUC normalized by dose and BSA were higher in **15* carriers compared to *1a/*1a patients (39.27 *vs* 17.32, P=.003)	-	[103]

ANC: absolute neutrophil count; AUC: area under the curve; BSA: body surface area; CL: clearance; FOLFIRI: irinotecan plus 5-fluoururacil (continuous infusion) and leucovorin; FOLFIRINOX: irinotecan plus 5-fluoururacil; leucovorin and oxaliplatina; FUIRI: irinotecan plus high-dose 5FU; HR: hazard ratio; IFL: irinotecan plus fluorouracil and leucovorin; IRI: Irinotecan; Lv5FU2-IRI: irinotecan plus leucovorin and fluorouracil (bolus + continuous infusion) and irinotecan; NI: not informed; OR: odds ratio; OS: overall survival; PK: pharmacokinetic; PFS: progression-free survival; RR: relative risk; SN-38: 7-ethyl-10-hydroxycamptothecin; SN-38G: SN-38 glucuronide (10-O-glucuronyl-SN-38); TEGAFIRI: iriniteca plus tegafur/uracil oral leucovorin; TTP: time to tumor progression; XELIRI: irinotecan plus capecitabine.

Moreover, the association of the *UGT1A1*28* and **6* polymorphisms with an increased chance of developing diarrhea and neutropenia was validated by meta-analysis. This relationship persists for neutropenia regardless of IRI dose; however, it is not significant for diarrhea in patients receiving low-doses [80]. In contrast, most of the studies on patients' clinical responses to IRI chemotherapy found no significant association of the *UGT1A1*28* and **6* polymorphisms with any change in response rate [64,65,70,71,81], time to progression [64], progression-free or overall survival [63–65,68,81,82].

Since the UGT1A7 and UGT1A9 enzymes mediate to some extent the inactivation of SN-38, it has been suggested that the *UGT1A7* and *UGT1A9* genes polymorphisms might be associated with IRI toxicities as well [70,71,75]. Although UGT1A9 is highly expressed in human liver, UGT1A7 is present in extrahepatic tissues and is most likely to be relevant to the SN-38 enterohepatic circulation. Additionally, recent studies suggest that a combined signature of the haplotypes of *UGT1A1*, *UGT1A7*, and *UGT1A9* could provide more precise information on IRI pharmacogenetic, rather than individual SNPs [69,83].

As the *UGT1A* genotypes explain only part of the IRI treatment variability, interest has turned to other polymorphisms. Genes encoding transporters and other enzymes involved in IRI pharmacokinetic have, somewhat, been considered for association with drug exposure and outcomes (Table 2). The CYP3A4 and CYP3A5 enzymes mediate the formation of APC and NPC, other quantitatively abundant inactive metabolites of IRI, whereas the hCE1 (CES1 gene family) and hiCE (CES2 gene family) are responsible for the conversion of IRI to its active metabolite SN-38. There is only a limited number of pharmacogenetic studies concerning the impact of these genes polymorphisms on IRI therapy, with inconsistent results [52,74,75,84]. In a Japanese study [84] the incidence of severe neutropenia was not significantly influenced by the number of functional CES1 genes. Likewise, the *CES2* and *CYP3A4/5* variant genotypes showed no association with drug-induced toxicity in North Americans [52] and *CYP3A5* in Koreans [75]. In contrast, a Canadian study showed a significantly reduced risk of diarrhea in patients with the *CES1 27467A* variant, and more severe mucositis in *CYP3A5* expressers [74].

Studies on the transporter P-glycoprotein, encoded by the *ABCB1* gene, revealed conflicting results. There is some evidence that variant genotypes of *ABCB1* increase the bioavailability of IRI and SN-38 [53], while other studies showed opposite relation [74,83]. Data on toxicity and clinical outcomes are inconsistent as well. The wild-type *ABCB1 12677GG* was associated with severe neutropenia [83], whereas the variant *3435TT* was associated with diarrhea in Koreans [83], nausea/vomiting in Canadians [74] and increased

risk of early toxicity in Scandinavians [76]. The *ABCB1 1236T-2677T-3435T* variant haplotype responded to treatment less frequently and had shorter survived time in the Gimelius *et al*. [76] study. However, no difference in IRI pharmacokinetic, toxicity or clinical response was observed in an Italian study of *ABCB1* and IRI [85]. Polymorphisms in other transporters genes as *ABCC1*, *ABCC2*, *ABCG2* and the influx *SLCO1B1* have, to some degree, been associated with SN-38 exposure, toxicity and/or clinical outcomes [52,53,74,75,85] but the impact on IRI therapy remains unclear.

At present, the role of pharmacogenetic testing for *CYP3A4/5*, *CES*, and *ABC* and *SLCO1B1* transporters seems limited in elucidating the interindividual variability of IRI pharmacokinetic and treatment outcomes. Otherwise, due to the accumulated evidence on the increased risk for neutropenia, the *UGT1A1*28* polymorphism is a promising candidate for routine pretreatment genetic screening. Therefore, in 2005 the US FDA revised the package insert of Camptosar®, recommending a reduction in the starting dose by at least one level in **28/*28* carriers, but not for heterozygous patients. However, the precise dose reduction is unknown, and subsequent dose modifications should be considered based on individual patient tolerance to treatment [86]. Following the FDA recommendations, the Royal Dutch Association for the Advancement of Pharmacy [87] indicated a decrease of the theoretical dose by 30% in patients homozygous for **28* allele if dose >250 mg/m^2, then dose increase according to neutrophil count. The Association does not recommend changing the IRI dose for **1/*28* patients, because a reduction might result in under treatment.

Additionally, a recent review produced by a French joint workgroup comprising the Group of Clinical Onco-pharmacology (GPCO-Unicancer) and the National Pharmacogenetics Network (RNPGx), proposed a decision for *UGT1A1* genotyping depending on initially intended IRI dose. The French group recommended pretreatment *UGT1A1* genotyping (**28*,**36*,**37*) for all patients scheduled to receive an IRI dose ≥180 mg/m^2. For **28/*28* patients with scheduled doses between 180 and 230 mg/m^2 a 25 to 30% dose reduction at the first cycle is recommended, whereas a dose ≥240 mg/m^2 is contra-indicating in this genotyping group. In fact, the authors suggest that the administration of such intensified dose is only possible in **1/*1* and **1/*28* patients in the absence of additional risk factors and under strict medical observation [88].

In addition to the above recommendations, it is important to consider patient's ethnicity while performing a pharmacogenetic investigation. Given the high frequency and proven relation to IRI-induced toxicity, the evaluation of the variant **6* together with the **28* would be beneficial to Asians patients under IRI chemotherapy [69].

IRI DOSE INDIVIDUALIZATION STUDIES

Personalized dosing of drugs is a long-standing goal of clinical pharmacologists. IRI is an interesting drug for TDM due to its complex metabolism and increasing knowledge of its pharmacokinetic predictors, including genetic variations of drug metabolizing enzymes, drug transporters and tumor targets [55,56]. These new approaches should improve patient outcomes and prevent severe side effects by considering the pharmacologic profile of IRI in the individual patient into account, and could potentially replace dosing based only on body-surface area (BSA).

To date, only one study individualized IRI doses to reach a pharmacokinetic exposure target. Van der Bol *et al*. [15] evaluated the usefulness of an algorithm to calculate *a priori* an individual dose for IRI based on CYP3A4 phenotyping, through the determination of midazolam clearance. For the construction of the mathematical model, factors that could affect IRI clearance, such as demographic characteristics of the patients, pathophysiological factors and genetic variations involved in the metabolism of the drug were considered. There was a significant correlation between predicted and observed IRI clearance. The final IRI clearance equation took into account the patients' height, gamma-glutamyl transferase (GGT) activity and midazolam clearance [89]. The dose for patients was calculated by multiplying the predicted IRI clearance by 22.157 (µg x h/mL), which was the mean AUC of IRI observed in the study by Mathijssen *et al*. [89] which was arbitrarily assigned as the exposure target to IRI. The use of individual doses with the algorithm resulted in improved predictability in the pharmacokinetics and IRI toxicity profile compared to the dose calculated by BSA, reducing the incidence of severe neutropenia by more than four times (P = 0.013) [15].

UGT1A1 genotyping can identify patients at increased risk for myelosuppression owing to increased SN-38 exposure. In several studies, the variability of systemic exposure to SN-38 has been associated with the risk of neutropenia [54,90,91]. Thus, the presence of *UGT1A1*28* could be an indicator of myelosuppression risk and the genotype can be used to individualize dosing of IRI [54]. In an attempt to define precise genotype-based dose schedule a few number of clinical dose-escalation studies have suggested the IRI Maximum Tolerated Dose (MTD) based on patients' UGT1A1 genotype (Table 3). Satoh et al. [92] proposed a starting dose for IRI monotherapy of 150 mg/m^2 for patients who have two of **6* and/or **28* alleles, but many required dose reductions or delayed treatment in subsequent cycles. In this study, the clinical outcomes were not evaluated. The Innocenti et al. [54] study indicated the MTD for IRI monotherapy of 220 mg/m^2 for **28/*28* patients, 390 mg/m^2 for **1/*28* patients

and 470 mg/m^2 for wt genotype. No statistically significant difference on antitumor response was found within the genotypes groups using the proposed regimen. Additionally, the AUC of IRI increased according to the increase in the MTD in each genotype group, but the mean of the SN-38 AUC was similar among the different MTDs in each genotype group. This normalization of SN-38 AUC by genotype-directed dosing may be the key to preserving antitumor efficacy, even in patients with the **28/*28* genotype, which would be treated at lower doses [54]. In the trial of Fukuda *et al*. [93] the two **1/*28* patients were treated with an initial IRI dose of 60 mg/m^2, but did not completed the planned treatment because of dose-limiting toxicities. Thus, 60 mg/m^2 was considered to be the MTD of IRI for these patients.

The MTD for FOLFIRI regimen (associated or not with bevacizumab) proposed by six studies ranged from 130 to 210 mg/m^2 for patients with two **6* and/or **28* alleles, 240 to 350 mg/m^2 for heterozygous patients with one wt allele and 260 to 390 mg/m^2 for **1/*1* patients [73,91,94–97]. In the Lu et al. [95] study, colorectal cancer patients with IRI dose escalation based on UGT1A1 genotyping presented better clinical response rate than those without dose escalation. Marcuello et al. [96] found an overall response rate (ORR) lower in patients carrying the defective allele, while a dose ≥ 260 mg/m^2, in carriers of at least one wt allele, was an independent predictor of better clinical outcome, indicating a possible benefit of increasing IRI dosage in *UGT1A1*1/*1* subjects.

Table 3. Dose-finding studies based on *UGT1A1* genotype.

Type of cancer	**Chemotherapy**	***UGT1A1* genotype/n**	**Starting dose** (mg/m^2)	**Maximum Tolerated Dose** (mg/m^2)	**Genotype related outcomes**	**Ref.**
Gastrointestinal	IRI	**1/*1* (n=41) **1/*28, *1/*6* (n=20) **28/*28*, *6/*6, *6/*28 (n=21)	150 150 150	 >150 150	-	[92]
Gastrointestinal Lung and Other	IRI	**1/*1* (n=31) **1/*28* (n=28) **28/*28* (n=9)	390 390 280	470 390 220	No statistically significant difference on antitumor response within genotypes groups	[54]
Lung	IRI	**1/*28* (n=2)	60	60	Dose limiting toxicities	[93]
Colorectal	FOLFIRI/ bevacizumab	**1/*1* (n=25) **1/*28* (n=23)	260 260	310 260	The overall median PFS was 9.0 months (95% CI = 6.6 - 13.1). PFS curves do not clearly separate by *UGT1A1* genotype	[94]
Colorectal	FOLFIRI/ bevacizumab	**1/*1* **1/*28*	180 180	260 240	Clinical response rate of patients treated under *UGT1A1* genotyping	[95]

		**28/*28*	120	210	based dose escalation (n=79) was better than that of those without dose escalation (n=28) (P = 0.028)	
Colorectal	FOLFIRI	**1/*1* (n=35) **1/*28* (n=24)	215 215	370 310	The response rate was higher in **28* carriers (OR: 4.35, P=.03) or patients treated at doses ≥MTD (OR: 5.57, P=.014)	[91]
Colorectal	FOLFIRI	**1/*1* (n=23) **1/*28, *1/*6* (n=20) **28/*28*, *6/*6, *6/*28 (n=7)	280 240 240	350 350 200	Homozygous carriers for defective allele had lower ORR (28.6%, vs 61.5% and 80%)	[73]
Colorectal	FOLFIRI	**1/*1* (n=42) **1/*28* (n=38) *28/*28* (n=14)	180 110 90	390 340 130	The ORR was lower in carriers of the *28 allele (13% in **28/*28*, 60% in **1/*1* and 39% in **1/*28* and P<.049) A dose ≥260 mgm^2 was an independent predictor of better response and higher TTP in patients (*1/*1 and **1/*28*)	[96]
Colorectal	FOLFIRI	**1/*1* (n=10)	150	RD: 180	-	[97]

		**1/*28, *1/*6* (n=2)	150			
		**28/*28*, *6/*6, *6/*28 (n=3)	150			
		**1/*1* (n=21)	150	150		
Solid tumors	CAPIRINOX	**1/*28* (n=18)	150	150	-	[104]
		**28/*28* (n=11)	150	75		

CAPIRINOX: Irinotecan/Oxaliplatin/Capecitabine; FOLFIRI: irinotecan plus 5-fluoururacil (continuous infusion) and leucovorin; IRI: Irinotecan; MTD: maximum tolerated dose; OR: odds ratio; ORR: overall response rate; PFS: progression-free survival RD: recommended dose; TTP: time to tumor progression.

The economic impact of a pretreatment screening for the *UGT1A1*28* polymorphism was estimated by Roncato *et al*. [98]. In the retrospective study with colorectal patients treated with FOLFIRI, the cost of toxicity management was calculated according to the *UGT1A1* genotype. The predicted cost per patient increased according to the number of variant allele, with a mean of € 812 for **1/*1* (n=109), € 1,119 for **1/*28* (n=112), and € 4,886 for **28/*28* patients (n=22). The authors attributed this finding to the different toxicity profile among the genotypes, and the higher frequency of costly interventions like hospitalization among patients with the mutant allele. The results of this study point-out the cost-effectiveness of the test, supporting its implementation in routine practice [98].

Since SN-38 is much more cytotoxic than IRI, plasma levels of SN-38, clearance of SN-38, and/or polymorphism of *UGT1A1* have clinical relevance. The clearance ability of SN-38 can be predicted by determining the SN-38G/SN-38 plasma concentration ratio. Seventeen colorectal cancer patients with wild-type *UGT1A1* gene were treated with FOLFIRI regimen, with 2 h infusion of IRI 150 mg/m^2 and the blood collection time was at 15 min after the end of infusion. The values of plasma SN-38G/SN-38 ratios were between 1.03 and 7.09, a variation greater than 6x, indicating that UGT activity is highly variable among patients with the wt *UGT1A1* gene [57]. After this, Hirose *et al*. [42] suggest a one-point plasma SN-38G/SN-38 concentration ratio to define IRI induced neutropenia and to guide IRI dose adjustments. The blood collection time was as mentioned above, because they have stated that the plasma SN-38G/SN-38 concentration ratio at this time was associated to IRI induced neutropenia [57]. Seventy Japanese outpatients with colorectal cancer were treated with the above FOLFIRI regimen. There were 38 wt patients, 26 patients were 6* or **28* heterozygote and 6 patients were **6* homozygote or **6/*28* compound homozygote. They suggest that the dose of IRI in patients with a plasma SN-38G/SN-38 concentration ratio of <3 should be reduced to approximately 100-110 mg/m^2. Because the total continuous dose was different among patients with a plasma SN-38G/SN-38 concentration ratio of < 3 compared with those with a ratio of ≥ 3 [42]. Hirose *et al*. [42] propose a scheme to individualize IRI dose, at the first cycle the dose should be given on the basis of genetic testing. Than the plasma SN-38G/SN-38 concentration ratio should be determined for subsequent dose adjustments if necessary.

Nal-IRI in combination with 5-fluorouracil and folinic acid represents an relevant step forward in improving second line treatment options in patients with progression of metastatic pancreatic cancer [99]. Although this new formulation in combination with these agents presents a manageable safety profile in patients, it is necessary to check *UGT1A1* gene status

in all patients. In the phase III NAPOLI-1, patients with homozygous *UGT1A1*28*, the starting dose of Nal-IRI was lower, initial dose of 50 mg/m^2 and subsequently increased after first cycle without severe toxicity. But if toxicity grade 3/4 occurs for these patients, the dose reduction should be from 50 mg/m^2 to 43 mg/m^2 after the first occurrence and from 43 to 35 mg/m^2 after a second adverse event. The dose reductions for nal-IRI for patients without *UGT1A1*28* homozygosity who have present a grade 3/4 adverse event should be subsequently from 70 to 50 mg/m^2 and to 43 mg/m^2 for the first and second adverse events, respectively [99].

There is data supporting the effectiveness of *UGT1A1* genotype-based dose adjustment to potentially reduce the incidence of severe toxicity and improve survival. However, further randomized trials of IRI decreasing dose in patients with at-risk genotypes and increasing it in wt patients is warranted.

PROSPECTS

The estimation of pharmacokinetic parameters of IRI and its metabolites in previously published population pharmacokinetic models required complicated blood sampling schedules, limiting their clinical application [28,29], which can justify the lack of clinical studies of pharmacokinetic dose individualization. In this context, the use of dried blood spots (DBS), usually obtained from finger pricks, can potentially allow multiple sampling from the same patient, even at remote sites [100]. Thus, the quantification of IRI and its active metabolite SN-38 in DBS may be an alternative to individualize the drug dose through a minimally invasive collection method [101]. Hahn *et al*. [101] collected DBS from patients on IRI therapy as single agent or combined regimen. The samples were collected 1 hour and 24 hours after the beginning of IRI infusion. With these two collections it was possible to determine the AUC of IRI. They suggested that estimation of IRI AUC using DBS is a promising alternative, particularly considering the complex sampling usually required for limited sampling strategies. The use of such alternative sampling strategy eventually could allow larger studies to evaluate the relation between exposure to IRI and its metabolites to toxicity and clinical responses, also supporting the establishment of exposure targets.

CONCLUSIONS

Studies with pharmacokinetic and pharmacogenetic assays demonstrate that the identification of patients at risk of severe toxicities from IRI is feasible and allows the individualization of doses. Currently, the most straightforward approach for IRI dose individualization is *UGT1A1* genotyping. However, this strategy is sub-optimal due to several other genetic and environmental contributions to the variable pharmacokinetics of IRI and its active metabolites. Pharmacokinetically-based IRI dose individualization studies are needed to improve safety and effectiveness of this important chemotherapeutic drug. The use of DBS sampling could allow the clinical application of complex sampling for the clinical use of limited sampling and population pharmacokinetic models for IRI doses individualization.

ACKNOWLEDGEMENTS

This work was supported by a research grant (Process 17/2551-0001430-8) from Fundação de Amparo à Pesquisa do Rio Grande do Sul (Chamada FAPERGS/MS/CNPq/SESRS 03/2017).

REFERENCES

[1] Carrillo, J. A.; Munoz, C. A. Alternative Chemotherapeutic Agents: Nitrosoureas, Cisplatin, Irinotecan. *Neurosurg. Clin. N. Am.*, **2012**, *23* (2), 297–306.

[2] Kawamura, K.; Hashimoto, H.; Ogawa, M.; Yui, J.; Wakizaka, H.; Yamasaki, T.; Hatori, A.; Xie, L.; Kumata, K.; Fujinaga, M.; Zhang, M. R. Synthesis, Metabolite Analysis, and in Vivo Evaluation of [11C]irinotecan as a Novel Positron Emission Tomography (PET) Probe. *Nucl. Med. Biol.*, **2013**, *40* (5), 651–657.

[3] Basu, S.; Zeng, M.; Yin, T.; Gao, S.; Hu, M. Development and Validation of an UPLC-MS/MS Method for the Quantification of Irinotecan, SN-38 and SN-38 Glucuronide in Plasma, Urine, Feces, Liver and Kidney: Application to a Pharmacokinetic Study of Irinotecan in Rats. *J. Chromatogr. B Anal. Technol. Biomed. Life Sci.*, **2016**, *1015–1016*, 34–41.

[4] Fuchs, C.; Mitchell, E. P.; Hoff, P. M. Irinotecan in the Treatment of Colorectal Cancer. *Cancer Treat. Rev.*, **2006**, *32* (7), 491–503.

[5] Petrelli, F.; Inno, A.; Ghidini, A.; Rimassa, L.; Tomasello, G.; Labianca, R.; Barni, S.

Second Line with Oxaliplatin- or Irinotecan-Based Chemotherapy for Gemcitabine-Pretreated Pancreatic Cancer: A Systematic Review. *Eur. J. Cancer*, **2017**, *81*, 174–182.

[6] Schønnemann, K. R.; Yilmaz, M.; Bjerregaard, J. K.; Nielsen, K. M.; Pfeiffer, P. Phase II Study of Biweekly Cetuximab in Combination with Irinotecan as Second-Line Treatment in Patients with Platinum-Resistant Gastro-Oesophageal Cancer. *Eur. J. Cancer*, **2012**, *48* (4), 510–517.

[7] Ueda, Y.; Miyatake, T.; Nagamatsu, M.; Yamasaki, M.; Nishio, Y.; Yoshino, K.; Fujita, M.; Tsutsui, T.; Enomoto, T.; Kimura, T. A Phase II Study of Combination Chemotherapy Using Docetaxel and Irinotecan for TC-Refractory or TC-Resistant Ovarian Carcinomas (GOGO-OV2 Study) and for Primary Clear or Mucinous Ovarian Carcinomas (GOGO-OV3 Study). *Eur. J. Obstet. Gynecol. Reprod. Biol.*, **2013**, *170* (1), 259–263.

[8] Algeciras-Schimnich, A.; O'Kane, D. J.; Snozek, C. L. H. Pharmacogenomics of Tamoxifen and Irinotecan Therapies. *Clin. Lab. Med.*, **2008**, *28* (4), 553–567.

[9] Etienne-Grimaldi, M. C.; Boyer, J. C.; Thomas, F.; Quaranta, S.; Picard, N.; Loriot, M. A.; Narjoz, C.; Poncet, D.; Gagnieu, M. C.; Ged, C.; Broly, F.; Le Morvan, V.; Bouquié, R.; Gaub, M. P.; Philibert, L.; Ghiringhelli, F.; Le Guellec, C. UGT1A1 Genotype and Irinotecan Therapy: General Review and Implementation in Routine Practice. *Fundam. Clin. Pharmacol.*, **2015**, *29* (3), 219–237.

[10] Zashikhina, N. N.; Volokitina, M. V.; Korzhikov-Vlakh, V. A.; Tarasenko, I. I.; Lavrentieva, A.; Scheper, T.; Rühl, E.; Orlova, R. V.; Tennikova, T. B.; Korzhikova-Vlakh, E. G. Self-Assembled Polypeptide Nanoparticles for Intracellular Irinotecan Delivery. *Eur. J. Pharm. Sci.*, **2017**, *109* (July), 1–12.

[11] Alimonti, A.; Gelibter, A.; Pavese, I.; Satta, F.; Cognetti, F.; Ferretti, G.; Rasio, D.; Vecchione, A.; Di Palma, M. New Approaches to Prevent Intestinal Toxicity of Irinotecan-Based Regimens. *Cancer Treat. Rev.*, **2004**, *30* (6), 555–562.

[12] Kweekel, D.; Guchelaar, H. J.; Gelderblom, H. Clinical and Pharmacogenetic Factors Associated with Irinotecan Toxicity. *Cancer Treat. Rev.*, **2008**, *34* (7), 656–669.

[13] Lam, S. W.; Guchelaar, H. J.; Boven, E. The Role of Pharmacogenetics in Capecitabine Efficacy and Toxicity. *Cancer Treat. Rev.*, **2016**, *50*, 9–22.

[14] Wang-Gillam, A.; Li, C. P.; Bodoky, G.; Dean, A.; Shan, Y. S.; Jameson, G.; MacArulla, T.; Lee, K. H.; Cunningham, D.; Blanc, J. F.; Hubner, R. A.; Chiu, C. F.; Schwartsmann, G.; Siveke, J. T.; Braiteh, F.; Moyo, V.; Belanger, B.; Dhindsa, N.;

Bayever, E.; Von Hoff, D. D.; Chen, L. T. Nanoliposomal Irinotecan with Fluorouracil and Folinic Acid in Metastatic Pancreatic Cancer after Previous Gemcitabine-Based Therapy (NAPOLI-1): A Global, Randomised, Open-Label, Phase 3 Trial. *Lancet*, **2016**, *387* (10018), 545–557.

[15] Van Der Bol, J. M.; Mathijssen, R. H. J.; Creemers, G. J. M.; Planting, A. S. T.; Loos, W. J.; Wiemer, E. A. C.; Friberg, L. E.; Verweij, J.; Sparreboom, A.; De Jong, F. A. A CYP3A4 Phenotype-Based Dosing Algorithm for Individualized Treatment of Irinotecan. *Clin. Cancer Res.*, **2010**, *16* (2), 736–742.

[16] Adiwijaya, B.; Kim, J.; Lang, I.; Csõszi, T.; Cubillo, A.; Chen, J.-S.; Wong, M.; Park, J.; Kim, J.; Rau, K.; Melichar, B.; Gallego, J.; Fitzgerald, J.; Belanger, B.; Molnar, I.; Ma, W. Population Pharmacokinetics of Liposomal Irinotecan in Patients With Cancer. *Clin. Pharmacol. Ther.*, **2017**, *102* (6), 997–1005.

[17] Xu, Y.; Villalona-Calero, M. A. Irinotecan: Mechanisms of Tumor Resistance and Novel Strategies for Modulating Its Activity. *Ann. Oncol.*, **2002**, *13* (12), 1841–1851.

[18] Martino, E.; Della Volpe, S.; Terribile, E.; Benetti, E.; Sakaj, M.; Centamore, A.; Sala, A.; Collina, S. The Long Story of Camptothecin: From Traditional Medicine to Drugs. *Bioorganic Med. Chem. Lett.*, **2017**, *27* (4), 701–707.

[19] Morham, S. G.; Kluckman, K. D.; Voulomanos, N.; Smithies, O. Targeted Disruption of the Mouse Topoisomerase I Gene by Camptothecin Selection. *Mol. Cell. Biol.*, **1996**, *16* (12), 6804–6809.

[20] Fan, Y.; Mansoor, N.; Ahmad, T.; Khan, R. A.; Czejka, M.; Sharib, S.; Yang, D.-H.; Ahmed, M. Physiologically Based Pharmacokinetic Modeling for Predicting Irinotecan Exposure in Human Body. *Oncotarget*, **2017**, *8* (29), 48178–48185.

[21] Lu, A. J.; Zhang, Z. S.; Zheng, M. Y.; Zou, H. J.; Luo, X. M.; Jiang, H. L. 3D-QSAR Study of 20 (S)-Camptothecin Analogs. *Acta Pharmacol. Sin.*, **2007**, *28* (2), 307–314.

[22] Staker, B. L.; Hjerrild, K.; Feese, M. D.; Behnke, C. A.; Burgin, A. B.; Stewart, L. The Mechanism of Topoisomerase I Poisoning by a Camptothecin Analog. *Proc. Natl. Acad. Sci. U. S. A.*, **2002**, *99* (24), 15387–15392.

[23] Huisman, S. A.; De Bruijn, P.; Ghobadi Moghaddam-Helmantel, I. M.; Ijzermans, J. N. M.; Wiemer, E. A. C.; Mathijssen, R. H. J.; De Bruin, R. W. F. Fasting Protects against the Side Effects of Irinotecan Treatment but Does Not Affect Anti-Tumour Activity in Mice. *Br. J. Pharmacol.*, **2016**, *173* (5), 804–814.

[24] Zhang, X.; Yin, J. F.; Zhang, J.; Kong, S. J.; Zhang, H. Y.; Chen, X. M. UGT1A1*6 Polymorphisms Are Correlated with Irinotecan-Induced Neutropenia: A Systematic

Review and Meta-Analysis. *Cancer Chemother. Pharmacol.*, **2017**, *80* (1), 135–149.

[25] Conklin, K. A. Chemotherapy-Associated Oxidative Stress: Impact on Chemotherapeutic Effectiveness. *Integr. Cancer Ther.*, **2004**, *3* (4), 294–300.

[26] Chen, Y.; Jungsuwadee, P.; Vore, M.; Butterfield, D. A.; St. Clair, D. K. Collateral Damage in Cancer Chemotherapy: Oxidative Stress in Nontargeted Tissues. *Mol. Interv.*, **2007**, *7* (3), 147–156.

[27] Rothenberg, M. L.; Kuhn, J. G.; Schaaf, L. J.; Rodriguez, G. I.; Eckhardt, S. G.; Villalona-Calero, M. A.; Rinaldi, D. A.; Hammond, L. A.; Hodges, S.; Sharma, A.; Elfring, G. L.; Petit, R. G.; Locker, P. K.; Miller, L. L.; Von Hoff, D. D. Phase I Dose-Finding and Pharmacokinetic Trial of Irinotecan (CPT-11) Administered Every Two Weeks. *Ann. Oncol.*, **2001**, *12* (11), 1631–1641.

[28] Poujol, S.; Pinguet, F.; Ychou, M.; Abderrahim, A. G.; Duffour, J.; Bressolle, F. M. M. A Limited Sampling Strategy to Estimate the Pharmacokinetic Parameters of Irinotecan and Its Active Metabolite, SN-38, in Patients with Metastatic Digestive Cancer Receiving the FOLFIRI Regimen. *Oncol. Rep.*, **2007**, *18* (6), 1613–1621.

[29] Klein, C. E.; Gupta, E.; Reid, J. M.; Atherton, P. J.; Sloan, J. A.; Pitot, H. C.; Ratain, M. J.; Kastrissios, H. Population Pharmacokinetic Model for Irinotecan and Two of Its Metabolites, SN-38 and SN-38 Glucuronide. *Clin. Pharmacol. Ther.*, **2002**, *72* (6), 638–647.

[30] Chabot, G. G.; Abigerges, D.; Catimel, G.; Culine, S.; de Forni, M.; Extra, J. M.; Mahjoubi, M.; Hérait, P.; Armand, J. P.; Bugat, R. Population Pharmacokinetics and Pharmacodynamics of Irinotecan (CPT-11) and Active Metabolite SN-38 during Phase I Trials. *Ann. Oncol. Off. J. Eur. Soc. Med. Oncol.*, **1995**, *6* (2), 141–151.

[31] Canal, P.; Gay, C.; Dezeuze, A.; Douillard, J. Y.; Bugat, R.; Brunet, R.; Adenis, A.; Herait, P.; Lokiec, F.; Mathieu-Boue, A. Pharmacokinetics and Pharmacodynamics of Irinotecan during a Phase II Clinical Trial in Colorectal Cancer. Pharmacology and Molecular Mechanisms Group of the European Organization for Research and Treatment of Cancer. *J. Clin. Oncol.*, **1996**, *14* (10), 2688–2695.

[32] Saltz, L. B.; Kanowitz, J.; Kemeny, N. E.; Schaaf, L.; Spriggs, D.; Staton, B. A.; Berkery, R.; Steger, C.; Eng, M.; Dietz, A.; Locker, P.; Kelsen, D. P. Phase I Clinical and Pharmacokinetic Study of Irinotecan, Fluorouracil, and Leucovorin in Patients with Advanced Solid Tumors. *J. Clin. Oncol.*, **1996**, *14* (11), 2959–2967.

[33] Sparreboom A, de Jonge MJ, de Bruijn P, Brouwer E, Nooter K, Loos WJ, van Alphen RJ, Mathijssen RH, Stoter G, V. J. Irinotecan Metabolism and Disposition in Cancer.

Clin. Cancer Res., **1998**, *4* (November), 2747–2754.

[34] Pitot, H. C.; Goldberg, R. M.; Reid, J. M.; Sloan, J. A.; Skaff, P. A.; Erlichman, C.; Rubin, J.; Burch, P. A.; Adjei, A. A.; Alberts, S. A.; Schaaf, L. J.; Elfring, G.; Miller, L. L. Phase I Dose-Finding and Pharmacokinetic Trial of Irinotecan Hydrochloride (CPT-11) Using a Once-Every-Three-Week Dosing Schedule for Patients with Advanced Solid Tumor Malignancy. *Clin. Cancer Res.*, **2000**, *6* (6), 2236–2244.

[35] de Jonge, M. J. A.; Verweij, J.; de Bruijn, P.; Brouwer, E.; Mathijssen, R. H. J.; van Alphen, R. J.; de Boer-Dennert, M. M.; Vernillet, L.; Jacques, C.; Sparreboom, A. Pharmacokinetic, Metabolic, and Pharmacodynamic Profiles in a Dose-Escalating Study of Irinotecan and Cisplatin. *J. Clin. Oncol.*, **2000**, *18* (1), 195–195.

[36] Slatter, J. G.; Schaaf, L. J.; Sams, J. P.; Feenstra, K. L.; Johnson, M. G.; Bombardt, P. A.; Cathcart, K. S.; Verburg, M. T.; Pearson, L. K.; Compton, L. D.; Miller, L. L.; Baker, D. S.; Pesheck, C. V. Pharmacokinetics, Metabolism, and Excretion of Irinotecan (Cpt-11) Following I. V. Infusion of [14C] Cpt-11 in Cancer Patients. *Drug Metab. Dispos.*, **2000**, *28* (4), 423–433.

[37] Poujol, S.; Pinguet, F.; Malosse, F.; Astre, C.; Ychou, M.; Culine, S.; Bressolle, F. Sensitive HPLC-Fluorescence Method for Irinotecan and Four Major Metabolites in Human Plasma and Saliva: Application to Pharmacokinetic Studies. *Clin. Chem.*, **2003**, *49* (11), 1900–1908.

[38] Satoh, T.; Yasui, H.; Muro, K.; Komatsu, Y.; Sameshima, S.; Yamaguchi, K.; Sugihara, K. Pharmacokinetic Assessment of Irinotecan, SN-38, and SN-38-Glucuronide: A Substudy of the FIRIS Study. *Anticancer Res.*, **2013**, *33* (9), 3845–3854.

[39] Mullangi, R.; Ahlawat, P.; Srinivas, N. R. Irinotecan and Its Active Metabolite, SN-38: Review of Bioanalytical Methods and Recent Update from Clinical Pharmacology Perspectives. *Biomed. Chromatogr.*, **2010**, *24* (1), 104–123.

[40] Boyd, G.; Smyth, J. F.; Jodrell, D. I.; Cummings, J. High-Performance Liquid Chromatographic Technique for the Simultaneous Determination of Lactone and Hydroxy Acid Forms of Camptothecin and SN-38 in Tissue Culture Media and Cancer Cells. *Anal. Biochem.*, **2001**, *297* (1), 15–24.

[41] Poujol, S.; Bressolle, F.; Duffour, J.; Abderrahim, A. G.; Astre, C.; Ychou, M.; Pinguet, F. Pharmacokinetics and Pharmacodynamics of Irinotecan and Its Metabolites from Plasma and Saliva Data in Patients with Metastatic Digestive Cancer Receiving Folfiri Regimen. *Cancer Chemother. Pharmacol.*, **2006**, *58* (3), 292–305.

[42] Hirose, K.; Yamashita, K.; Takada, H.; Kaneda, N.; Fukami, K.; Maruo, E.; Kitamura, M.; Hasegawa, J.; Maeda, Y. Usefulness of One-Point Plasma SN-38G/SN-38 Concentration Ratios as a Substitute for UGT1A1 Genetic Information after Irinotecan Administration. *Int. J. Clin. Oncol.*, **2014**, *19* (2), 397–402.

[43] Van Schaik, R. H. N. Implications of Cytochrome P450 Genetic Polymorphisms on the Toxicity of Antitumor Agents. *Ther. Drug Monit.*, **2004**, *26* (2), 236–240.

[44] Santos, A.; Zanetta, S.; Cresteil, T.; Deroussent, A.; Pein, F.; Raymond, E.; Vernillet, L.; Risse, M. L.; Boige, V.; Gouyette, A.; Vassal, G. Metabolism of Irinotecan (CPT-11) by CYP3A4 and CYP3A5 in Humans. *Clin. Cancer Res.*, **2000**, *6* (5), 2012–2020.

[45] Kehrer, D. F. S.; Mathijssen, R. H. J.; Verweij, J.; de Bruijn, P.; Sparreboom, A. Modulation of Irinotecan Metabolism by Ketoconazole. *J. Clin. Oncol.*, **2002**, *20* (14), 3122–3129.

[46] Mathijssen, R. H. J.; Verweij, J.; Bruijn, P. de; Loos, W. J.; Sparreboom, A. Effects of St. John's Wort on Irinotecan Metabolism. *J Natl Cancer Inst*, **2002**, *94* (16), 1247–1249.

[47] Khanna, R.; Morton, C. L.; Danks, M. K.; Potter, P. M. Proficient Metabolism of Irinotecan by a Human Intestinal Carboxylesterase. *Cancer Res.*, **2000**, *60* (17), 4725–4728.

[48] Humerickhouse, R.; Lohrbach, K.; Li, L.; Bosron, W. F.; Dolan, M. E. Characterization of CPT-11 Hydrolysis by Human Liver Carboxylesterase Isoforms hCE-1 and hCE-2. *Cancer Res.*, **2000**, *60* (5), 1189–1192.

[49] Hatfield, M. J.; Tsurkan, L.; Garrett, M.; Shaver, T. M.; Hyatt, J. L.; Edwards, C. C.; Hicks, L. D.; Potter, P. M. Organ-Specific Carboxylesterase Profiling Identifies the Small Intestine and Kidney as Major Contributors of Activation of the Anticancer Prodrug CPT-11. *Biochem. Pharmacol.*, **2011**, *81* (1), 24–31.

[50] Iusuf, D.; Ludwig, M.; Elbatsh, A.; van Esch, A.; van de Steeg, E.; Wagenaar, E.; van der Valk, M.; Lin, F.; van Tellingen, O.; Schinkel, A. H. OATP1A/1B Transporters Affect Irinotecan and SN-38 Pharmacokinetics and Carboxylesterase Expression in Knockout and Humanized Transgenic Mice. *Mol. Cancer Ther.*, **2014**, *13* (2), 492–503.

[51] Fujiwara, Y.; Minami, H. An Overview of the Recent Progress in Irinotecan Pharmacogenetics R Eview. **2010**, *11* (June 2005), 391–406.

[52] Innocenti, F.; Kroetz, D. L.; Schuetz, E.; Dolan, M. E.; Ram??rez, J.; Relling, M.; Chen, P.; Das, S.; Rosner, G. L.; Ratain, M. J. Comprehensive Pharmacogenetic Analysis of Irinotecan Neutropenia and Pharmacokinetics. *J. Clin. Oncol.*, **2009**, *27*

(16), 2604–2614.

[53] Sai, K.; Saito, Y.; Maekawa, K.; Kim, S. R.; Kaniwa, N.; Nishimaki-Mogami, T.; Sawada, J. I.; Shirao, K.; Hamaguchi, T.; Yamamoto, N.; Kunitoh, H.; Ohe, Y.; Yamada, Y.; Tamura, T.; Yoshida, T.; Matsumura, Y.; Ohtsu, A.; Saijo, N.; Minami, H. Additive Effects of Drug Transporter Genetic Polymorphisms on Irinotecan Pharmacokinetics/pharmacodynamics in Japanese Cancer Patients. *Cancer Chemother. Pharmacol.*, **2010**, *66* (1), 95–105.

[54] Innocenti, F.; Schilsky, R. L.; Ramiŕez, J.; Janisch, L.; Undevia, S.; House, L. K.; Das, S.; Wu, K.; Turcich, M.; Marsh, R.; Karrison, T.; Maitland, M. L.; Salgia, R.; Ratain, M. J. Dose-Finding and Pharmacokinetic Study to Optimize the Dosing of Irinotecan according to the UGT1A1 Genotype of Patients with Cancer. *J. Clin. Oncol.*, **2014**, *32* (22), 2328–2334.

[55] Ratain, M. J.; Innocenti, F. Individualizing Dosing of Irinotecan. *Clin. Cancer Res.*, **2010**, *16* (2), 371–372.

[56] Di Paolo, A.; Bocci, G.; Polillo, M.; Del Re, M.; Di Desidero, T.; Lastella, M.; Danesi, R. Pharmacokinetic and Pharmacogenetic Predictive Markers of Irinotecan Activity and Toxicity. *Curr. Drug Metab.*, **2011**, *12* (10), 932–943.

[57] Hirose, K.; Kozu, C.; Yamashita, K.; Maruo, E.; Kitamura, M.; Hasegawa, J.; Omoda, K.; Murakami, T.; Maeda, Y. Correlation between Plasma Concentration Ratios of SN-38 Glucuronide and Sn-38 and Neutropenia Induction in Patients with Colorectal Cancer and Wild-Type UGT1A1 Gene. *Oncol. Lett.*, **2012**, *3* (3), 694–698.

[58] Chabot, G. G. Clinical Pharmacokinetics of Irinotecan. *Clin. Pharmacokinet.*, **1997**, *33* (4), 245–259.

[59] Roy, A. C.; Park, S. R.; Cunningham, D.; Kang, Y. K.; Chao, Y.; Chen, L. T.; Rees, C.; Lim, H. Y.; Tabernero, J.; Ramos, F. J.; Kujundzic, M.; Cardic, M. B.; Yeh, C. G.; de Gramont, A. A Randomized Phase II Study of PEP02 (MM-398), Irinotecan or Docetaxel as a Second-Line Therapy in Patients with Locally Advanced or Metastatic Gastric or Gastro-Oesophageal Junction Adenocarcinoma. *Ann. Oncol.*, **2013**, *24* (6), 1567–1573.

[60] Ando, Y.; Saka, H.; Ando, M.; Sawa, T.; Muro, K.; Ueoka, H.; Yokoyama, A.; Saitoh, S.; Shimokata, K.; Hasegawa, Y. Polymorphisms of UDP-Glucuronosyltransferase Gene and Irinotecan Toxicity: A Pharmacogenetic Analysis. *Cancer Res.*, **2000**, *60* (24), 6921–6926.

[61] Iyer, L.; Das, S.; Janisch, L.; Wen, M.; Ramírez, J.; Karrison, T.; Fleming, G. F.;

Vokes, E. E.; Schilsky, R. L.; Ratain, M. J. UGT1A1*28 Polymorphism as a Determinant of Irinotecan Disposition and Toxicity. *Pharmacogenomics J.*, **2002**, *2* (1), 43–47.

[62] Innocenti, F.; Undevia, S. D.; Iyer, L.; Chen, P. X.; Das, S.; Kocherginsky, M.; Karrison, T.; Janisch, L.; Ramírez, J.; Rudin, C. M.; Vokes, E. E.; Ratain, M. J. Genetic Variants in the UDP-Glucuronosyltransferase 1A1 Gene Predict the Risk of Severe Neutropenia of Irinotecan. *J. Clin. Oncol.*, **2004**, *22* (8), 1382–1388.

[63] Marcuello, E.; Altés, A.; Menoyo, A.; del Rio, E.; Gómez-Pardo, M.; Baiget, M. UGT1A1 Gene Variations and Irinotecan Treatment in Patients with Metastatic Colorectal Cancer. *Br. J. Cancer*, **2004**, *2*, 678–682.

[64] McLeod, H. L. Individualizing Cancer Chemotherapy. *Clin. Adv. Hematol. Oncol.*, **2006**, *4* (4), 259–261.

[65] Li, M.; Wang, Z.; Guo, J.; Liu, J.; Li, C.; Liu, L.; Shi, H.; Liu, L.; Li, H.; Xie, C.; Zhang, X.; Sun, W.; Fang, S.; Bi, X. Clinical Significance of UGT1A1 Gene Polymorphisms on Irinotecan-Based Regimens as the Treatment in Metastatic Colorectal Cancer. *Onco. Targets. Ther.*, **2014**, *7*, 1653–1661.

[66] Shulman, K.; Cohen, I.; Barnett-Griness, O.; Kuten, A.; Gruber, S. B.; Lejbkowicz, F.; Rennert, G. Clinical Implications of UGT1A1*28 Genotype Testing in Colorectal Cancer Patients. *Cancer*, **2011**, *117* (14), 3156–3162.

[67] Xiao, X. G.; Xia, S.; Zou, M.; Mei, Q.; Zhou, L.; Wang, S. J.; Chen, Y. The Relationship between UGT1A1 Gene Polymorphism and Irinotecan Effect on Extensive-Stage Small-Cell Lung Cancer. *Onco. Targets. Ther.*, **2015**, *8*, 3575–3583.

[68] Toffoli, G.; Cecchin, E.; Corona, G.; Russo, A.; Buonadonna, A.; D'Andrea, M.; Pasetto, L. M.; Pessa, S.; Errante, D.; De Pangher, V.; Giusto, M.; Medici, M.; Gaion, F.; Sandri, P.; Galligioni, E.; Bonura, S.; Boccalon, M.; Biason, P.; Frustaci, S. The Role of UGT1A1*28 Polymorphism in the Pharmacodynamics and Pharmacokinetics of Irinotecan in Patients with Metastatic Colorectal Cancer. *J. Clin. Oncol.*, **2006**, *24* (19), 3061–3068.

[69] Minami, H.; Sai, K.; Saeki, M.; Saito, Y.; Ozawa, S.; Suzuki, K.; Kaniwa, N.; Sawada, J.; Hamaguchi, T.; Yamamoto, N.; Shirao, K.; Yamada, Y.; Ohmatsu, H.; Kubota, K.; Yoshida, T.; Ohtsu, A.; Saijo, N. Irinotecan Pharmacokinetics/pharmacodynamics and UGT1A Genetic Polymorphisms in Japanese: Roles of UGT1A1*6 and *28. *Pharmacogenet. Genomics*, **2007**, *17*, 497–504.

[70] Martinez-Balibrea, E.; Abad, A.; Martínez-Cards, A.; Ginés, A.; Valladares, M.;

Navarro, M.; Aranda, E.; Marcuello, E.; Benavides, M.; Massutí, B.; Carrato, A.; Layos, L.; Manzano, J. L.; Moreno, V. UGT1A and TYMS Genetic Variants Predict Toxicity and Response of Colorectal Cancer Patients Treated with First-Line Irinotecan and Fluorouracil Combination Therapy. *Br. J. Cancer*, **2010**, *103* (4), 581–589.

[71] Carlini, L. E.; Meropol, N. J.; Bever, J.; Andria, M. L.; Hill, T.; Gold, P.; Rogatko, A.; Wang, H.; Blanchard, R. L. UGT1A7 and UGT1A9 Polymorphisms Predict Response and Toxicity in Colorectal Cancer Patients Treated with Capecitabine / Irinotecan UGT1A7 and UGT1A9 Polymorphisms Predict Response and Toxicity in Colorectal Cancer Patients Treated with Capecitabine / Irin. **2005**, *11*, 1226–1236.

[72] Lévesque, E.; Bélanger, A.-S.; Harvey, M.; Couture, F.; Jonker, D.; Innocenti, F.; Cecchin, E.; Toffoli, G.; Guillemette, C. Refining the UGT1A Haplotype Associated with Irinotecan-Induced Hematological Toxicity in Metastatic Colorectal Cancer Patients Treated with 5-Fluorouracil/irinotecan-Based Regimens. *J. Pharmacol. Exp. Ther.*, **2013**, *345* (1), 95–101.

[73] Kim, K. P.; Kim, H. S.; Sym, S. J.; Bae, K. S.; Hong, Y. S.; Chang, H. M.; Lee, J. L.; Kang, Y. K.; Lee, J. S.; Shin, J. G.; Kim, T. W. A UGT1A1*28 and*6 Genotype-Directed Phase I Dose-Escalation Trial of Irinotecan with Fixed-Dose Capecitabine in Korean Patients with Metastatic Colorectal Cancer. *Cancer Chemother. Pharmacol.*, **2013**, *71* (6), 1609–1617.

[74] Teft, W. A.; Welch, S.; Lenehan, J.; Parfitt, J.; Choi, Y. H.; Winquist, E.; Kim, R. B. OATP1B1 and Tumour OATP1B3 Modulate Exposure, Toxicity, and Survival after Irinotecan-Based Chemotherapy. *Br. J. Cancer*, **2015**, *112* (5), 857–865.

[75] Han, J.-Y.; Lim, H.-S.; Park, Y. H.; Lee, S. Y.; Lee, J. S. Integrated Pharmacogenetic Prediction of Irinotecan Pharmacokinetics and Toxicity in Patients with Advanced Non-Small Cell Lung Cancer. *Lung Cancer*, **2009**, *63* (1), 115–120.

[76] Glimelius, B.; Garmo, H.; Berglund, A.; Fredriksson, L. a; Berglund, M.; Kohnke, H.; Byström, P.; Sørbye, H.; Wadelius, M. Prediction of Irinotecan and 5-Fluorouracil Toxicity and Response in Patients with Advanced Colorectal Cancer. *Pharmacogenomics J.*, **2011**, *11* (1), 61–71.

[77] UGT Alleles Nomenclature Home Page. UGT Nomenclature Commitee. June 2005. Access 2017-12. https://www.pharmacogenomics.pha.ulaval.ca/ugt-alleles-nomenclature/.

[78] Hoskins, J. M.; Goldberg, R. M.; Qu, P.; Ibrahim, J. G.; McLeod, H. L. UGT1A1*28 Genotype and Irinotecan-Induced Neutropenia: Dose Matters. *J. Natl. Cancer Inst.*,

2007, *99* (17), 1290–1295.

[79] Saito, Y.; Maekawa, K.; Ozawa, S.; Sawada, J. Genetic Polymorphisms and Haplotypes of Major Drug Metabolizing Enzymes in East Asians and Their Comparison with Other Ethnic Populations. *Current*, **2007**, 49–78.

[80] Campbell, J. M.; Stephenson, M. D.; Bateman, E.; Peters, M. D. J.; Keefe, D. M.; Bowen, J. M. Irinotecan-Induced Toxicity Pharmacogenetics: An Umbrella Review of Systematic Reviews and Meta-Analyses. *Pharmacogenomics J.*, **2017**, *17* (1), 21–28.

[81] Chen, X.; Liu, L.; Guo, Z.; Liang, W.; He, J.; Huang, L.; Deng, Q.; Tang, H.; Pan, H.; Guo, M.; Liu, Y.; He, Q.; He, J. UGT1A1 Polymorphisms with Irinotecan-Induced Toxicities and Treatment Outcome in Asians with Lung Cancer: A Meta-Analysis. *Cancer Chemother. Pharmacol.*, **2017**, *79* (6), 1109–1117.

[82] Kim, S. Y.; S Hong, Y.; K Shim, E.; Kong, S.-Y.; Shin, A.; Baek, J. Y.; Jung, K. H. S-1 plus Irinotecan and Oxaliplatin for the First-Line Treatment of Patients with Metastatic Colorectal Cancer: A Prospective Phase II Study and Pharmacogenetic Analysis. *Br. J. Cancer*, **2013**, *109* (6), 1420–1427.

[83] Han, J. Y.; Lim, H. S.; Yoo, Y. K.; Eun, S. S.; Yong, H. P.; Sung, Y. L.; Lee, J. E.; Dea, H. L.; Heung, T. K.; Jin, S. L. Associations of ABCB1, ABCC2, and ABCG2 Polymorphisms with Irinotecan-Pharmacokinetics and Clinical Outcome in Patients with Advanced Non-Small Cell Lung Cancer. *Cancer*, **2007**, *110* (1), 138–147.

[84] Sai, K.; Saito, Y.; Tatewaki, N.; Hosokawa, M.; Kaniwa, N.; Nishimaki-Mogami, T.; Naito, M.; Sawada, J. I.; Shirao, K.; Hamaguchi, T.; Yamamoto, N.; Kunitoh, H.; Tamura, T.; Yamada, Y.; Ohe, Y.; Yoshida, T.; Minami, H.; Ohtsu, A.; Matsumura, Y.; Saijo, N.; Okuda, H. Association of Carboxylesterase 1A Genotypes with Irinotecan Pharmacokinetics in Japanese Cancer Patients. *Br. J. Clin. Pharmacol.*, **2010**, *70* (2), 222–233.

[85] De Mattia, E.; Toffoli, G.; Polesel, J.; D'Andrea, M.; Corona, G.; Zagonel, V.; Buonadonna, A.; Dreussi, E.; Cecchin, E. Pharmacogenetics of ABC and SLC Transporters in Metastatic Colorectal Cancer Patients Receiving First-Line FOLFIRI Treatment. *Pharmacogenet. Genomics*, **2013**, *23* (10), 549–557.

[86] *Camptosar Prescribing Information*; 2012.

[87] Swen, J. J.; Nijenhuis, M.; De Boer, A.; Grandia, L.; Maitland-Van Der Zee, A. H.; Mulder, H.; Rongen, G. A. P. J. M.; Van Schaik, R. H. N.; Schalekamp, T.; Touw, D. J.; Van Der Weide, J.; Wilffert, B.; Deneer, V. H. M.; Guchelaar, H. J. Pharmacogenetics: From Bench to Byte an Update of Guidelines. *Clin. Pharmacol.*

Ther., **2011**, *89* (5), 662–673.

[88] Etienne-Grimaldi, M.-C.; Bennouna, J.; Formento, J.-L.; Douillard, J.-Y.; Francoual, M.; Hennebelle, I.; Chatelut, E.; Francois, E.; Faroux, R.; El Hannani, C.; Jacob, J.-H.; Milano, G. Multifactorial Pharmacogenetic Analysis in Colorectal Cancer Patients Receiving 5-Fluorouracil-Based Therapy Together with Cetuximab-Irinotecan. *Br. J. Clin. Pharmacol.*, **2012**, *73* (5), 776–785.

[89] Mathijssen Ron, H. H. J.; de Jong, F. A.; van Schaik, R. H. N.; Lepper, E. R.; Friberg, L. E.; Rietveld, T.; de Bruijn, P.; Graveland, W. J.; Figg, W. D.; Verweij, J.; Sparreboom, A. Prediction of Irinotecan Pharmacokinetics by Use of Cytochrome P450 3A4 Phenotyping Probes. *J. Natl. Cancer Inst.*, **2004**, *96* (21), 1585–1592.

[90] Ramchandani, R. P.; Wang, Y.; Booth, B. P.; Ibrahim, A.; Johnson, J. R.; Rahman, A.; Mehta, M.; Innocenti, F.; Ratain, M. J.; Gobburu, J. V. S. The Role of SN-38 Exposure, UGT1A1*28 Polymorphism, and Baseline Bilirubin Level in Predicting Severe Irinotecan Toxicity. *J. Clin. Pharmacol.*, **2007**, *47* (1), 78–86.

[91] Toffoli, G.; Cecchin, E.; Gasparini, G.; D'Andrea, M.; Azzarello, G.; Basso, U.; Mini, E.; Pessa, S.; De Mattia, E.; Re, G. Lo; Buonadonna, A.; Nobili, S.; De Paoli, P.; Innocenti, F. Genotype-Driven Phase I Study of Irinotecan Administered in Combination with Fluorouracil/leucovorin in Patients with Metastatic Colorectal Cancer. *J. Clin. Oncol.*, **2010**, *28* (5), 866–871.

[92] Satoh, T.; Ura, T.; Yamada, Y.; Yamazaki, K.; Tsujinaka, T.; Munakata, M.; Nishina, T.; Okamura, S.; Esaki, T.; Sasaki, Y.; Koizumi, W.; Kakeji, Y.; Ishizuka, N.; Hyodo, I.; Sakata, Y. Genotype-Directed, Dose-Finding Study of Irinotecan in Cancer Patients with UGT1A1*28 And/or UGT1A1*6 Polymorphisms. *Cancer Sci.*, **2011**, *102* (10), 1868–1873.

[93] Fukuda, M.; Shimada, M.; Kitazaki, T.; Nagashima, S.; Hashiguchi, K.; Ebi, N.; Takayama, K.; Nakanishi, Y.; Semba, H.; Harada, T.; Seto, T.; Okamoto, I.; Ichinose, Y.; Sugio, K. Phase I Study of Irinotecan for Previously Treated Lung Cancer Patients with the UGT1A1*28 or *6 Polymorphism: Results of the Lung Oncology Group in Kyushu (LOGIK1004A). *Thorac. Cancer*, **2017**, *8* (1), 40–45.

[94] Toffoli, G.; Sharma, M. R.; Marangon, E.; Posocco, B.; Gray, E.; Mai, Q.; Buonadonna, A.; Polite, B. N.; Miolo, G.; Tabaro, G.; Innocenti, F. Genotype-Guided Dosing Study of FOLFIRI plus Bevacizumab in Patients with Metastatic Colorectal Cancer. *Clin. Cancer Res.*, **2017**, *23* (4), 918–924.

[95] Lu, C. Y.; Huang, C. W.; Hu, H. M.; Tsai, H. L.; Huang, C. M.; Yu, F. J.; Huang, M.

Y.; Chang, S. F.; Huang, M. L.; Wang, J. Y. Prognostic Advantage of Irinotecan Dose Escalation according to Uridine Diphosphate Glucuronosyltransferase 1A1 (UGT1A1) Genotyping in Patients with Metastatic Colorectal Cancer Treated with Bevacizumab Combined with 5-Fluorouracil/leucovorin with Irinote. *Transl. Res.*, **2014**, *164* (2), 169–176.

[96] Marcuello, E.; Páez, D.; Paré, L.; Salazar, J.; Sebio, a; del Rio, E.; Baiget, M. A Genotype-Directed Phase I-IV Dose-Finding Study of Irinotecan in Combination with Fluorouracil/leucovorin as First-Line Treatment in Advanced Colorectal Cancer. *Br. J. Cancer*, **2011**, *105* (1), 53–57.

[97] Yamashita, K.; Nagashima, F.; Fujita, K.; Yamamoto, W.; Endo, H.; Miya, T.; Narabayashi, M.; Kawara, K.; Akiyama, Y.; Ando, Y.; Ando, M.; Sasaki, Y. Phase I/II Study of FOLFIRI in Japanese Patients with Advanced Colorectal Cancer. *Jpn. J. Clin. Oncol.*, **2011**, *41* (2), 204–209.

[98] Roncato, R.; Cecchin, E.; Montico, M.; De Mattia, E.; Giodini, L.; Buonadonna, A.; Solfrini, V.; Innocenti, F.; Toffoli, G. Cost Evaluation of Irinotecan-Related Toxicities Associated With the UGT1A1*28 Patient Genotype. *Clin. Pharmacol. Ther.*, **2017**, *102* (1), 123–130.

[99] Passero, F. C.; Grapsa, D.; Syrigos, K. N.; Saif, M. W. The Safety and Efficacy of Onivyde (Irinotecan Liposome Injection) for the Treatment of Metastatic Pancreatic Cancer Following Gemcitabine-Based Therapy. *Expert Rev. Anticancer Ther.*, **2016**, *16* (7), 697–703.

[100] Antunes, M. V.; Charão, M. F.; Linden, R. Dried Blood Spots Analysis with Mass Spectrometry: Potentials and Pitfalls in Therapeutic Drug Monitoring. *Clin. Biochem.*, **2016**, *49* (13–14), 1035–1046.

[101] Hahn, R. Z.; Arnhold, P. C.; Andriguetti, N. B.; Schneider, A.; Klück, H. M.; dos Reis, S. L.; Bastiani, M. F.; Kael, I.; da Silva, A. C. C.; Schwartsmann, G.; Antunes, M. V.; Linden, R. Determination of Irinotecan and Its Metabolite SN-38 in Dried Blood Spots Using High-Performance Liquid-Chromatography with Fluorescence Detection. *J. Pharm. Biomed. Anal.*, **2018**, *150*, 51–58.

[102] Huang, L.; Zhang, T.; Xie, C.; Liao, X.; Yu, Q.; Feng, J.; Ma, H.; Dai, J.; Li, M.; Chen, J.; Zang, A.; Wang, Q.; Ge, S.; Qin, K.; Cai, J.; Yuan, X. SLCO1B1 and SLC19A1 Gene Variants and Irinotecan-Induced Rapid Response and Survival: A Prospective Multicenter Pharmacogenetics Study of Metastatic Colorectal Cancer. *PLoS One*, **2013**, *8* (10), 1–10.

[103] Xiang, X.; Rao Jada, S.; Hua Li, H.; Fan, L.; San Tham, L.; Ing Wong, C.; Chin Lee, S.; Lim, R.; Yu Zhou, Q.; Cher Goh, B.; Huat Tan, E.; Chowbay, B. Pharmacogenetics of SLCO1B1 Gene and the Impact of *1b and *15 Haplotypes on Irinotecan Disposition in Asian Cancer Patients. *Pharmacogenet. Genomics*, **2006**, *16* (9), 683–691.

[104] Goetz, M. P.; McKean, H. A.; Reid, J. M.; Mandrekar, S. J.; Tan, A. D.; Kuffel, M. A.; Safgren, S. L.; McGovern, R. M.; Goldberg, R. M.; Grothey, A. A.; McWilliams, R.; Erlichman, C.; Ames, M. M. UGT1A1 Genotype-Guided Phase I Study of Irinotecan, Oxaliplatin, and Capecitabine. *Invest. New Drugs*, **2013**, *31* (6), 1559–1567.

3. CAPÍTULO 2 – AN EASILY IMPLEMENTABLE LIQUID CHROMATOGRAPHY ASSAY FOR THERAPEUTIC DRUG MONITORING OF IRINOTECAN AND MAJOR METABOLITES IN PLASMA

Roberta Z. HAHN [1,2], Priscila C. ARNHOLD [1], Natalia B. ANDRIGUETTI [1,2], Anelise SCHNEIDER [1], Helena KLÜCK [3], Ramon M.M. VILELA [3], Simone L. DOS REIS [3], Gilberto SCHWARTSMANN [3], Marina V. ANTUNES [1,2] & Rafael LINDEN [1,2] *

1 *Analytical Toxicology Laboratory, Universidade Feevale, Novo Hamburgo-RS, Brazil*
2 *Graduate Program on Toxicology and Analytical Toxicology, Universidade Feevale, Novo Hamburgo-RS, Brazil*
3 *Serviço de Oncologia, Hospital de Clínicas de Porto Alegre, Porto Alegre-RS, Brazil*

Latin American Journal of Pharmacy **36**,12 (2017) 2363–2368.

SUMMARY. The objective of this study was to develop an easily implementable liquid-chromatographic assay for clinical application in therapeutic drug monitoring of irinotecan (IRI), including the metabolite SN-38 and its glucuronide SN-38G. IRI and the metabolites SN-38 and SN-38G were extracted from plasma, after protein precipitation, with methyl-*tert*-butyl ether. SN-38G levels were estimated by treating plasma with β-glucuronidase and evaluating the difference of SN-38 levels. Separation was performed in a reversed phase column with isocratic elution and fluorescence detection. Total chromatographic run time was 19 min. The assay was linear in the range of 10 to 3,000 ng/mL for IRI and 1 to 300 ng/mL for SN-38. Accuracy was 97.8-105.2%, intra-assay precision was 2.1-4.72% and inter-assay precision was of 1.66-4.37%. The assay was applied in samples from 10 patients under IRI chemotherapy. The assay was validated and due to its simple setup can be implemented in clinical laboratories aiming to pharmacokinetically individualize IRI doses. Particularly, the simple estimation of the glucuronidation ratio of the active metabolite SN-38 can be used to identify patients on risk for severe toxicity.

RESUMEN. El objetivo de este estudio fue desarrollar un ensayo cromatográfico líquido fácilmente implementable para la aplicación clínica en la monitorización terapéutica del fármaco del irinotecán (IRI), que incluye el metabolito SN-38 y su glucurónido SN-38G. IRI y los metabolitos SN-38 y SN-38G se extrajeron del plasma, después de la precipitación de proteínas, con metil-*terc*-butil éter. Los niveles de SN-38G se estimaron tratando el plasma con β-glucuronidasa y evaluando la diferencia de los niveles de SN-38. La separación se realizó en uma columna de fase invertida con elución isocrática y detección de fluorescencia. El tiempo total de ejecución cromatográfica fue de 19 min. El ensayo fue lineal en el intervalo de 10 a 3.000 ng/mL para IRI y de 1 a 300 ng/mL para SN-38. La precisión fue de 97.8-105.2%, la precisión intra-ensayo fue de 2.1-4.72% y la precisión entre ensayos fue de 1.66-4.37%. El ensayo se aplicó en muestras de 10 pacientes con quimioterapia IRI. El ensayo fue validado y debido a su configuración simple puede implementarse en laboratorios clínicos con el objetivo de individualizar farmacocinéticamente las dosis de IRI. Particularmente, la simple estimación de la relación de glucuronidación del metabolito activo SN-38 puede usarse para identificar pacientes con riesgo de toxicidad grave.

KEYWORDS: HPLC-FL; irinotecan; SN-38; therapeutic drug monitoring.

INTRODUCTION

Irinotecan is a chemotherapeutic drug used as a first-line treatment for colorectal cancer (1) and advanced pancreatic cancer (2). The primary active metabolite of IRI is SN-38 (7-ethyl-10-hydroxycamptothecin), formed by liver carboxylesterases. SN-38 is 100 to 1,000 times more cytotoxic than the parent drug and is detoxified through the formation of its glucuronide, SN-38G, mainly by UGT1A1. Antineoplastic activity is attributed to the inhibitory effect on DNA topoisomerase I, which plays an important role in DNA replication and transcription and leading to cell death (3). Like most oncological drugs, IRI has a narrow therapeutic window (4). Therefore, an important limitation associated with its use is the wide interindividual variability in tolerability with occurrence of severe toxicity, especially neutropenia and severe diarrhea, and efficacy, partly due to the complex metabolism of this drug (5). This variability is partially related to interindividual pharmacokinetic and pharmacogenetic differences, especially in the glucuronidation of the active metabolite through the action of UGT. The risk of severe neutropenia associated with IRI administration is related to a variant allele of the UGT gene, which reduces the elimination rate of SN-38

(6,7). Therefore, the concentration ratio [SN-38G]/[SN-38] was described as a useful pharmacokinetic index to identify patients at risk for severe adverse effects (8,9).

Besides being an approved drug by the Food and Drug Administration (FDA) for more than twenty years, IRI has recently gained renewed interest due to results showing an extended survival of pancreatic cancer patients treated with a new nanolipossomal formulation when compared to standard chemotherapy (10). The observed relation between exposure to IRI and its main active metabolite SN-38 and its clinical effects, both for the classical (4) and the new nanolipossomal formulation (11), suggest this drug can be a candidate for therapeutic drug monitoring (TDM).

TDM of IRI requires the availability of reliable and cost-effective analytical methods. Determination of plasma levels of IRI and SN-38 has been accomplished by the use of liquid chromatography, coupled to either tandem mass spectrometric (LC-MS/MS) or fluorescence detection (HPLC-FL), usually based on only precipitation technique, some by solid phase extraction and by liquid-liquid extraction (12). HPLC-FL is a particularly interesting analytical method due to its selectivity and robustness, with reduced implementation costs when compared to LC-MS/MS.

In this paper, we describe a simple, selective, highly sensitive and cost-effective HPLC–FL method, requiring small volumes of human plasma, for the quantification of IRI and SN-38, along with the estimation of SN-38G, suitable for clinical use on TDM of IRI and could be used for future dose adjustments.

MATERIALS AND METHODS

Reagents and reference standard samples

IRI hydrochloride, camptothecin (CPT, internal standard-IS), SN-38, β-glucuronidase (β-GLU, 100,000 UI mL^{-1}) and metil-tert-butyl-ether (MTBE) were purchased from Sigma-Aldrich. Acetonitrile, methanol, acetone, hydrochloric acid, orthophosphoric acid and monopotassium phosphate were purchased from Merck. Ultrapure water was obtained through an Elga Purelab Ultra® apparatus from Elga Labwater. For method validation, human plasma was obtained from pooled samples collected from healthy volunteers.

Sample preparation

Plasma sample preparation was based on protein precipitation followed by liquid-liquid extraction. Aliquots of 200 µL of plasma were transferred to micro tubes containing 30

ng of IS (CPT, dried acetone extract) and vortex mixed. Proteins were precipitated with the addition of 400 µL of a mixture of acetonitrile and methanol (50:50, v/v), followed by vortex mixing and centrifugation at 15.000 g for 10 min. An aliquot of 400 µL of the resulting supernatant was transferred to another tube and added with 1 mL of MTBE, followed, again, by vortex mixing and 10 min centrifugation at 15.000 g. The organic layer was dried at 60 ºC. After recovery with 200 µL of a mixture of mobile phase and hydrochloric acid 1M (3:1, v/v), to avoid conversion of IRI to its carboxylate form, 50 µL were injected into the HPLC-FL. For estimation of SN-38G concentrations, enzymatic hydrolysis with β-glucuronidase was carried out just in a separate plasma sample with the addition of 15 µL of β-GLU and incubation for 120 min at 37 ºC, followed by the extraction procedure described above. SN-38G concentrations in ng mL^{-1} were estimated by multiplying the difference in SN-38 levels between plasma samples treated and untreated with β-GLU by 1.448, as a molar equivalency factor.

Instrumental analysis

Chromatographic analyses were performed with a Shimadzu Class VP HPLC system, with an RF-10AXL fluorescence detector, controlled by Class VP 6.13 SP2 software. Separation was performed in an Eclipse Plus C8 column (150 x 4.6 mm, 5 µm, Agilent), protected by a C8 guard cartridge (4 x 3.0 mm, Phenomenex). The column temperature was set at 25 °C. Mobile phase was composed of a mixture of phosphate buffer 0.1 M pH 4.0 with acetonitrile (80:20, v/v), with a flow rate of 1 mL min^{-1}. Total run time was 19 min. Chromatograms were acquired at an excitation wavelength of 370 nm and an emission wavelength of 470 nm for IRI. Emission was set at 534 nm for SN-38 and IS. Detector sensitivity was set at an initial gain of 32x and increased to 128x at 10 min.

Linearity

Calibration models were evaluated at 8 levels, with sextuplicate analysis at the levels of 10, 25, 50, 100, 250, 500, 1,500 and 3,000 ng mL^{-1} for IRI and 1, 2.5, 5, 10, 25, 50, 150 and 300 ng mL^{-1} for SN-38. Calibration curves were constructed by calculating the ratios of the peak area of the analytes to the peak area of the IS and with the nominal concentrations of the calibration samples. Homoscedasticity of calibration data was evaluated with F-test at the confidence level of 95%, and calibration curves were fitted using least-squares linear regression using several weighting factors ($1/x$, $1/x^2$, $1/x^{0.5}$ $1/y$, $1/y^2$, $1/y^{0.5}$). The calibration models were evaluated by their correlation coefficients (r) and cumulative percentage relative

error (∑%RE) (13). Daily calibration curves using the same concentrations (single measurement per concentration) were prepared with each batch of validation and patients samples.

Precision and accuracy

Plasma samples containing IRI and SN-38 at the concentrations levels low (QCL), medium (QCM) and high concentrations (QCH), were analyzed in triplicate on each of 5 days. The nominal concentrations of QCL, QCM and QCH for IRI and SN-38 were 70, 700 and 2,000 ng mL^{-1} and 7, 70 and 200 ng mL^{-1}, respectively. Within-assay precision and between-day precision were calculated by ANOVA and expressed as CV%. Accuracy was calculated as the percentage of nominal concentration measured in the analytical procedure. The acceptance criteria for accuracy were mean values within ±15% of the theoretical value and for precision a maximum CV of 15% (14).

Lower limit of quantification

An independent plasma quality control sample at the lowest point of the calibration curve, 10 and 1 ng ml^{-1} for IRI and SN-38 respectively, was included in the accuracy and precision experiments (quality control at the limit of quantitation, QCLOQ) and was also tested in triplicate on five different days. The acceptance criteria established for the limit of quantification was accuracy within 100 ± 20% of the nominal value and a maximum CV of 20%.

Extraction efficiency

Extraction efficiency was calculated by the ratio of peak areas of IRI and SN-38 obtained at the QC samples to those obtained with the respective standard solutions corresponding to complete recovery, measured in triplicate. The extraction yield was calculated as percentage comparing the area of IRI and SN-38 in spiked samples and the reference solutions.

Selectivity

Selectivity was evaluated by testing 6 blank plasma samples obtained from 6 different human sources. They were prepared as described above to check for the presence of chromatographic peaks that might interfere with the detection of IRI, SN-38 or the IS.

Stability

For evaluation of stability at the HPLC autosampler, control samples of plasma containing IRI and SN-38 at the concentration levels of QCL and QCH were extracted, pooled and injected at time intervals of 1 h, during 12 h. Stability of analytes was tested by regression analysis plotting absolute peak areas corresponding to each compound at each concentration vs. injection time. Using the obtained linear regression, the concentration after 12 h was calculated. A decrease or increase of up to 10% in the measured peak areas was considered as acceptable. For estimation of freeze–thaw stability, plasma samples of patients were pooled to obtain two levels of controls, at low and high concentrations. They were analysed in triplicate before and after 3 freeze–thaw cycles. Differences in the measured concentrations from the end to the beginning of the series of up to 15% were accepted as indication of stability.

Method application

The method was applied to the measurement of IRI, SN-38, and SN-38G in plasma samples of patients receiving IRI in single or combined chemotherapy regimens. The study was cleared by the Ethics Review Board and informed consent was provided by all participants. Samples were collected 1 and 24 h after the beginning of the infusion, according to a population pharmacokinetics and limited sampling strategy previously described (15,16). The area under the curve (AUC) of IRI was calculated by minimizing an objective Bayesian function using the solver add-in from Microsoft Excel.

RESULTS AND DISCUSSION

Chromatography and sample preparation

Retention times were 8.2, 14.0 and 16.2 min for IRI, SN-38 and IS, respectively, with no interfering peaks present in blank samples (Figure 1). The sample preparation technique based on protein precipitation followed by liquid-liquid extraction provided extracts with a high degree of purity, potentially increasing the column working life. Differently from this study, most of the previously described HPLC-FL assays for IRI used ion pair reagents in the mobile phase, which requires longer equilibration times and extensive cleaning after use. Quantitation of SN-38G is essential to evaluate the metabolic detoxification of SN-38. However, SN-38G reference standards are hardly accessible, requiring sophisticated approaches such as biosynthesis by human expressed UGTs (17). Alternatively, estimation of SN-38G concentrations by enzymatic hydrolysis is an easy and straightforward approach to

evaluate the levels of this important IRI metabolite. The hydrolysis conditions applied in this study, including incubation time and β-GLU concentration, were optimized to render the highest hydrolysis efficiency. IRI and SN-38 present native fluorescence, allowing its sensitive and selective determination by FL detectors, dispensing the need for LC-MS/MS for measuring clinically relevant concentrations.

Considering the potential clinical applications of this method for dose individualization, in this study we present an optimized HPLC method with FL detection, with adequate sensibility for TDM of this important chemotherapeutic drug.

Figure 1. Chromatograms obtained with the assay.

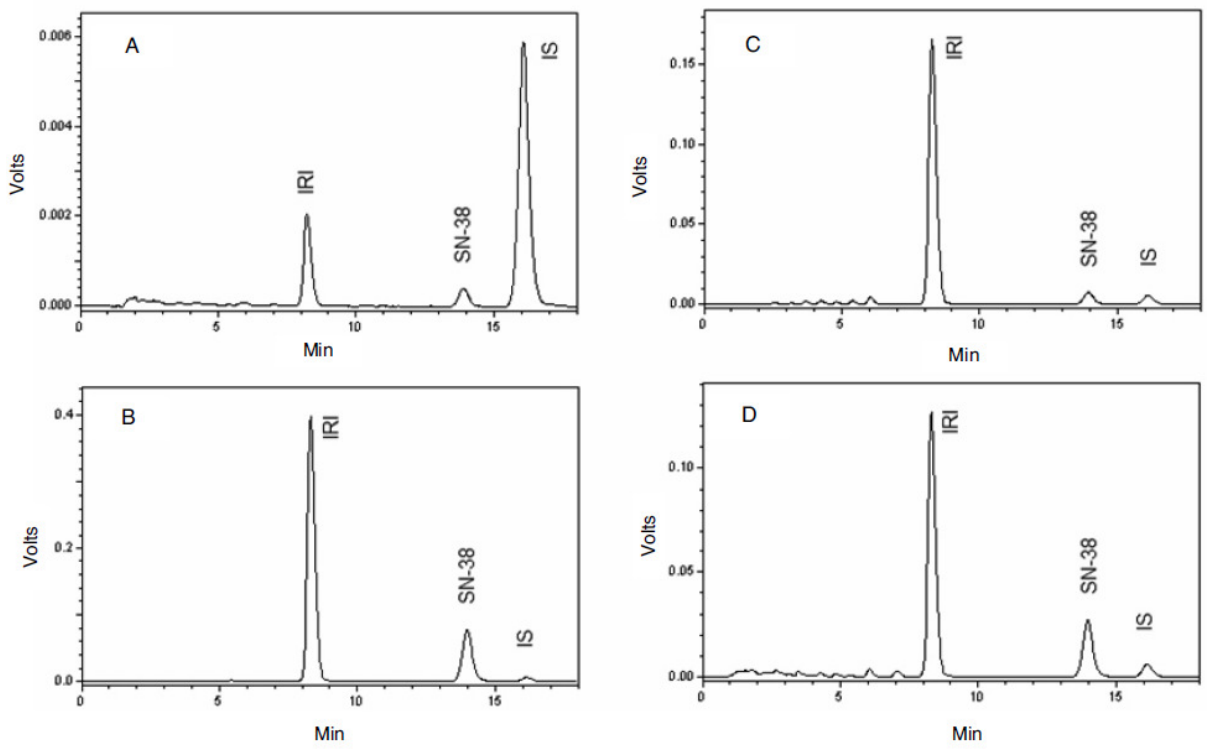

A: QCLOQ with IRI at 10 ng mL^{-1} and SN-38 at 1 ng mL^{-1}. **B:** QCH with IRI at 2,000 ng mL^{-1} and SN-38 at 200 ng mL^{-1}. C: Patient sample with IRI at 972.1 ng mL^{-1} and SN-38 at 21.9 ng mL^{-1}. **D:** Same patient sample as in C, but after β-GLU hydrolysis, with SN-38 at 67.5 ng mL^{-1} (SN-38G estimated as 65.9 ng mL^{-1}).

Method validation

Linearity was demonstrated in the range of 10 to 3,000 ng mL^{-1} IRI and from 1 to 300 ng mL^{-1} for SN-38, covering the wide range of concentrations expected in the employed limited sampling. With this wide calibration range, it was possible to quantify with a single calibration curve, samples from patients with high and low concentrations, corresponding to the collections of 1 and 24 hours after the start of the infusion, allowing calculating the AUC

with only two concentrations. Calibration data had significant heteroscedasticity (F_{IRI} = 81.190 and F_{SN-38} = 16.387; *F*crit (5,5; 0,95) = 5.05) and the best weighting factor for IRI and SN-38 was $1/x^2$, with Σ%RE of 9.9 x 10^{-14} and of 3.6 x 10^{-15} (Σ%RE of unweighted regression was -140.06 and -76.64, respectively) and was used for the further validation studies and for the routine application of the method. Coefficients of correlation were above 0.9999, exhibiting acceptable linearity.

The method's accuracy was within the range of 97.8-105.2%, intra-assay precision was 2.1-4.72%, and inter-assay precision was of 1.66-4.37% (Table 1). The QCLOQ sample presented accuracy of 99.4 and 100.3%, intra-assay precision of 5.7 and 10.3%, and inter-assay precision of 1.5 and 5.1% for IRI and SN-38, respectively. Extraction efficiency was greater than 40%. The limits of quantification for analytes were satisfactory for application of the method to clinical samples, at 10 ng mL^{-1} IRI and 1 ng mL^{-1} SN-38.

Table 1. Method validation parameters: precision, accuracy and extraction yield.

Analyte	QC sample	Nominal concentration (ng mL^{-1})	Precision (CV %)		Accuracy (%)	Extraction yield (%)
			Intra-assay	Inter-assay		
IRI	QCLOQ	10	5.70	1.54	99.4	-
	QCL	70	2.47	1.66	103.0	41.3
	QCM	700	4.22	2.57	98.2	40.3
	QCH	2000	4.24	2.94	97.8	41.0
SN-38	QCLOQ	1	10.30	5.12	100.3	-
	QCL	7	2.10	3.52	105.2	41.8
	QCM	70	4.02	3.04	98.5	42.1
	QCH	200	4.72	4.37	98.6	42.6

QCLOQ: quality control at the limit of quantification, QCL: quality control low, QCM: quality control medium, QCH: quality control high. (precision and accuracy n=45, extraction yield n= 9).

The chromatographic conditions employing a reversed phase column and isocratic elution with fluorescence detection proved capable of selectively separating analytes and endogenous compounds. No interfering peaks were detected in the tested blank samples. There was no indication of instability of the analytes in any of the tested conditions, demonstrating the feasibility of its processing in usual laboratory conditions. The extracts maintained in the autosampler were stable with a maximum variation in peak area ratios after 12 h of 98.6%, from the values in the beginning of the series (Table 2). It is therefore possible to conduct simultaneous extraction from a number of samples, storing them at room

temperature before proceeding to injection. And there was no indication of instability after three freeze–thaw cycles (Table 2).

Table 2. Processed sample stability at autosampler and freeze-thaw cycles.

Analyte	QC sample	Nominal concentration (ng mL^{-1})	Processed sample Concentration change after 12 h in AS (%)	QC sample	Nominal concentration (ng mL^{-1})	Freeze-thaw stability Concentration change after third cycle (%)
IRI	QCL	70	+0.7	PLL	53.9	-0.6
	QCH	2000	-0.8	PHL	1764.0	+0.9
SN-38	QCL	7	-0.7	PLL	2.1	-4.8
	QCH	200	-1.4	PHL	12.5	-4.0

QCL: quality control low, QCH: quality control high, AS: autosampler, PLL: patient low level, PHL: patient high level. (processed sample stability n=10, freeze–thaw cycles of pooled patient samples n=24).

Method application

IRI, SN-38 and SN-38G concentrations, measured in samples obtained from 10 patients, were in the range of 26.1 to 2802.1 ng mL^{-1}, of 1.23 to 18.08 ng mL^{-1} and of 8.93 to 210.5 ng mL^{-1}, respectively, with patients receiving IRI doses of 180 or 350 mg/m^2. IRI AUC was in the range of 4,843 to 17,502 ng h mL^{-1}. The glucuronidation ratio was in the range 2.92 to 12.5 and 5.9 to 26.8 in samples collected 1 and 24 h after the beginning of the infusion, respectively.

CONCLUSIONS

This work provides a fully validated and easily implementable method for the determination of IRI, SN-38, and SN-38G in human plasma samples using HPLC-FL equipment, fitted to the application of therapeutic drug monitoring of IRI in patients receiving common infusional chemotherapeutic regimens.

REFERENCES

(1) Tournigand C., T. André, E. Achille, G. Lledo, M. Flesh, D. Mery-Mignard, *et al.* (2004) *J. Clin. Oncol*. **22**: 229–237.

(2) Conroy T., C. Gavoille, E. Samalin, M. Ychou & M. Ducreux (2013) *Curr. Oncol.*

Rep. **15**: 182–189.

(3) Di Paolo A., G. Bocci, M. Polillo, M. Del Re, T. Di Desidero, M. Lastella, *et al*. (2011) *Curr. Drug Metab*. **12**: 932–43.

(4) Van Der Bol J.M., R.H.J. Mathijssen, G.J.M. Creemers, A.S.T. Planting, W.J. Loos, E.A.C. Wiemer, *et al.* (2010) *Clin. Cancer Res*. **16**: 736–742.

(5) Meyerhardt J. A. & R. J. Mayer (2005) *N. Engl. J. Med.* **352**: 476–87.

(6) Innocenti F. & M.J. Ratain (2006) *Pharmacogenomics.* **7**: 1211–1221.

(7) Toffoli G., E. Cecchin, G. Gasparini, M. D'Andrea, G. Azzarello, U. Basso, *et al.* (2010) *J. Clin. Oncol.* **28**: 866–871.

(8) Hirose K., C. Kozu, K. Yamashita, E. Maruo, M. Kitamura, J. Hasegawa, *et al.* (2012) *Oncol. Lett.* **3**: 694–698.

(9) Hirose K., K. Yamashita, H. Takada, N. Kaneda, K. Fukami, E. Maruo, *et al.* (2014) *Int. J. Clin. Oncol.* **19**: 397–402.

(10) Wang-Gillam A., C.P. Li, G. Bodoky, A. Dean, Y.S. Shan, G. Jameson, *et al.* (2016) *Lancet.* **387**: 545–557.

(11) Adiwijaya B., J. Kim, I. Lang, T. Csõszi, A. Cubillo, J.-S. Chen, *et al.* (2017) *Clin. Pharmacol. Ther.* **0**: 1–9.

(12) Mullangi R., P. Ahlawat & N.R. Srinivas (2010) *Biomed. Chromatogr.* **24**: 104–123.

(13) Almeida A.M., M.M. Castel-Branco & A.C. Falcão (2002) *J. Chromatogr. B.* **774:** 215–222.

(14) FDA, "Guidance for Industry: Bioanalytical Method Validation". Available at (http://www.fda.gov/downloads/Drugs/Guidance/ucm070107.pdf).

(15) Klein C.E., E. Gupta, J.M. Reid, P.J. Atherton, J.A. Sloan, H.C. Pitot, *et al*. (2002) *Clin. Pharmacol. Ther.* **72**: 638–647.

(16) Poujol S., F. Pinguet, M. Ychou, A.G. Abderrahim, J. Duffour & F.M.M. Bressolle (2007) *Oncol. Rep.* **18**: 1613–1621.

(17) Corona G., C. Elia, B. Casetta & G. Toffoli (2010) *Ther. Drug Monit*. **32**: 638–646.

4. CAPÍTULO 3 – DETERMINATION OF IRINOTECAN AND ITS METABOLITE SN-38 IN DRIED BLOOD SPOTS USING HIGH-PERMORMANCE LIQUID-CHROMATOGRAPHY WITH FLUORESCENCE DETECTION

Roberta Z Hahn[a,b], Priscila C Arnhold[a], Natália B Andriguetti[a,b], Anelise Schneider[a], Helena M Klück[c], Simone L dos Reis[c], Marcos Frank Bastiani[a,b], Igor Kael[a], Anne Caroline Cezimbra da Silva[a], Gilberto Schwartsmann[c], Marina V Antunes[a,b], Rafael Linden[a,b*]

[a]Analytical Toxicology Laboratory, Universidade Feevale, Novo Hamburgo-RS, Brazil
[b]Graduate Program on Toxicology and Analytical Toxicology, Universidade Feevale, Novo Hamburgo-RS, Brazil
[c]Oncology Service, Hospital de Clínicas de Porto Alegre, Porto Alegre-RS, Brazil

*Corresponding author

Journal of Pharmaceutical and Biomedical Analysis 150 (2018) 51–58.

HIGHLIGHTS

Irinotecan and SN-38 can be measured in clinical relevant concentrations in DBS by HPLC-FL.

Irinotecan and SN-38 are stable in DBS for 14 days at 42 °C.

Validation data support the clinical use of the assay.

Irinotecan and SN-38 have higher concentrations in whole blood than in plasma.

Irinotecan and SN-38 concentrations in DBS have higher correlation with plasma levels at high concentrations.

ABSTRACT

Irinotecan (IRI) is an antineoplastic drug widely used for the treatment of colorectal and advanced pancreatic cancer. Despite its clinical utility, the clinical use of IRI is associated with potentially severe hematopoietic and gastrointestinal toxicities. The quantification of IRI and its active metabolite SN-38 in dried blood spots (DBS) may be an alternative to individualize the drug dose through a minimally invasive and easy collection method. The aim of this study was to develop and validate a simple and fast HPLC-FL assay for simultaneous IRI and SN-38 measurement in DBS, with adequate analytical performance for clinical use. The method employs liquid extraction of one 8 mm disk of whole blood, followed by separation in a reversed phase Eclipse Plus C8 column (150 × 4.6 mm, 5 μm). Detection was performed with a fluorescence detector, with excitation wavelength of 370 and emission of 420 for IRI and 534 nm for SN-38 and internal standard (camptothecin). Total analytical run time was 17 min. Mobile phase was a mixture of 0.1 M phosphate buffer pH 4.0 and acetonitrile (80:20, v/v), at 1 mL min^{-1}. The assay was linear in the range 10 to 3,000 ng mL^{-1} and from 0.5 to 300 ng mL^{-1} for IRI and SN-38, respectively. Precision assays presented CV% of 2.71-5.65 and 2.15-10.07 for IRI and SN-38, respectively, and accuracy in the range of 94.26-100.93 and 94.24-99.33 %. IRI and SN-38 were stable at 25 and 42 °C for 14 days in DBS samples. The method was applied to DBS samples obtained from fingerpicks from 19 volunteers receiving IRI in single or combined chemotherapy regimens, collected 1 and 24 hours after beginning of the infusion. The estimated plasma concentration of IRI and SN-38 in sample collected 1 h after star of infusion presents 16 of 19 values within the ±20% range of the measured plasma concentrations. On the other hand, predictions of IRI and SN-38 plasma concentrations from DBS measurements obtained 24 h after the beginning of the infusion were poor. AUC of IRI that was calculated using plasma and DBS-estimated concentrations, with a high correlation (r = 0.918). The method presented suitable characteristics for the clinical use. However, translation of IRI and SN-38 DBS to plasma concentrations is challenging due to the compound's variable plasma/blood partition.

Keywords: Irinotecan; SN-38; dried blood spots; high-performance liquid chromatography; fluorescence detection; therapeutic drug monitoring.

GRAPHICAL ABSTRACT

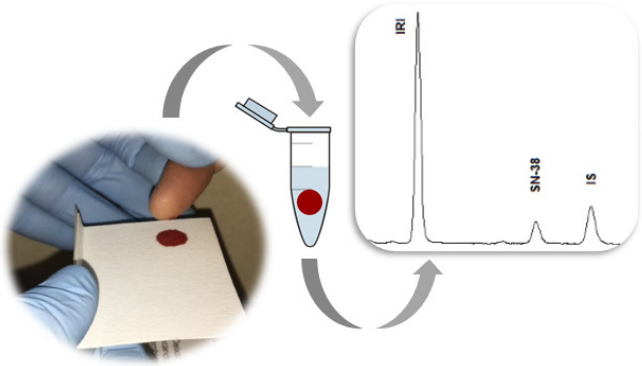

1. INTRODUCTION

Irinotecan (IRI) is a chemotherapeutic drug used in the treatment of colorectal [1] and advanced pancreatic cancer [2]. The primary active metabolite of IRI is SN-38 (7-ethyl-10-hydroxycamptothecin), formed by liver carboxylesterases. SN-38 is at least 100 times more cytotoxic than the parent drug and is detoxified through the formation of its glucuronide, SN-38G, mainly by UGT1A1. The antineoplastic activity of IRI and SN-38 is attributed to their inhibitory effect on DNA topoisomerase I, required for cellular DNA replication and transcription [3]. IRI, as most anticancer drugs, is a toxic compound at clinically used doses [4], and its use is associated to a wide interindividual variability in tolerability, with frequent occurrence of severe toxicity, primarily neutropenia and severe diarrhea [5]. This variability is partially related to interindividual pharmacokinetic differences, with a previous study being successful in adjusting IRI doses targeting a selected area under the curve (AUC) in order to minimize the occurrence of toxicity [4]. Alternative dose adjustment studies selected IRI doses based on genotyping or phenotyping approaches [6,7]. The observed relation between exposure to IRI and its principal active metabolite SN-38 with clinical effects, both for the classical [4] and the new, recently FDA approved, nanolipossomal formulation [8], suggest this drug may be a candidate for therapeutic drug monitoring (TDM). The estimation of pharmacokinetic parameters of IRI and its metabolites in previously published population pharmacokinetic models required complicated blood sampling schedules, limiting their clinical application [9,10]. In this context, the use of dried blood spots (DBS), usually obtained from fingerpricks, can potentially allow multiple sampling with minimal patient

burden [11]. Alongside with the minimally invasive sampling, potential advantages of DBS for TDM analyses includes reduced logistic costs for storage and transportation of specimens, analyte stabilization due to drying, increased biosafety, and the possibility of self-sampling [11–13]. However, as most reference drug concentration levels were established for plasma samples, translating DBS to plasma concentrations is the major limitation for the disseminated use of DBS in the TDM field. The major hurdle in this context is the effect of the hematocrit of the blood sample, which impacts the blood-to-plasma partition ratio, as well as the volume on the spot and, eventually, the drug extraction yield [14]. Particularly in the case of IRI and SN-38, the low concentration levels observed after usual doses and the small available blood volume in the DBS require highly sensitive analytical methods. There is no previous report of a DBS assay for IRI. The measurement of plasma levels of IRI and SN-38 has been accomplished by the use of liquid chromatography, coupled to either tandem mass-spectrometric (LC-MS/MS) or fluorescence detection (HPLC-FL), as reviewed by others [15]. HPLC-FL is a particularly interesting analytical method due to its selectivity and robustness, with reduced implementation costs when compared to LC-MS/MS. Considering the lack of assays for the determination of IRI and SN-38 in DBS and its potential applications for the individualization of chemotherapy, the aim of this study was to develop and validate a simple, selective, highly sensitive and cost-effective HPLC–FL method for the quantification of IRI and SN-38 in DBS.

2. EXPERIMENTAL

2.1. Reagents, materials and reference standard samples

Irinotecan hydrochloride (96.15% of IRI base), camptothecin (CPT) and SN-38 were acquired from Sigma-Aldrich (Saint Louis, United States). Methanol, acetonitrile, dimethyl-sulfoxide (DMSO), hydrochloric acid, orthophosphoric acid and monopotassium phosphate were purchased from Merck (Darmstadt, Germany). Whatman 903® paper was obtained from GE Healthcare (Westborough, United States). Ultrapure water was produced in an Elga Purelab Ultra® apparatus from Elga Labwater (High Wycombe, United Kingdom). For method validation, human blood was collected from healthy volunteers, and the hematocrit was measured by Sysmex KX-21N (Kobe, Japan). Blank blood used for the preparation of validation DBS samples had a Hct% of 40 unless otherwise stated.

2.2 Preparation of solutions and standards

IRI and CPT stock solutions at the concentrations of 1 and 0.2 mg mL^{-1}, respectively, were prepared by powder dissolution in a mixture of acetonitrile: orthophosphoric acid 1 mM (90:10, v/v). SN-38 stock solution was prepared in DMSO at the concentration of 0.5 mg mL^{-1}. IRI and SN-38 combined working solutions were prepared by dilution of the stock with acetonitrile to render concentrations of 100, 250, 500, 1,000, 2,500, 5,000, 15,000, 30,000 and 60,000 ng mL^{-1} and 5, 12.5, 25, 50, 125, 250, 750, 1,500 and 3,000 ng mL^{-1}, respectively. DBS extraction solvent was a mixture of acetonitrile and methanol (1:4, v/v), containing CPT (internal standard, IS) at 10 ng mL^{-1}. HPLC eluent was composed of phosphate buffer 0.1 M pH 4.0 and acetonitrile (80:20, v/v). Dried DBS extracts were recovered with a mixture of mobile phase and hydrochloric acid 1M (3:1, v/v). The presence of hydrochloric acid 1M is required to avoid the *in vitro* formation of the carboxylate form of both IRI and SN-38 [15].

2.3. Chromatography equipment and conditions

Chromatographic analyses were performed with a Class-VP HPLC-FL system, from Shimadzu (Kyoto, Japan). Separation was performed in an Eclipse Plus C8 column (150 × 4.6 mm, 5 μm), from Agilent Technologies (Santa Clara, United States), protected by a C8 guard cartridge (4 x 3.0 mm), from Phenomenex (Torrance, United States). The column temperature was set to 55 °C, with eluent flow rate fixed at 1.0 mL min^{-1}. Total chromatographic run time was 17 min. Chromatograms were acquired at the excitation wavelength of 370 nm, with emission wavelengths of 420 nm for IRI and 534 nm for SN-38 and IS. Detector sensitivity was set at an initial gain of 128 times, increasing to 16,384 times after 10 min.

2.4. Sample preparation

One punched DBS disk, with a fixed diameter of 8 mm, was used for extraction. The disc was transferred to a polypropylene microtube and added with 350 μL of extraction solution. After 30 min shaking at 500 rpm in a ThermoMixer® (Eppendorf), at 45 °C, an aliquot of 300 μL of the supernatant was transferred to another microtube and evaporated to dryness in a vacuum centrifuge at 45 °C (Concentrator Plus®, Eppendorf). The resulting dried extract was recovered with 150 μL of a mixture of mobile phase and hydrochloric acid 1M (3:1), vortex mixed and centrifuged at 15,000 g for 10 min, and 50 μL was injected into the HPLC-FL.

2.5. Selectivity

Blank DBS samples obtained from 10 different human sources were prepared as described above to check for the presence of chromatographic peaks that might interfere with detection of IRI, SN-38 or IS.

2.6. Linearity

Aliquots of 40 μL of the combined IRI and SN-38 working solutions were transferred to polypropylene microtubes and evaporated to dryness with an in a vacuum centrifuge at 45 °C (Concentrator Plus, Eppendorf). Dried working solutions were recovered with 400 μL of drug-free blood (Hct%=40) and gently homogenized for 5 min at 20 rpm. DBS calibration samples were prepared by pipetting 50 μL of blood in Whatman 903® paper, followed for a minimum drying time of 3 hours before extraction. Resulting calibrator concentrations were 10, 25, 50, 100, 250, 500, 1,500, 3,000 and 6,000 ng mL^{-1} for IRI, and 0.5, 1.25, 2.5, 5, 12.5, 25, 75, 150 and 300 ng mL^{-1} for SN-38. Six replicates at each concentration were analyzed, and calibration curves were calculated relating the area ratios of IRI and SN-38 peak to the IS peak with the nominal concentrations. Homoscedasticity of calibration data was evaluated with *F*-test at the confidence level of 95%. Weighted least-squares linear regression was used to generate calibration models, which were evaluated through their coefficients of correlation (*r*) and cumulative percentage relative error (Σ%RE) [15]. Daily calibration curves were analyzed within each batch of validation and clinical samples.

2.7. Precision and accuracy

Aliquots of blank blood were enriched with the working solutions and applied to paper to obtain quality control (QC) DBS samples containing IRI and SN-38 at concentrations of 70 and 7 (quality control low, QCL), 700 and 70 (quality control medium, QCM) and 2,000 and 200 ng mL^{-1} (quality control high, QCH), respectively. QC samples were processed and analyzed in triplicate, in each of 5 days. Within-assay precision and between-day precision were calculated by one-way analysis of variance and expressed as CV%. Accuracy was evaluated as the percentage of the nominal concentration represented by the concentration calculated with the calibration curve. The acceptance criteria for accuracy were mean values within ±15% of the theoretical value, and for precision, a maximum CV of 15% was accepted [16].

2.8. Lower limit of quantification

Precision and accuracy were also evaluated at the concentration level of the lowest calibrator, being tested in triplicate on five different days. These DBS QC sample (Quality control at the limit of quantification, QCLOQ), containing IRI and SN- 38 at 10 and 0.5 ng mL^{-1}, respectively, were prepared and processed as previously described. The acceptance criteria were accuracy within 100±20% of the nominal concentration and a maximum CV% of 20 [16].

2.9. Extract stability at the autosampler

DBS QC samples at low (QCL) and high (QCH) concentrations (n=6 each) were extracted as described above and the extracts obtained at each concentration level were pooled. Aliquots of these pooled extracts at each concentration were transferred to autosampler vials and injected under the conditions of a regular analytical run at time intervals of 1 h, during 12 h. Peak area ratios between beginning and end of the series were compared. A decrease or an increase of up to 15% in the measured peak areas was considered as acceptable [17].

2.10. Stability at varying temperatures

For evaluation of thermal stability of IRI and SN-38 in DBS, QC samples at low (QCL) and high (QCH) concentrations, were maintained at 25 and 42 °C and analyzed in triplicate 1, 7 and 14 days after spotting on the paper. Stability was considered acceptable if all results were within the range of 85–115% of the concentrations measured at the beginning of the series.

2.11. Determination of IRI and SN-38 in plasma

IRI and SN-38 were measured in plasma by HPLC-FL after protein precipitation, followed by liquid-liquid extraction. Briefly, 200 μL aliquots of plasma were transferred to polypropylene microtubes containing 100 μl of the IS solution (CPT, 300 ng mL^{-1} in acetone), previously dried in a vacuum centrifugal evaporator at 30 °C. After mixing, proteins were precipitated by the addition of 400 μL of a mixture of acetonitrile-methanol (50:50, v/v), followed by centrifugation at 15,000 g for 10 min. An aliquot of 400 μL of the obtained supernatant was transferred to a fresh polypropylene microtube and added with 1 mL of MTBE. After additional homogenization and centrifugation steps, an 850 μL aliquot of the supernatant was evaporated to dryness and recovered with 200 μL of a mixture of mobile

phase and hydrochloric acid 1M (3:1), being 50 µL injected into the HPLC-FL. Instrumental conditions were similar as those used for DBS samples, excluding the column temperature, which was set at 25 °C, and the emission wavelength for IRI, which was 470 nm. Linearity was demonstrated in the range of 10 to 3,000 ng mL^{-1} for IRI and from 0.5 to 300 ng mL^{-1} for SN-38. The method accuracy was within the range of 97.8-105.2%, with an intra-assay precision of 2.1 - 4.72% and inter-assay precision of 1.66-4.37% [18].

2.14. Influence of hematocrit on accuracy

Aliquots of blood containing differing hematocrit levels (Hct% of 25, 35 and 50) were prepared by adding or removing plasma to blank blood collected into EDTA containing tubes [19]. IRI and SN-38 were added to these aliquots of blood with differing hematocrit levels to achieve the concentrations of CQL and CQH and were pipetted onto Whatman 903® paper, followed by drying at room temperature for at least 3 h. The DBS thus created were analyzed as described above. The influence of the Hct% on IRI and SN-38 measurements was determined as the percentages of nominal concentrations that were measured in the DBS. Acceptance criteria were values in the range of 85-115%.

2.15. Influence of hematocrit on extraction yield

Aliquots of 18 µL of blood (Hct% 25, 35 and 50) containing IRI and SN-38 at concentrations of QCL and QCH, and non-spiked blood were added to Whatman 903® paper and allowed to dry at ambient temperature for at least 3 hours. Whole spots were cut and extracted, as described previously, in triplicate. Non-spiked extracts were added with IRI and SN-38 solutions to obtain final concentrations equivalent to 100% extraction yield. Extraction yield was calculated comparing the area ratios of IRI and SN-38 to the internal standard in control and non-spiked samples.

2.16. Influence of spotted blood volume on accuracy

Blood with Hct% of 40 was prepared as described above and IRI and SN-38 were added to achieve concentrations of CQL and CQH, and was then pipetted onto Whatman 903® paper at the volumes of 30, 40 and 55 µL, consistent with fingerprick blood drops. After drying, the obtained DBS were analyzed as described above and IRI and SN-38 were quantified with a calibration curve prepared after pipetting 50 µL of blood to paper. In all extractions, 8 mm disks were used for testing. The influence of the Hct on IRI and SN-38 measurements was determined as the percentages of the nominal concentrations that were

actually measured in the DBS. The acceptance criterion was a maximum deviation of ± 15% from nominal concentrations.

2.17. Method application

DBS, obtained after fingerpricks, and venous blood samples, from which plasma was separated by centrifugation, were obtained simultaneously (within 3 min) from 19 volunteers receiving IRI in single or combined chemotherapy regimens. Samples were collected 1 and 24 h after the beginning of the infusion (90 minutes), according to a population pharmacokinetics and limited sampling strategy previously described [9,10]. Hct was measured from an aliquot of the venous blood by standard hematology procedures. The study was approved by the institutional review board of Hospital de Clínicas de Porto Alegre, and performed according to the Helsinki declaration principles. Informed consent was obtained from all volunteers.

2.18. Comparison between concentrations measured in DBS and plasma samples

An estimated plasma concentration was calculated using the equation EPCHct = (DBSconc/[1-(Hct/100)]) × fp where DBSconc is the concentration measured in DBS, Hct is the individual hematocrit of patient and fp is the fraction of the drug in plasma, according to Antunes et al. [11]. The fp value was adjusted to obtain a mean ratio between the measured IRI and SN-38 plasma concentrations and EPC of 1, using the above equation. EPC was also calculated using a correction factor based on the mean ratio of IRI and SN-38 plasma to DBS concentrations, without considering the individual Hct nor fp (EPCfactor). A third approach for the calculation of estimated plasma concentrations from DBS measurements (EPCequation) was to apply the regression equation obtained after correlating plasma (y) to DBS concentrations (x). Area under the curve (AUC) for IRI was calculated using the Solver supplement in Microsoft Excel and applying a three-compartment pharmacokinetic model and population data previously described [10]. Considering that AUC of IRI was successfully used in the past as a predictor of toxicity after chemotherapy [4] we arbitrarily defined the mean AUC of the used chemotherapy regimens, ± 1 standard deviation (CV% of 30), as a exposure target to evaluate the concordance of prediction based on plasma and DBS IRI concentrations [7,10]. In this arbitrary classification, patients presenting AUC within ± 1 standard deviation of the mean were classified as adequately exposed, and patients with AUC values below and above this range were classified as under or overexposed to IRI, respectively.

3. RESULTS AND DISCUSSION

3.1. Chromatography and sample preparation

Fluorescence detection coupled to liquid-chromatographic separation has been reported for determination of IRI and SN-38 in plasma [15], but there is no report of an assay for these compounds in DBS. However, the high sensitivity of these assays makes HPLC-FL a viable and cost-effective alternative for IRI determination in a typical DBS, which usually contains 16-18 μL of blood [20]. Using the chromatographic conditions described in this manuscript, IRI, SN-38 and IS had retention times of 8.20, 13.03 and 15.33 min, respectively (Figure 1), with a total run time of 17 min. Whatman 903® paper was used as DBS substrate due to its wide availability, low purchase cost and high degree of standardization [11]. Sample preparation was based on a simple, single step, solvent extraction, followed by extract evaporation and injection of the extract recovered with a mixture of mobile phase and hydrochloric acid 1M (3:1).

Figure 1. Chromatograms obtained with the assay.

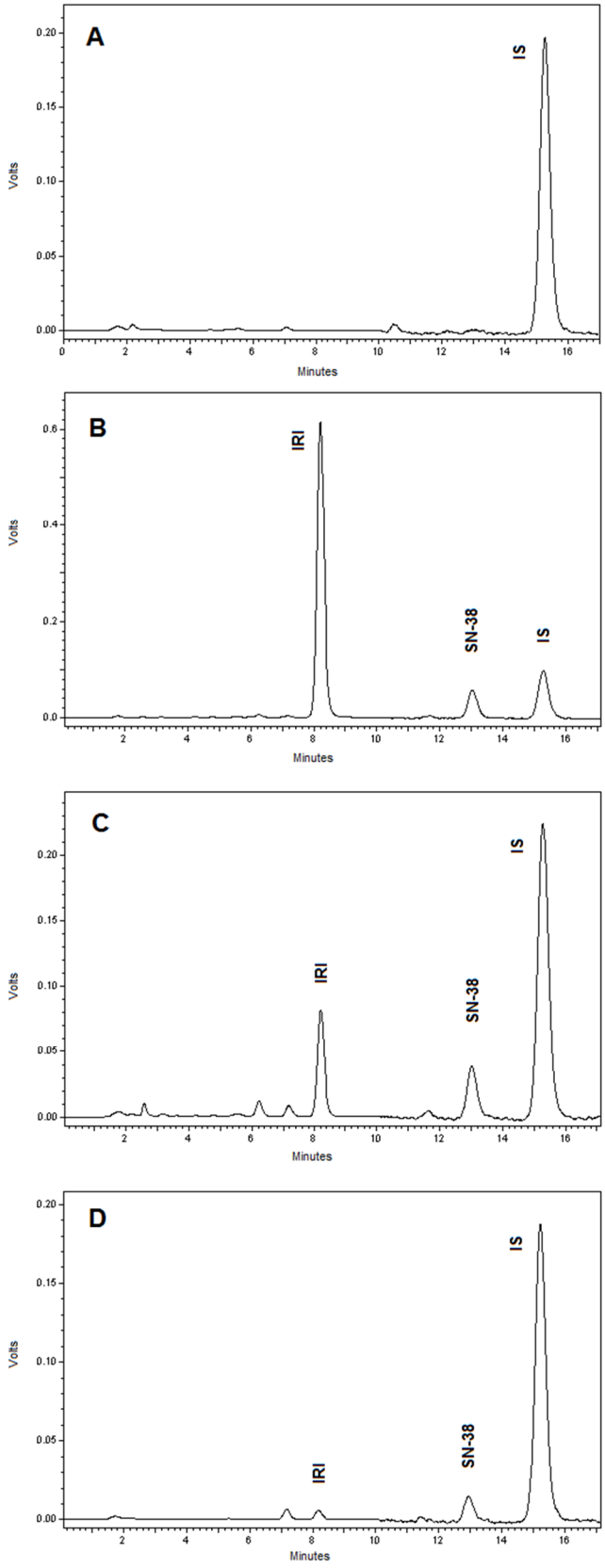

A: Blank DBS. **B:** Patient sample collected 1 hour after the start of the infusion, with IRI at 2068 ng mL^{-1} and SN-38 at 9.7 ng mL^{-1} **C**: Same patient sample as in B, but sample collected 24 hours after the start of the infusion, with IRI at 118.0 ng mL^{-1} and SN-38 at 2.9 ng mL^{-1}. **D**: Quality control at the limit of quantification (QCLOQ) containing IRI and SN-38 at 10 and 0.5 ng mL^{-1}, respectively.

3.2. General method validation

Fluorescence detection at selected wavelengths was highly selective and no interfering peaks were detected in the tested blank samples. Processed sample stability was tested with control samples of IRI and SN-38 at low (QCL) and high (QCH) concentrations, being both stable at the chromatograph's autosampler, with signal variations in the range of -1.97 to +3.55% and -6.61 to +2.78% after 12 hours, respectively (Table 1).

Table 1. Method validation parameters: precision, accuracy and processed sample stability at autosampler.

Analyte	QC sample	Nominal concentration (ng mL^{-1})	Precision (CV %)		Accuracy (%)	Processed sample concentration change after 12 h in AS (%)
			Intra-assay	Inter-assay		
IRI	QCLOQ	10	5.65	5.35	100.93	-
	QCL	70	3.38	5.35	99.95	-1.97
	QCM	700	2.71	3.02	96.46	-
	QCH	2,000	4.16	3.70	94.26	+3.55
SN-38	QCLOQ	0.5	10.07	9.61	99.33	-
	QCL	7	3.67	6.24	97.43	-6.61
	QCM	70	2.41	2.15	94.24	-
	QCH	200	4.19	3.74	96.07	+2.78

QCLOQ: quality control at the limit of quantitation, QCL: quality control low, QCM: quality control medium, QCH: quality control high, AS: autosampler (precision and accuracy n=45, processed sample stability n=12).

Calibration data presented significant heteroscedasticity (*F* values of 2757.6 and 716.6 for IRI and SN-38, respectively, against *Ftab* of 5.05). Several weighting factors were tested to the calibration data, and among the evaluated weighting factors, $1/x^2$ presented the lowest cumulative error for IRI and SN-38 (Σ%RE= 1.3 x 10^{-13} and 1.9 x10^{-13}) and was used for all quantitative measurements. Precision and accuracy fulfilled the acceptance criteria (Table 1), with intra-assay precision in the range of 2.71 to 4.16% and 2.41 to 4.19% for IRI and SN-38, respectively, whereas inter-assay precision ranged between 3.02 and 5.35% and 2.15 and 6.24% for both compounds. Accuracy was in the range of 94.3 to 99.9% for IRI and 94.2 to 97.4% for SN-38. The lower quantifiable concentration of the method was 10 ng mL^{-1} for IRI and 0.5 ng mL^{-1} for SN-38, which were selected based on expected clinical concentrations. It is important to note that such sensitivity was obtained using only one DBS, with 8 mm of diameter, which has, in average, 18 μL of whole blood. The lowest limit of quantification

presented intra-assay and inter-assay precision of 5.65 and 5.35% for IRI and 10.07 and 9.61% for SN-38, with an accuracy of 100.9 and 99.3% for the same compounds.

3.3. Specific DBS method validation

IRI and SN-38 stability in DBS were tested at room and high temperatures (25 and 42 °C, respectively) in an attempt to simulate transport conditions in the regular mail service and long laboratory handling times (Table 2). Considering an acceptance range of 85-115% for accuracy, both compounds were stable for 14 days under the tested conditions, with measured concentrations in the range 87.1-98.6% for IRI and 97.0-108.6% for SN-38 (Table 2). Considering the standard transport time of the mail service, we believe that a 14 days stability of IRI and SN-38 in DBS is acceptable for clinical use.

Table 2. Long term stability of IRI and SN-38 in DBS maintained at different temperatures (percentage of nominal concentration).

Analyte	QC sample	Nominal concentration (ng mL $^{-1}$)	Temperature (°C)	Day 7	Day 14
IRI	QCL	70	25	92.7	88.8
			42	90.5	87.1
	CQH	2,000	25	98.6	95.4
			42	98.5	96.0
SN-38	QCL	7	25	97.1	104.2
			42	97.0	101.8
	QCH	200	25	99.9	101.0
			42	108.6	108.1

QCL: quality control low, QCH: quality control high (n=3 for each concentration at each day and temperature).

As the blood Hct can affect the amount of blood in a spot with a fixed diameter, as well as the extraction yield of the analytes from the cellulose matrix, the impact of the Hct on the IRI and SN-38 measurements in DBS was also evaluated. Considering the existence of patients with widely different Hct values in the clinical setting, we evaluated the effect of Hct on measurement accuracy at the Hct% values of 25, 35 and 50 (Table 3). Accuracy was in the range of 93.7 to 104.6% for IRI and between 92.5 to 108.0% for SN-38, being the smaller value observed in a control sample with Hct% value of 25, due to the reduced viscosity of the blood, which results in a smaller volume of blood in the 8 mm punch. On the other hand, the

higher value observed in a control sample with Hct% of 50, due to a higher volume of blood in the disk. Although being acceptable, the accuracy could be improved if the corrected blood volume of blood in the DBS is taken into consideration [20]. In this case, accuracy values were in the range of 95.2 to 102.0%, and of 96.2 to 105.4 %, for IRI and SN-38, respectively (Table 3). Extraction yield was moderately affected by Hct and presented variations according to IRI and SN-38 concentrations, decreasing at high concentrations, an effect that can be compensated by matrix-matched calibration curves. Extraction yield for IRI was in the range of 55.9 to 64.4% and of 44.6 to 55.2% for QCL and QCH levels, respectively, being smaller with the increase of the Hct%.

Table 3. Evaluation of the influence of Hct on the accuracy and extraction yield of IRI and SN-38 in DBS.

Analyte	Hct (%)	QC sample	Nominal concentration (ng mL^{-1})	Accuracy (%)	Volume-corrected accuracy (%)	Extraction yield (%)
IRI	25	QCL	70	94.8	102.0	64.37
		QCH	2,000	93.7	100.8	55.22
	35	QCL	70	99.3	100.8	62.21
		QCH	2,000	97.4	98.9	50.51
	50	QCL	70	104.6	95.5	55.87
		QCH	2,000	104.3	95.2	44.58
SN-38	25	QCL	7	97.9	105.4	64.49
		QCH	200	92.5	99.5	54.76
	35	QCL	7	101.5	103.0	63.08
		QCH	200	98.4	99.9	49.41
	50	QCL	7	105.3	96.2	55.59
		QCH	200	108.0	98.6	43.28

QCL: quality control low, QCH: quality control high (n =3 for each control sample, at each Hct% value).

Calibration and QC samples were prepared by spotting 50 μL of whole blood fortified with IRI and SN-38 in Whatman 903® paper. When spotting other volumes, consistent with drops obtained from fingerpricks (30, 40 and 55 μL), no significant impact on the accuracy of both analytes measurements at two concentration levels was observed, with measured IRI and SN-38 levels in the range of 88.8 to 106.4% and 91.2 to 106.5% of nominal values, respectively (Table 4).

Table 4. Evaluation of the influence of spotted volume on the accuracy of IRI and SN-38 measurements in DBS.

Analyte	Volume (µL)	QC sample	Nominal concentration (ng mL $^{-1}$)	Accuracy (%)
IRI	30	QCL	70	104.9
		QCH	2,000	88.8
	40	QCL	70	103.1
		QCH	2,000	90.2
	55	QCL	70	106.4
		QCH	2,000	92.2
SN-38	30	QCL	7	106.5
		QCH	200	91.2
	40	QCL	7	100.8
		QCH	200	92.0
	55	QCL	7	100.6
		QCH	200	94.0

QCL: quality control low, QCH: quality control high (n =3 for each control sample, at each volume).

3.4. Method application

The developed method was applied to samples obtained from 19 patients receiving IRI chemotherapy. Patients received regimens containing IRI as single chemotherapeutic agent at the dose of 350 mg m^{-2} (n= 4) or the combined FOLFIRI regimen, with IRI doses ranging from 133 to 200 mg m^{-2} (n=15). Patients had Hct% in the range of 26.1 to 45.1. Plasma concentrations were estimated from DBS collected by fingerpricks using three different approaches (EPCHct, EPCfactor and EPCequation). Measured concentrations are presented in table 5. DBS samples collected 1 h after the beginning of the infusion presented IRI concentrations in the range of 1,091 to 5,213 ng mL^{-1} (606 to 2,802 ng mL^{-1} in plasma) and SN-38 concentrations in the range of 3.45 to 18.93 ng mL^{-1} (3.09 to 19.29 ng mL^{-1} in plasma). The average plasma/DBS ratio for IRI in this collection time was 0.57 (range 0.44-0.85) and 0.85 (range 0.57-1.08) for SN-38. DBS samples collected 24 h after the beginning of the infusion presented IRI concentrations in the range of 38.4 to 393.1 ng mL^{-1} (12.8 to 110.0 ng mL^{-1} in plasma) and SN-38 concentrations in the range of 0.56 to 3.08 ng mL^{-1} (0.58 to 2.97 ng mL^{-1} in plasma). The average plasma/DBS ratio for IRI in this collection time was 0.39 (range 0.17-0.72) and 0.97 (range 0.60-1.74) for SN-38.

Table 5. Summary of measured and estimated irinotecan and SN-38 concentrations obtained from patients (n=19).

	Sample collection time (h)	Irinotecan					SN-38		
		Plasma (ng mL^{-1})	DBS (ng mL^{-1})	$EPC_{Equation}$ (% of plasma levels)	AUC from plasma levels (µg x h mL^{-1})	AUC from $EPC_{Equation}$ (µg x h mL^{-1})	Plasma (ng mL^{-1})	DBS (ng mL^{-1})	EPC_{Factor} (% of plasma levels)
1	1	2802.10	5213.31	95.20	17.502	16.272	18.08	17.94	84.00
	24	77.66	214.73	80.47			2.12	2.36	107.69
2	1	2237.02	3868.26	91.41	10.225	10.503	16.81	18.62	93.82
	24	29.24	105.57	140.33			2.97	2.15	70.34
3	1	1687.70	2925.00	95.29	12.169	10.906	15.16	15.84	88.49
	24	68.12	160.16	75.99			2.91	3.08	102.81
4	1	1287.88	2324.15	103.27	9.230	9.228	7.08	8.78	105.04
	24	42.54	87.20	87.97			1.89	1.86	95.33
5	1	1435.56	2304.97	92.03	10.065	9.285	9.91	11.28	96.41
	24	44.73	108.11	92.85			1.23	1.40	109.94
6	1	972.15	1144.82	80.65	6.688	5.561	19.29	18.93	83.09
	24	39.10	85.15	94.67			1.28	1.39	104.68
7	1	1566.26	2574.29	92.31	9.851	9.622	10.82	11.87	92.93
	24	47.34	176.13	115.97			1.81	2.54	135.63
8	1	2391.85	5090.77	109.16	17.105	17.446	13.07	16.15	104.61
	24	109.97	393.12	88.72			1.57	2.47	152.75
9	1	982.20	1770.48	109.32	6.762	9.359	7.51	10.36	116.84
	24	21.52	90.69	177.08			0.91	0.89	94.21
10	1	605.99	1091.34	125.29	4.780	6.807	7.10	9.89	117.93
	24	42.24	249.77	164.26			2.19	2.49	110.23
11	1	1220.24	2307.62	108.37	8.442	9.987	7.90	9.83	105.36
	24	42.39	209.88	145.16			1.41	2.36	162.72
12	1	1300.08	2080.10	93.61	4.859	6.768	8.90	8.23	78.30
	24	12.77	38.40	217.96			0.58	0.56	93.58
13	1	1653.58	3389.83	110.27	10.310	11.282	14.07	17.65	106.21

	24	43.64	127.45	103.87			1.63	1.71	101.39
14	1	1076.66	2437.22	128.40	8.539	8.382	3.09	3.43	94.41
	24	64.64	118.67	67.46			1.16	0.67	55.67
15	1	1223.41	2169.52	102.86	7.426	6.908	14.26	14.84	88.12
	24	31.12	43.22	92.47			1.12	0.97	83.93
16	1	1878.69	3282.42	94.41	12.710	12.338	9.64	13.38	117.47
	24	41.02	148.49	120.60			1.21	1.15	92.45
17	1	1331.02	2536.56	107.32	9.763	9.866	8.95	13.71	129.70
	24	46.36	86.52	80.43			2.67	2.82	102.20
18	1	1057.00	2068.38	114.63	7.249	7.777	5.56	9.71	148.00
	24	46.49	118.04	93.54			1.74	2.86	159.16
19	1	1598.12	2142.40	77.96	11.176	8.268	9.83	11.33	97.53
	24	54.09	82.68	67.53			1.48	1.44	94.57

IRI concentrations measured in DBS obtained from fingerpricks, and DBS obtained from venous blood, after phlebotomy, were highly correlated, with r = 0.954 and 0.976 for the collection times of 1 and 24 h post-infusion, respectively. IRI plasma and DBS concentrations presented a higher correlation at the collection time of 1 h post infusion when compared with levels measured after 24 h, with r values of 0.949 and 0.766, respectively. For SN-38, there was also a high correlation between concentrations in DBS obtained from fingerpricks and venous blood, with r = 0.934 and 0.925 at the collection times of 1 and 24 h post-infusion. SN-38 levels in plasma and DBS also presented a higher correlation in measurements from samples obtained at the collection time of 1 h than at 24 h, with r = 0.933 and 0.796, respectively. The estimation of IRI plasma concentrations from DBS obtained from fingerpricks using the EPCHct approach at the sample collection time of 1 h after the beginning of the infusion, utilizing an fp value of 0.37, allowed to estimate 14 of 19 values within ±20% of the measured plasma concentrations. For the same set of data, EPCfactor, using a multiplication factor of 0.57, presented 15 of 19 values within ±20% of the measured plasma concentrations. The best predictive performance for these concentration data was obtained using the regression equation (y=0.463x+253.96), with EPCequation presenting 16 of 19 values within the ±20% range and all estimated concentrations within a ±30% range. In the other hand, predictions of IRI plasma concentrations from DBS measurements obtained 24 h after the beginning of the infusion were poor, with EPCHct (fp=0.22), EPCfactor (multiplication factor of 0.39) and EPCequation (y=0.1966x+20.28) presenting only 6, 7 and 10 values, respectively, within the ±20% range of the 19 measured plasma levels. When calculating IRI AUC with EPCequation, 15 among 19 values were within a ±20% range of those obtained with measured plasma concentrations, and all AUC values were within a ±45% range of values calculated with plasma measurements.

The AUC of IRI was calculated using both plasma and EPCequation values (Table 5) were highly concordant, with r = 0.918. Using the mean AUC ± 1 standard deviation as an arbitrarily exposure target to classify the patient's exposure to IRI, 17 patients had concordant classification when using plasma or DBS levels to calculate AUC (5 patients had IRI with the target and 14 had exposures below the target). This preliminary result, with a small number of observations, indicate that estimation of IRI AUC using DBS is a promising alternative, particularly considering the complex sampling usually required for limited sampling strategies. However, additional evaluations in larger groups of patients are needed to validate the clinical use of DBS for estimation of IRI plasma AUC.

The estimation of plasma concentrations of SN-38 from DBS values was also more effective for samples collected 1 h after the beginning of the infusion. For this set of concentrations, EPCHct (fp=0.54) estimated 13 of 19 values within ±20% of the measured plasma concentrations, whereas EPCequation (y=0.9947x-1.7641) estimated 15 of 19 values within ±20% of the measured plasma concentrations. Differently, for IRI, the best predictive performance was obtained using a multiplication factor of 0.85, EPCfactor presenting 16 of 19 values within ±20% range and with 18 out of 19 with a ±30% range. As well as was observed with IRI, predictions of SN-38 plasma concentrations from DBS measurements obtained 24 h after the beginning of the infusion were also poor. In this case, EPCHct (fp=0.59), EPCfactor (multiplication factor of 0.97) and EPCequation (y=0.6623x+0.4524) presented 12, 13 and 13 values, out of 19, within the ±20% range of actual plasma levels.

Translation of DBS concentrations to plasma levels, biological matrix in which most of the pharmacokinetic information is based, is a major challenge. The distribution of drug between plasma and blood cells is affected by a number of individual and pathological variables, such as inflammatory and nutritional status, disease state, smoking habits [21], renal functions [22], etc. The plasma protein binding of IRI and SN-38 was reported as is 65 and 95%, respectively [23]. As it is usually accepted that only the unbound fraction of drug in plasma in able to partition into erythrocytes, it is to be expect relatively more IRI in the red blood cells compared with SN-38 in vivo, what was confirmed by our observations. In this study, IRI levels in DBS were shown to be a promising alternative suitable to predict exposure to the drug through AUC, whereas the correlation between SN-38 concentrations in DBS and plasma levels was poorer. Additional studies, with larger groups of patients, are needed to evaluate if DBS concentrations can be correlated with clinical endpoints, allowing its clinical use for IRI dose individualization.

4. CONCLUSIONS

A high-performance liquid chromatography-fluorescence detection assay for the simultaneous quantification of IRI and SN-38 in a single dried blood spot, with about 18 μL of whole blood, was developed and validated. IRI and SN-38 were stable in DBS for up to two weeks at 42 °C. IRI and SN-38 concentrations in plasma and DBS from patients receiving IRI chemotherapy presented concentration-dependent correlations. Besides the difficulties to translate DBS measurements to IRI and SN-38 plasma levels, due to its unique blood/plasma

distribution behavior, the relation of IRI and SN-38 DBS concentrations with clinical endpoints requires further investigation.

REFERENCES

[1] C. Tournigand, T. André, E. Achille, G. Lledo, M. Flesh, D. Mery-Mignard, E. Quinaux, C. Couteau, M. Buyse, G. Ganem, B. Landi, P. Colin, C. Louvet, A. De Gramont, FOLFIRI followed by FOLFOX6 or the reverse sequence in advanced colorectal cancer: A randomized GERCOR study, J. Clin. Oncol. 22 (2004) 229–237. doi:10.1200/JCO.2004.05.113.

[2] T. Conroy, C. Gavoille, E. Samalin, M. Ychou, M. Ducreux, The role of the FOLFIRINOX regimen for advanced pancreatic cancer, Curr. Oncol. Rep. 15 (2013) 182–189. doi:10.1007/s11912-012-0290-4.

[3] A. Di Paolo, G. Bocci, M. Polillo, M. Del Re, T. Di Desidero, M. Lastella, R. Danesi, Pharmacokinetic and pharmacogenetic predictive markers of irinotecan activity and toxicity., Curr. Drug Metab. 12 (2011) 932–43. doi:10.2174/138920011798062283.

[4] J.M. Van Der Bol, R.H.J. Mathijssen, G.J.M. Creemers, A.S.T. Planting, W.J. Loos, E.A.C. Wiemer, L.E. Friberg, J. Verweij, A. Sparreboom, F.A. De Jong, A CYP3A4 phenotype-based dosing algorithm for individualized treatment of irinotecan, Clin. Cancer Res. 16 (2010) 736–742. doi:10.1158/1078-0432.CCR- 09-1526.

[5] M.D. Jeffrey A. Meyerhardt, M.D., M.P.H., and Robert J. Mayer, Systemic Therapy for Colorectal Cancer, N. Engl. J. Med. 352 (2005) 476–87.

[6] F. Innocenti, R.L. Schilsky, J. Ramírez, L. Janisch, S. Undevia, L.K. House, S. Das, K. Wu, M. Turcich, R. Marsh, T. Karrison, M.L. Maitland, R. Salgia, M.J. Ratain, Dose-finding and pharmacokinetic study to optimize the dosing of irinotecan according to the UGT1A1 genotype of patients with cancer, J. Clin. Oncol. 32 (2014) 2328–2334. doi:10.1200/JCO.2014.55.2307.

[7] H.H.J. Mathijssen Ron, F.A. de Jong, R.H.N. van Schaik, E.R. Lepper, L.E. Friberg, T. Rietveld, P. de Bruijn, W.J. Graveland, W.D. Figg, J. Verweij, A. Sparreboom, Prediction of irinotecan pharmacokinetics by use of cytochrome P450 3A4 phenotyping probes, J. Natl. Cancer Inst. 96 (2004) 1585–1592. doi:10.1093/jnci/djh298.

[8] B. Adiwijaya, J. Kim, I. Lang, T. Csõszi, A. Cubillo, J.-S. Chen, M. Wong, J. Park, J. Kim, K. Rau, B. Melichar, J. Gallego, J. Fitzgerald, B. Belanger, I. Molnar, W. Ma,

Population Pharmacokinetics of Liposomal Irinotecan in Patients With Cancer, Clin. Pharmacol. Ther. 0 (2017) 1–9. doi:10.1002/cpt.720.
[9] C.E. Klein, E. Gupta, J.M. Reid, P.J. Atherton, J.A. Sloan, H.C. Pitot, M.J. Ratain, H. Kastrissios, Population pharmacokinetic model for irinotecan and two of its metabolites, SN-38 and SN-38 glucuronide, Clin. Pharmacol. Ther. 72 (2002) 638–647. doi:10.1067/mcp.2002.129502.
[10] S. Poujol, F. Pinguet, M. Ychou, A.G. Abderrahim, J. Duffour, F.M.M. Bressolle, A limited sampling strategy to estimate the pharmacokinetic parameters of irinotecan and its active metabolite, SN-38, in patients with metastatic digestive cancer receiving the FOLFIRI regimen, Oncol. Rep. 18 (2007) 1613–1621.
[11] M.V. Antunes, M.F. Charão, R. Linden, Dried blood spots analysis with mass spectrometry: Potentials and pitfalls in therapeutic drug monitoring, Clin. Biochem. 49 (2016) 1035–1046. doi:10.1016/j.clinbiochem.2016.05.004.
[12] T.V. Popov, L.C. Maričič, H. Prosen, D.B. Vončina, Development and validation of dried blood spots technique for quantitative determination of topiramate using liquid chromatography-tandem mass spectrometry., Biomed. Chromatogr. 27 (2013) 1054–61. doi:10.1002/bmc.2905.
[13] E. Shokry, F. Villanelli, S. Malvagia, A. Rosati, G. Forni, S. Funghini, D. Ombrone, M. Della Bona, R. Guerrini, G. La Marca, Therapeutic drug monitoring of carbamazepine and its metabolite in children from dried blood spots using liquid chromatography and tandem mass spectrometry, J. Pharm. Biomed. Anal. 109 (2015) 164–170. doi:10.1016/j.jpba.2015.02.045.
[14] Y. Enderle, K. Foerster, J. Burhenne, Journal of Pharmaceutical and Biomedical Analysis Clinical feasibility of dried blood spots : Analytics , validation , and applications, 130 (2016) 231–243.
[15] R. Mullangi, P. Ahlawat, N.R. Srinivas, Irinotecan and its active metabolite, SN38: Review of bioanalytical methods and recent update from clinical pharmacology perspectives, Biomed. Chromatogr. 24 (2010) 104–123. doi:10.1002/bmc.1345.
[16] A.M. Almeida, M.M. Castel-Branco, A.C. Falcão, Linear regression for calibration lines revisited: Weighting schemes for bioanalytical methods, J. Chromatogr. B Anal. Technol. Biomed. Life Sci. 774 (2002) 215–222. doi:10.1016/S1570-0232(02)00244-1.
[17] FDA, Guidance for Industry: Bioanalytical Method Validation, (2001).
[18] R.Z. Hahn, P.C. Arnhold, N.B. Andriguetti, A. Schneider, H.M. Klück, R.M.M. Vilela, S.L. Dos Reis, G. Schwartsmann, M. V Antunes, R. Linden, An Easily Implementable Liquid

Chromatography Assay for Therapeutic Drug Monitoring of Irinotecan and Major Metabolites in Plasma, Lat. Am. J. Pharm. 36 (2017) 1–6.
[19] R.A. Koster, J.W. Alffenaar, R. Botma, B. Greijdanus, D.J. Touw, D.R. Uges, J.G. Kosterink, What is the right blood hematocrit preparation procedure for standards and quality control samples for dried blood spot analysis?, Bioanalysis. 7 (2015) 345–351. doi:10.4155/bio.14.298 [doi].
[20] R.Z. Hahn, M.V. Antunes, P. Costa Arnhold, N.B. Andriguetti, S.G. Verza, R. Linden, Determination of topiramate in dried blood spots using singlequadrupole gas chromatography–mass spectrometry after flash methylation with trimethylanilinium hydroxide, J. Chromatogr. B Anal. Technol. Biomed. Life Sci. 1046 (2017) 131–137. doi:10.1016/j.jchromb.2017.01.047.
[21] H. Dumez, G. Guetens, G. De Boeck, M.S. Highley, E.A. de Bruijin, A.T. van Oosterom, R.A. Maes, In vitro partition of irinotecan (CPT-11) in human volunteer blood: the influence of concentration, gender and smoking, Anticancer. Drugs. 16 (2005) 893–895. doi:10.1097/01.cad.0000175585.24317.ca.
[22] K. Fujita, Y. Masuo, H. Okumura, Y. Watanabe, H. Suzuki, Y. Sunakawa, K. Shimada, K. Kawara, Y. Akiyama, M. Kitamura, M. Kunishima, Y. Sasaki, Y. Kato, Increased Plasma Concentrations of Unbound SN-38, the Active Metabolite of Irinotecan, in Cancer Patients with Severe Renal Failure, Pharm. Res. 33 (2016) 269–282. doi:10.1007/s11095-015-1785-0.
[23] G.G. Chabot, Clinical pharmacokinetics of irinotecan., Clin. Pharmacokinet. 33 (1997) 245–259. doi:10.2165/00003088-199733040-00001.

5. CONSIDERAÇÕES FINAIS

IRI é um fármaco amplamente utilizado no tratamento do câncer colorretal e pancreático avançado e seu uso está associado com efeitos adversos imprevisíveis, principalmente diarreia e neutropenia (TOURNIGAND et al., 2004). Esses efeitos podem ser muito graves, podendo levar à interrupção do tratamento e severa morbidade, ou até mesmo fatais. Anos de pesquisa elucidaram o metabolismo complexo do IRI, que envolve várias enzimas de fase I e II, além de transportadores de fármacos (**capítulo 1**). Apesar deste conhecimento, ainda não existem estratégias amplamente aceitas para a individualização de doses de IRI, bem como alvos farmacocinéticos estabelecidos para este fármaco.

Nesta dissertação, foram desenvolvidas e validadas duas metodologias altamente sensíveis para análise de IRI e metabólitos. Um método para determinação da concentração plasmática de IRI, SN-38 e SN-38G (**capítulo 2**), aliada a uma estratégia de amostragem limitada (POUJOL et al., 2007) e parâmetros farmacocinéticos populacionais (KLEIN et al., 2002), possibilitou determinar a exposição sistêmica ao IRI através do cálculo da ASC do paciente. O desenvolvimento do primeiro método com a amostragem alternativa por DBS para a quantificação de IRI e SN-38 (**capítulo 3**), forneceu uma estratégia de amostragem que facilita a execução de amostragens complexas para posterior cálculo da ASC. Ambos os ensaios desenvolvidos nesta dissertação empregaram o CLAE-FL, que é uma metodologia particularmente interessante devido à sua seletividade e robustez, com custos de implementação reduzidos quando comparados ao CL-EM/EM.

Em particular, o uso de DBS é promissor para a caracterização da exposição individual ao IRI e seus metabólitos visto permitir uma coleta minimamente invasiva, além de coletas múltiplas do mesmo paciente sem necessidade de infraestrutura ou profissionais especializados. Com treinamento, o próprio paciente pode realizar a coleta e usar o serviço postal para enviar o DBS até o laboratório.

O ensaio inédito para determinação de IRI e SN-38 em DBS apresentado no capítulo 3, combinado com ferramentas computacionais apropriadas, permitirá uma avaliação farmacocinética detalhada de pacientes sob tratamento quimioterápico com IRI e o estabelecimento de relações entre parâmetros farmacocinéticos e a ocorrência de efeitos adversos. Estes estudos futuros poderão resultar no estabelecimento de doses personalizadas com base nas características farmacocinéticas individuais.

REFERÊNCIAS

ANTUNES, Marina Venzon; CHARÃO, Mariele Feiffer; LINDEN, Rafael. Dried blood spots analysis with mass spectrometry: Potentials and pitfalls in therapeutic drug monitoring. **Clinical biochemistry**, v. 49, n. 13, p. 1035-1046, 2016.

BASU, Sumit et al. Development and validation of an UPLC–MS/MS method for the quantification of irinotecan, SN-38 and SN-38 glucuronide in plasma, urine, feces, liver and kidney: Application to a pharmacokinetic study of irinotecan in rats. **Journal of Chromatography B**, v. 1015, p. 34-41, 2016.

BJÖRKHEM-BERGMAN, Linda et al. Comparison of endogenous 4β-hydroxycholesterol with midazolam as markers for CYP3A4 induction by rifampicin. **Drug Metabolism and Disposition**, v. 41, n. 8, p. 1488-1493, 2013.

CANAL, PCAJYRRAPFA et al. Pharmacokinetics and pharmacodynamics of irinotecan during a phase II clinical trial in colorectal cancer. Pharmacology and Molecular Mechanisms Group of the European Organization for Research and Treatment of Cancer. **Journal of clinical oncology**, v. 14, n. 10, p. 2688-2695, 1996.

CONROY, Thierry et al. The role of the FOLFIRINOX regimen for advanced pancreatic cancer. **Current oncology reports**, v. 15, n. 2, p. 182-189, 2013.

DE JONG, Floris A. et al. Flat-Fixed Dosing of Irinotecan. **Clinical Cancer Research**, v. 10, n. 12, p. 4068-4071, 2004.

DI PAOLO, Antonello et al. Pharmacokinetic and pharmacogenetic predictive markers of irinotecan activity and toxicity. **Current drug metabolism**, v. 12, n. 10, p. 932-943, 2011.

FERLAY, Jacques et al. Cancer incidence and mortality worldwide: sources, methods and major patterns in GLOBOCAN 2012. **International journal of cancer**, v. 136, n. 5, p. E359-E386, 2015.

HIROSE, Koichi et al. Correlation between plasma concentration ratios of SN-38 glucuronide and SN-38 and neutropenia induction in patients with colorectal cancer and wild-type UGT1A1 gene. **Oncology letters**, v. 3, n. 3, p. 694-698, 2012.

HIROSE, Kouichi et al. Usefulness of one-point plasma SN-38G/SN-38 concentration ratios as a substitute for UGT1A1 genetic information after irinotecan administration. **International journal of clinical oncology**, v. 19, n. 2, p. 397-402, 2014.

INNOCENTI, Federico et al. Dose-finding and pharmacokinetic study to optimize the dosing of irinotecan according to the UGT1A1 genotype of patients with cancer. **Journal of Clinical Oncology**, v. 32, n. 22, p. 2328-2334, 2014.

KEHRER, Diederik FS et al. Modulation of irinotecan metabolism by ketoconazole. **Journal of clinical oncology**, v. 20, n. 14, p. 3122-3129, 2002.

KLEIN, Cheri Enders et al. Population pharmacokinetic model for irinotecan and two of its metabolites, SN-38 and SN-38 glucuronide. **Clinical Pharmacology & Therapeutics**, v. 72, n. 6, p. 638-647, 2002.

MATHIJSSEN, Ron HJ et al. Clinical pharmacokinetics and metabolism of irinotecan (CPT-11). **Clinical cancer research**, v. 7, n. 8, p. 2182-2194, 2001.

MATHIJSSEN, Ron HJ et al. Effects of St. John's wort on irinotecan metabolism. **Journal of the National Cancer Institute**, v. 94, n. 16, p. 1247-1249, 2002.

MEYERHARDT, Jeffrey A.; MAYER, Robert J. Systemic therapy for colorectal cancer. **New England Journal of Medicine**, v. 352, n. 5, p. 476-487, 2005.

POUJOL, Sylvain et al. Pharmacokinetics and pharmacodynamics of irinotecan and its metabolites from plasma and saliva data in patients with metastatic digestive cancer receiving Folfiri regimen. **Cancer chemotherapy and pharmacology**, v. 58, n. 3, p. 292-305, 2006.

POUJOL, Sylvain et al. A limited sampling strategy to estimate the pharmacokinetic parameters of irinotecan and its active metabolite, SN-38, in patients with metastatic digestive cancer receiving the FOLFIRI regimen. **Oncology reports**, v. 18, n. 6, p. 1613-1622, 2007.

ROUITS, E. et al. Pharmacokinetic and pharmacogenetic determinants of the activity and toxicity of irinotecan in metastatic colorectal cancer patients. **British journal of cancer**, v. 99, n. 8, p. 1239-1245, 2008.

SALEEM, Mohamed et al. Target concentration intervention in oncology: where are we at?. **Therapeutic drug monitoring**, v. 34, n. 3, p. 257-265, 2012.

SANTOS, Alexandre et al. Metabolism of irinotecan (CPT-11) by CYP3A4 and CYP3A5 in humans. **Clinical Cancer Research**, v. 6, n. 5, p. 2012-2020, 2000.

TOFFOLI, Giuseppe et al. Genotype-driven phase I study of irinotecan administered in combination with fluorouracil/leucovorin in patients with metastatic colorectal cancer. **Journal of Clinical Oncology**, v. 28, n. 5, p. 866-871, 2010.

TOURNIGAND, Christophe et al. FOLFIRI followed by FOLFOX6 or the reverse sequence in advanced colorectal cancer: a randomized GERCOR study. **Journal of Clinical Oncology**, v. 22, n. 2, p. 229-237, 2004.

VAN DER BOL, Jessica M. et al. A CYP3A4 phenotype–based dosing algorithm for individualized treatment of irinotecan. **Clinical Cancer Research**, v. 16, n. 2, p. 736-742, 2010.

VAN SCHAIK, Ron HN. Implications of cytochrome P450 genetic polymorphisms on the toxicity of antitumor agents. **Therapeutic drug monitoring**, v. 26, n. 2, p. 236-240, 2004.

ANEXO I

Comprovante da submissão do artigo " Pharmacokinetic and pharmacogenetic markers of irinotecan toxicity" à revista *Current Medicinal Chemistry*.

Roberta Zilles Hahn

De: Beenish Anwer <onbehalfof@manuscriptcentral.com>
Enviado em: quinta-feira, 4 de janeiro de 2018 15:34
Para: Roberta Zilles Hahn
Assunto: Current Medicinal Chemistry - Account Created in ScholarOne Manuscripts

04-Jan-2018

Dear Miss Hahn:

A manuscript titled Pharmacokinetic and pharmacogenetic markers of irinotecan toxicity (CMC-2018-0009) has been submitted by Miss Roberta Hahn to the Current Medicinal Chemistry.

You are listed as a co-author for this manuscript. The online peer-review system, ScholarOne Manuscripts, automatically creates a user account for you. Your USER ID and PASSWORD for your account is as follows:

Site URL: https://mc04.manuscriptcentral.com/crmc
USER ID: betahahn@feevale.br
PASSWORD: For security reasons your password is not contained in this email. To set your password click the link below.

You can use the above USER ID and PASSWORD (once set) to log in to the site and check the status of papers you have authored/co-authored. Please log in to https://mc04.manuscriptcentral.com/crmc to update your account information via the edit account tab at the top right.

Thank you for your participation.

Sincerely,
Current Medicinal Chemistry Editorial Office

ANEXO II

Comprovante da publicação do artigo "An Easily Implementable Liquid Chromatography Assay for Therapeutic Drug Monitoring of irinotecan and Major Metabolites in Plasma" na revista *Latin American Journal of Pharmacy*.

Latin American Journal of Pharmacy
(formerly *Acta Farmacéutica Bonaerense)*
Lat. Am. J. Pharm. **36** (12): 2363-8 (2017)

Received: October 1, 2017
Accepted: October 18, 2017

An Easily Implementable Liquid Chromatography Assay for Therapeutic Drug Monitoring of Irinotecan and Major Metabolites in Plasma

Roberta Z. HAHN [1,2], Priscila C. ARNHOLD [1], Natalia B. ANDRIGUETTI [1,2], Anelise SCHNEIDER [1], Helena KLÜCK [3], Ramon M.M. VILELA [3], Simone L. DOS REIS [3], Gilberto SCHWARTSMANN [3], Marina V. ANTUNES [1,2] & Rafael LINDEN [1,2] *

[1] *Analytical Toxicology Laboratory, Universidade Feevale, Novo Hamburgo-RS, Brazil*
[2] *Graduate Program on Toxicology and Analytical Toxicology, Universidade Feevale, Novo Hamburgo-RS, Brazil*
[3] *Serviço de Oncologia, Hospital de Clínicas de Porto Alegre, Porto Alegre-RS, Brazil*

SUMMARY. **The objective of this study was to develop an easily implementable liquid-chromatographic assay for clinical application in therapeutic drug monitoring of irinotecan (IRI), including the metabolite SN-38 and its glucuronide SN-38G. IRI and the metabolites SN-38 and SN-38G were extracted from plasma, after protein precipitation, with methyl-*tert*-butyl ether. SN-38G levels were estimated by treating plasma with β-glucuronidase and evaluating the difference of SN-38 levels. Separation was performed in a reversed phase column with isocratic elution and fluorescence detection. Total chromatographic run time was 19 min. The assay was linear in the range of 10 to 3,000 ng/mL for IRI and 1 to 300 ng/mL for SN-38. Accuracy was 97.8-105.2%, intra-assay precision was 2.1-4.72% and inter-assay precision was of 1.66-4.37%. The assay was applied in samples from 10 patients under IRI chemotherapy. The assay was validated and due to its simple setup can be implemented in clinical laboratories aiming to pharmacokinetically individualize IRI doses. Particularly, the simple estimation of the glucuronidation ratio of the active metabolite SN-38 can be used to identify patients on risk for severe toxicity.**

RESUMEN. El objetivo de este estudio fue desarrollar un ensayo cromatográfico líquido fácilmente implementable para la aplicación clínica en la monitorización terapéutica del fármaco del irinotecán (IRI), que incluye el metabolito SN-38 y su glucurónido SN-38G. IRI y los metabolitos SN-38 y SN-38G se extrajeron del plasma, después de la precipitación de proteínas, con metil-*terc*-butil éter. Los niveles de SN-38G se estimaron tratando el plasma con β-glucuronidasa y evaluando la diferencia de los niveles de SN-38. La separación se realizó en una columna de fase invertida con elución isocrática y detección de fluorescencia. El tiempo total de ejecución cromatográfica fue de 19 min. El ensayo fue lineal en el intervalo de 10 a 3.000 ng/mL para IRI y de 1 a 300 ng/mL para SN-38. La precisión fue de 97.8-105.2%, la precisión intra-ensayo fue de 2.1-4.72% y la precisión entre ensayos fue de 1.66-4.37%. El ensayo se aplicó en muestras de 10 pacientes con quimioterapia IRI. El ensayo fue validado y debido a su configuración simple puede implementarse en laboratorios clínicos con el objetivo de individualizar farmacocinéticamente las dosis de IRI. Particularmente, la simple estimación de la relación de glucuronidación del metabolito activo SN-38 puede usarse para identificar pacientes con riesgo de toxicidad grave.

INTRODUCTION

Irinotecan (IRI) is widely used as a first-line chemotheraphy for colorectal cancer [1] and advanced pancreatic cancer [2]. SN-38 (7-ethyl-10-hydroxycamptothecin) is the main active metabolite of IRI being 100 to 1,000 times more cytotoxic than the parent drug. SN-38 is detoxified by the formation of its glucuronide, SN-38G, mainly by UGT1A1 enzymes. Antineoplastic activity of IRI and SN-38 is attributed to the inhibitory effect on DNA topoisomerase I, which plays an important role in DNA replication and transcription and leading to cell death [3]. IRI has a narrow therapeutic window [4] and an important limitation associated with its use is the wide interindividual variability in tolerability with occurrence of severe toxicity, especially neutropenia and severe diarrhea, partly due to the complex metabolism of this drug [5]. This variability is partially related to interindividual pharmacokinetic and pharmacogenetic differences, especially in the metabolic inactivation of the active metabolite. The risk of severe neutropenia associated with IRI administration is associated to

KEY WORDS: HPLC-FL ; irinotecan; SN-38; therapeutic drug monitoring.

* Author to whom correspondence should be addressed. *E-mail:* rafael.linden@feevale.br

ISSN 0326 2383 (printed ed.)
ISSN 2362-3853 (on line ed.)

ANEXO III

Comprovante da publicação do artigo "Determination of irinotecan and its metabolite SN-38 in dried blood spots using high-performance liquid-chromatography with fluorescence detection" na revista *Journal of Pharmaceutical and Biomedical Analysis*.

Journal of Pharmaceutical and Biomedical Analysis 150 (2018) 51–58

Contents lists available at ScienceDirect

Journal of Pharmaceutical and Biomedical Analysis

journal homepage: www.elsevier.com/locate/jpba

Determination of irinotecan and its metabolite SN-38 in dried blood spots using high-performance liquid-chromatography with fluorescence detection

Roberta Z. Hahn[a,b], Priscila C. Arnhold[a], Natália B. Andriguetti[a,b], Anelise Schneider[a], Helena M. Klück[c], Simone L. dos Reis[c], Marcos Frank Bastiani[a,b], Igor Kael[a], Anne Caroline Cezimbra da Silva[a], Gilberto Schwartsmann[c], Marina V. Antunes[a,b], Rafael Linden[a,b,*]

[a] Analytical Toxicology Laboratory, Universidade Feevale, Novo Hamburgo, RS, Brazil
[b] Graduate Program on Toxicology and Analytical Toxicology, Universidade Feevale, Novo Hamburgo, RS, Brazil
[c] Oncology Service, Hospital de Clínicas de Porto Alegre, Porto Alegre, RS, Brazil

ARTICLE INFO

Article history:
Received 3 November 2017
Received in revised form
28 November 2017
Accepted 30 November 2017

Keywords:
Irinotecan
SN-38
Dried blood spots
High-performance liquid chromatography
Fluorescence detection
Therapeutic drug monitoring

ABSTRACT

Irinotecan (IRI) is an antineoplastic drug widely used for the treatment of colorectal and advanced pancreatic cancer. Despite its clinical utility, the clinical use of IRI is associated with potentially severe hematopoietic and gastrointestinal toxicities. The quantification of IRI and its active metabolite SN-38 in dried blood spots (DBS) may be an alternative to individualize the drug dose through a minimally invasive and easy collection method. The aim of this study was to develop and validate a simple and fast HPLC-FL assay for simultaneous IRI and SN-38 measurement in DBS, with adequate analytical performance for clinical use. The method employs liquid extraction of one 8 mm disk of whole blood, followed by separation in a reversed phase Eclipse Plus C8 column (150 × 4.6 mm, 5 μm). Detection was performed with a fluorescence detector, with excitation wavelength of 370 and emission of 420 for IRI and 540 nm for SN-38 and internal standard (camptothecin). Total analytical run time was 17 min. Mobile phase was a mixture of 0.1 M phosphate buffer pH 4.0 and acetonitrile (80:20, v/v), at 1 mL min^{-1}. The assay was linear in the range 10–3,000 ng mL^{-1} and from 0.5 to 300 ng mL^{-1} for IRI and SN-38, respectively. Precision assays presented CV% of 2.71-5.65 and 2.15-10.07 for IRI and SN-38, respectively, and accuracy in the range of 94.26-100.93 and 94.24-99.33%. IRI and SN-38 were stable at 25 and 42 °C for 14 days in DBS samples. The method was applied to DBS samples obtained from fingerpicks from 19 volunteers receiving IRI in single or combined chemotherapy regimens, collected 1 and 24 h after beginning of the infusion. The estimated plasma concentration of IRI and SN-38 in sample collected 1 h after star of infusion had 16 of 19 values within the ±20% range of the measured plasma concentrations. On the other hand, predictions of IRI and SN-38 plasma concentrations from DBS measurements obtained 24 h after the beginning of the infusion were poor. AUC of IRI that was calculated using plasma and DBS-estimated concentrations, with a high correlation ($r = 0.918$). The method presented suitable characteristics for the clinical use. However, translation of IRI and SN-38 DBS to plasma concentrations is challenging due to the compound's variable plasma/blood partition.

1. Introduction

Irinotecan (IRI) is a chemotherapeutic drug used in the treatment of colorectal [1] and advanced pancreatic cancer [2]. The primary active metabolite of IRI is SN-38 (7-ethyl-10-hydroxycamptothecin), formed by liver carboxylesterases. SN-38 is at least 100 times more cytotoxic than the parent drug and is detoxified through the formation of its glucuronide, SN-38G, mainly by UGT1A1. The antineoplastic activity of IRI and SN-38 is attributed to their inhibitory effect on DNA topoisomerase I, required for cellular DNA replication and transcription [3].

IRI, as most anticancer drugs, is a toxic compound at clinically used doses [4], and its use is associated to a wide interindividual

* Corresponding author at: Toxicological Analysis Laboratory Instituto de Ciências da Saúde Universidade Feevale, Novo Hamburgo-RS, Brazil Rodovia ERS 239, n. 2755 CEP 93525-075 Novo Hamburgo, RS, Brazil.
E-mail address: rafael.linden@feevale.br (R. Linden).

https://doi.org/10.1016/j.jpba.2017.11.079
0731-7085/